AD NUMBER

ADB014135

NEW LIMITATION CHANGE

TO

Distribution authorized to U.S. Gov't. agencies and their contractors; Specific Authority; Sep 1976. Other requests shall be referred to Director, Naval Research Lab., Washington, DC 20375.

FROM

Distribution authorized to U.S. Gov't. agencies only; Test and Evaluation; Sep 1976. Other requests shall be referred to Director, Naval Research Lab., Washington, DC 20375.

AUTHORITY

NRL, per DTIC Form 55

NRL Report 8005

Ambiguity-Resistant Three- and Four-Channel Interferometers

ROBERT L. GOODWIN
Tactical Electronic Warfare Division

September 9, 1976

NAVAL RESEARCH LABORATORY
Washington, D.C.

SECURITY CLASSIFICATION OF THIS PAGE (When Data Entered)

REPORT DOCUMENTATION PAGE

READ INSTRUCTIONS BEFORE COMPLETING FORM

1. REPORT NUMBER: NRL Report 8005	2. GOVT ACCESSION NO.
3. RECIPIENT'S CATALOG NUMBER	
4. TITLE (and Subtitle): AMBIGUITY-RESISTANT THREE- AND FOUR-CHANNEL INTERFEROMETERS	5. TYPE OF REPORT & PERIOD COVERED: Interim report on a continuing problem.
6. PERFORMING ORG. REPORT NUMBER	
7. AUTHOR(s): Robert L. Goodwin	8. CONTRACT OR GRANT NUMBER(s)
9. PERFORMING ORGANIZATION NAME AND ADDRESS: Naval Research Laboratory, Washington, D.C. 20375	10. PROGRAM ELEMENT, PROJECT, TASK AREA & WORK UNIT NUMBERS: NRL Problem R06-07B, RF12151401 62712N
11. CONTROLLING OFFICE NAME AND ADDRESS: Office of Naval Research, Arlington, Va. 22217	12. REPORT DATE: September 1976
	13. NUMBER OF PAGES: 132
14. MONITORING AGENCY NAME & ADDRESS (if different from Controlling Office)	15. SECURITY CLASS. (of this report): Unclassified
	15a. DECLASSIFICATION/DOWNGRADING SCHEDULE

16. DISTRIBUTION STATEMENT (of this Report)

Distribution limited to U.S. Government Agencies only; test and evaluation; September 1976. Other requests for this document must be referred to the Commanding Officer, Naval Research Laboratory, Washington, D.C. 20375.

17. DISTRIBUTION STATEMENT (of the abstract entered in Block 20, if different from Report)

NRL-R06-07
RF12-151

RF12-151-401

18. SUPPLEMENTARY NOTES

19. KEY WORDS (Continue on reverse side if necessary and identify by block number)

Ambiguity constraints	Emitter location
Array ratios	Interferometers
Arrays	Optimum-realizable arrays
Channel-pair phase errors	Probability-of-ambiguity
Direction-finding	

20. ABSTRACT (Continue on reverse side if necessary and identify by block number)

Interferometers are useful for implementing real-time estimates of the angle-of-arrival of radio-frequency energy from distant emitters. Although accuracy and resolution of these arrays improves with increasing length, so does their tendency toward ambiguous estimates of the spatial angle. Tolerance to ambiguity (caused by channel-pair phase errors) for three-element arrays of a given length improves dramatically when another antenna-receiver channel is added to the array.

(Continued)

DD FORM 1 JAN 73 1473 EDITION OF 1 NOV 65 IS OBSOLETE
S/N 0102-014-6601

SECURITY CLASSIFICATION OF THIS PAGE (When Data Entered)

251950

Extensions to array ambiguity theory clarifies the principles of three-element arrays, and provides exact synthesis procedures for four-element arrays of any length. The extended theory shows that while a three-element array 23 half-wavelengths long (subject to phase errors of 12 electrical degrees rms) has a probability-of-ambiguity (p_a') of 45%, the corresponding optimum four-element array has a p_a' of only 0.075%. Computer-aided syntheses define the optimum four-element arrays from 4 to 42 half-wavelengths, and provide the resultant p_a' (for system design purposes) for phase errors from 8 to 20 electrical degrees rms.

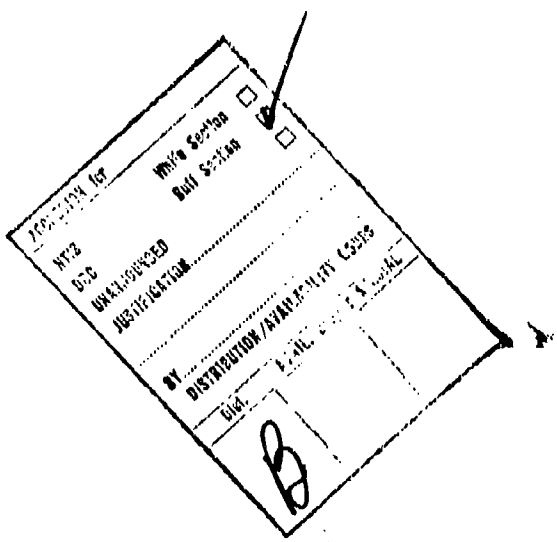

CONTENTS

AMBIGUITY-RESISTANT THREE- AND FOUR-CHANNEL INTERFEROMETERS

1.0 INTRODUCTION

Electronics support measures (ESM) systems used in military applications such as reconnaissance and threat reaction often require estimates of the angle of arrival (AOA) of radio-frequency signals from distant emitters. Accurate real-time AOAs—to 1° rms resolution and accuracy or better—facilitate efficient emitter sorting routines as well as establish emitter locations through the processing of successive relative bearing measurements. For ESM use, increasing emphasis is being placed on the implementation of AOA techniques that can provide azimuth coverage over wide fields of view, approaching ±60° with respect to the direction-finding (DF) system boresight. Multiple-element phase-only interferometers processing electrical phase differences between the signals received at spaced apertures turn out to be excellent for achieving accurate AOAs for certain ESM requirements. These techniques appear particularly applicable to implementing high-accuracy DF from airborne platforms in the frequency bands of interest above 1 GHz.

The three major goals of this report are

- To clarify some past misconceptions concerning the theory of multielement interferometers.

- To expound a general theory of interferometers which may stimulate research into the less-well-qualified aspects of phase-only interferometers, such as the constraints imposed by operation in severe multipath.

- To provide the ESM system designer with exact, readily applied techniques for obtaining the lowest probability of ambiguity for a given overall array length in three- and four-element arrays.

This report treats the phase-only interferometer exclusively. Interferometers that process relative amplitude information as well as phase difference information from multiple apertures—techniques prevalent in radio astronomy—are beyond the scope of this report. Attention will further be constrained to line arrays. Within these apparently severe restrictions of scope, there are many areas of applications for interferometers.

The reason for fixing attention exclusively on the phase-only interferometer is that in ESM systems, the designer often must maximize the instantaneous (nonscanned) field of view. He is faced with the choice of implementing directive-gain antenna/receiver channels, relatively nondirective antennas driving phase-only channels, or combinations of these approaches. For those requirements in which the loss in system detection sensitivity from nondirective apertures is acceptable, interferometer techniques that inherently

Manuscript submitted March 31, 1976.

achieve a large variation in output parameter for a small change in input bearing angle (large gradient) with comparatively few channels are quite suitable.

The simplest conceivable interferometer uses two essentially omnidirectional antennas and must employ supplementary techniques to discriminate against energy arriving from the rear hemisphere vs energy arriving from the front. In this elemental interferometer, the maximum allowable aperture spacing without ambiguous indications of AOA is one-half wavelength at the operating frequency. Arrays of n elements ($n \geq 3$) provide $(n-1)$ phase differences that can be used to resolve these ambiguities, even though the spacings between one or more pairs of adjacent channels exceeds one-half wavelength. Multielement arrays must be used in order to achieve both good angular resolution and low probability of ambiguity for realistic values of receiving channel phase errors.

The amount of published material on radio direction finding is incredible. Travers and Hixon [1] have assembled abstracts on the DF literature (including interferometers) covering the period 1899–1965. More recently, Barton [2–4] has included entries on interferometers in his index (and supplements) on material published in the *I.E.E.E. Transactions on Aerospace and Electronic Systems* and its predecessor publications. The emphasis of recent Russian work available in translation [5–7] is oriented more toward "frequency" interferometers (multifrequency ranging schemes) than toward addressing the "spatial" interferometer synthesis problem. Apparently, no work clarifying past inconsistencies in three-element arrays, and extending the theory to optimum arrays of four elements, has appeared to date.

Limiting the scope of this report to a consideration of only three- and four-element systems will not unduly restrict design freedom. These arrays are suitable for many requirements, as the following example will show.

The example pertains to locating surface emitters from an airborne platform and is offered to illustrate some of the tradeoffs between using arrays with either three or four elements. Figure 1-1 is a plan view of the geometry typical of an airborne collection system taking a series of relative bearings on a distant emitter. There are many treatments of the factors affecting location system performance [8–11] for the problem depicted in the illustration. The example shown is Butterly's [8] "asymmetrical 15° sector." The emitter range, normal to the assumed straight-line flight track, is 100 n.mi. (185.2 km). A flat-earth approximation is made, and errors because of altitude are neglected. The collection platform takes 16 successive bearings (forced to be equally spaced in Butterly's analysis, for convenience, with no great loss in generality). The first DF cut is made at an angle of 45° right of the array boresight; the last is taken at a bearing of 30°. Butterly's analysis shows that to restrict the area of uncertainty of emitter location to π n.mi.^{2} (3.43π km^2) to a probability of 0.95 requires accuracies of 0.21° rms on the bearings over this 15° range in angle.

The spatial accuracy in degrees rms, σ_{θ_a}, of an interferometer is related to the electrical phase error in the largest-spaced pair of antennas by the well-known expression

$$\sigma_{\theta_a} = \frac{\sigma_\phi}{\beta d \cos \theta_a}, \tag{1-1}$$

where

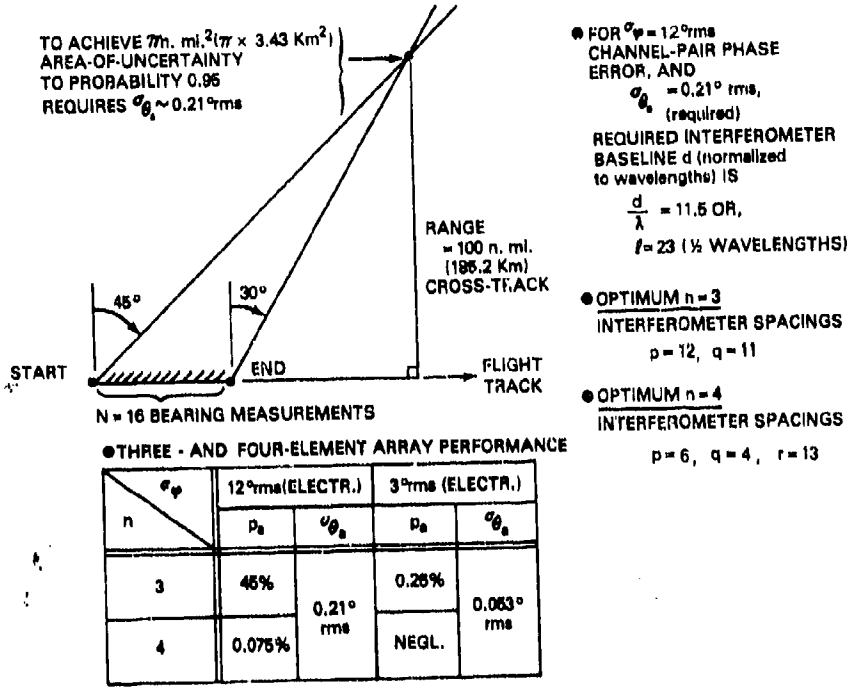

● THREE - AND FOUR-ELEMENT ARRAY PERFORMANCE

n \ σ_ψ	12°rms (ELECTR.)		3°rms (ELECTR.)	
	p_a	σ_{θ_a}	p_a	σ_{θ_a}
3	45%	0.21° rms	0.26%	0.053° rms
4	0.075%		NEGL.	

Fig. 1-1—Problem geometry for emitter location example

σ_ϕ = electrical phase error, degrees rms,

$\beta = 2\pi/\lambda$ = phase constant in the medium of propagation,

d = channel-pair spacing, longest-spaced channels.

If $\sigma_\phi = 12°$ rms (zero-mean) and if θ_a is in the vicinity of 37.5° (mean of 45° and 30°), to achieve an accuracy in AOA of 0.21° rms (zero-mean) requires an overall baseline length d = 11.5 wavelengths = 23 half-wavelengths. (Note: In developing the theory of low probability-of-ambiguity arrays, it is convenient to work with spacings expressed in integer half-wavelengths.) The optimum *three*-element array employs a channel 1 to 2 spacing of 12 half-wavelengths, and a channel 2 to 3 spacing of 11 half-wavelengths. For a readily obtained $\sigma_\phi = 12°$ rms, the probability of ambiguity of this array is 45%. This is clearly unacceptable performance.

The optimum *four*-element array, synthesized according to the principles presented in Secs. 4.0 and 5.0 of this report, has channel-pair element spacings of 6, 4, and 13 half-wavelengths between adjacent channels. For the same channel-pair phase error, 12° rms, the probability of ambiguity is 0.075%—a 600:1 improvement over the three-element array.

It is obvious that in dense signal environments, initial estimates of emitter location (and later refinements of these estimates) can be accomplished much more rapidly using

the more reliable estimates from the four-element array. It may also be observed that to reduce the probability of ambiguity of the three-element array to 0.26% requires a reduction in channel-pair phase error to approximately 3.0° rms. At the present state of the art in microwave component technology, it is doubtful whether such channel-pair phase tracking can be obtained over more than 5% to 10% bandwidths, even with automatic calibration.

The above example clearly shows the advantage of implementing a four-channel system, if the obtainable performance can be justified against the need for (a) the additional channel and (b) the additional processing. There are, of course, less stringent requirements that can be addressed very competently by a three-element array.

For example, suppose that it is possible to achieve system channel-pair phase tracking to 10° rms, and that a baseline length of $d/\lambda = 4$ ($\ell = 8$ half-wavelengths) is available. At boresight, the angular accuracy of such a system is 0.398° rms. Over the symmetric sector defined by a starting bearing of +15°, and an ending bearing of −15°, a direction-finding system need take only 21 bearing cuts, spaced at 1.5° increments, to attain a 0.95 probability of determining the location of an emitter to within a π n.mi.^{2} (3.43π km^2) area of uncertainty at a cross-track range of 102.65 n.mi. (190.1 km). This particular system has a probability of ambiguity of 1.01%, implying a somewhat longer initial processing interval, on the average, before "outliers" in the data could be identified and discarded (in contrast to the 0.075% p_a of the four-element system).

For many applications, the obtainable performance in three-element systems is quite satisfactory, provided that (a) the location geometry is favorable, (b) a sufficient number of bearing cuts can be taken, and (c) the system channel-pair phase tracking is good.

Figure 1-2 is one configuration of a four-element interferometer. The four functional elements shown are (a) relatively nondirective antennas for wide spatial coverage, (b) phase-tracked receiver channels incorporating hard limiting of channel signal levels to remove amplitude fluctuations, (c) phase comparators, and (d) an ambiguity-elimination and angle-processing circuit. As shown in the diagram, the channel at the far left is the phase reference. Other four-element array configurations are possible. Sec. 4.0 will show that this particular array configuration, called "cascaded end-phase," is the canonical configuration for a four-element array. Other array configurations can equal, but not exceed, its tolerance to angular ambiguities. This configuration is optimal because of its relatively simple processing compared with other array configurations.

For the configuration shown in Fig. 1-2, the electrical phase differences between a signal in the reference channel and signals in the other channels are

$$\varphi_{1,j} = \beta d_{1,j} \sin \theta_a , \tag{1-2}$$

where $d_{1,j}$ is the physical spacing between the phase centers of antennas 1 and j in the linear array ($j = 2, 3,$ or 4). Thus, three phase differences—the necessary and sufficient number to extract all the AOA-dependent electrical phase information the array can provide—are made available to the processing circuits.

Suppose $d_{1,4} = 4\, d_{1,3} = 16\, d_{1,2} = 8$ wavelengths. Normalized to half-wavelengths, the spacing integers (see Fig. 1-2) are $p = 1$, $p + q = 4$, and $p + q + r = 16$; these

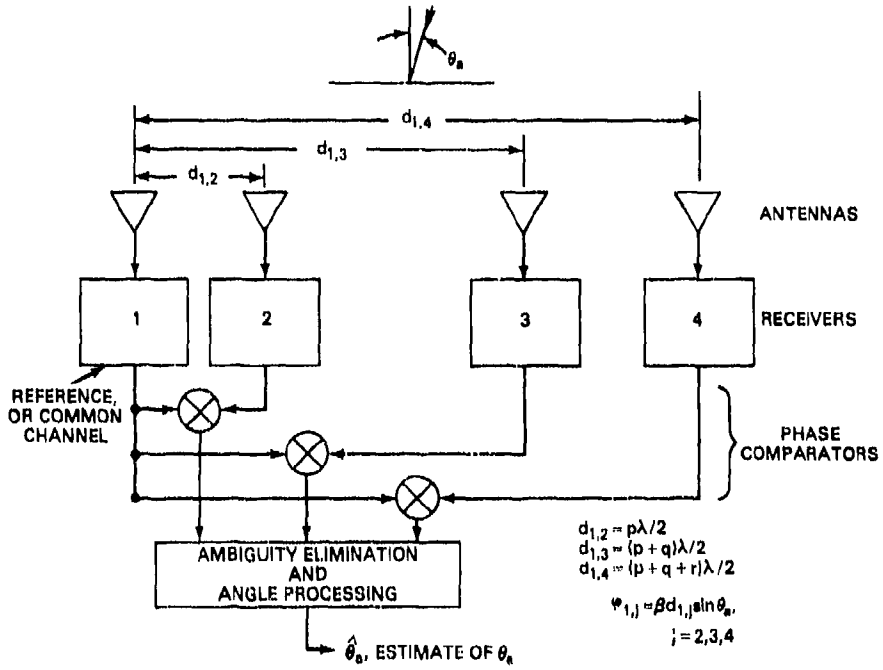

Fig. 1-2—Block diagram of four-element phase interferometer

define $q = 3$ and $r = 12$. According to Eq. (1-2), as θ_a increases, the electrical phase angles associated with channel-pair 1 and 4 and channel-pair 1 and 3 will eventually exceed $|\pm\pi|$ radians. However, since each member of the ensemble of phase comparator outputs can only be known modulo 2π, ambiguities—multiple-candidate AOAs—will be manifested in the phase comparator outputs. On the other hand, the phase comparator output associated with channel pair 1 and 2 can never exceed $|\pm\pi|$ radians. This fact can be exploited to yield an ambiguity resolution process that will enable an estimate of AOA associated with the *correct* mean AOA to be recovered.

There are $\ell - 1$ ambiguous θ_a in an array whose overall length is ℓ half-wavelengths. The probability that one of these ambiguous AOAs will be computed from the set of modulo 2π phase angles applied to the processing circuits is inversely related to the array spacings $d_{1,j}$ or more appropriately, to the spacing integers p, q, and r, when four-element arrays are under consideration.

The interferometer synthesis problem that is the main scope of this report is to determine p and q in three-element arrays; and p, q and r in four-element arrays so that an acceptable balance is achieved between the mutually incompatible objectives of maximizing the accuracy of the AOA estimate (increasing the overall array length) and minimizing the probability of ambiguity (minimizing the overall array length) subject to given channel-pair phase errors.

The two groups of readers to whom this report is addressed are (a) electronics support measure (ESM) system designers whose direction-finding requirements may be met

by implementing arrays synthesized according to the principles given here, and (b) those who may find the general theory of assistance as a point of departure in discovering the principles of arrays of more than four elements.

Array designs that achieve the best obtainable probability of ambiguity for given overall array length and channel-pair phase errors, and are guaranteed decodable, are described here. Thus, the report may be considered to be an extended "existence theorem" on low-ambiguity arrays. These arrays are guaranteed decodable because the spacing integers p, q, and r are relatively prime, but no specific decoding procedures are given in the report. The choice not to include some material on decoding was made reluctantly (in order to stress ambiguity aspects of array design), but was done in the knowledge that techniques based on the Chinese remainder theorem are well known.

Section 2.0 of this report is a short review of basic interferometer theory. It provides a thorough exposition of just what constitutes an ambiguity in arrays, and discusses the ambiguity constraints in arrays defined by two spacing integers.

Section 3.0 begins with a discussion of the phase-error sources in multichannel receiving systems, and the magnitudes of these errors in current-art receiver components. Then an expression for probability of ambiguity based on a channel-pair phase error formulation is given for three- and four-element, two-integer set arrays. Finally, the optimum spacings for these arrays is given, along with tabulations of p_a for various array lengths as a function of channel-pair phase error.

Section 4.0 treats the fundamentals of four-element, three-integer set interferometers by first considering the properties of various configurations of four elements. Resolvable and unresolvable ambiguities in the two distinct three-element subarrays that constitute a four-element array are then discussed. The role of the integer factor common to members of each of the subarray ratios as this factor influences overall array ambiguity is explored. Then, explicit forms are given for the ambiguity variables in each of the two subarrays, and some sample calculations are performed of probability of ambiguity. Last, it is shown that a particular form of four-element array, the cascaded end-phase array, is the optimum array configuration.

Section 5.0 provides the theoretical basis for synthesizing optimum arrays of various lengths. Two forms of array are introduced and defined to achieve a rapid, readily applied procedure; the "ideal unrealizable" array and the "optimum realizable" array. An approximate synthesis procedure, assuming independence of subarray ambiguities, is given. For most cases of current practical concern, this approximate synthesis procedure is very satisfactory. Indeed, this procedure often provides several arrays of the same overall length, but with differing p, q, and r spacings, that achieve the same overall probability of ambiguity. However, by treating the two subarray ambiguity variables as members of a joint probability density function, with correlation between the variables, it is possible to derive an exact formulation for the overall probability of ambiguity in four-element arrays. The impetus for presenting this exact analysis is threefold:

- The optimum array for a given overall array length and identical zero-mean channel-pair phase errors can be unequivocally specified.

- The analysis can be extended to arrays using antenna elements sequenced into a shared channel to achieve component-usage economies. (This analysis is not given in the present report, but it is a straightforward extension of the analyses given here.)

- Extensions of the basic analyses oriented toward other aspects of multielement array performance may be encouraged.

A convenient classification of overall array length that leads directly to a readily applied computer-aided synthesis is then given. The section closes with tabulations of probability of ambiguity for optimum arrays for a wide variety of array lengths.

Extensions of the research presented in this report are in progress, and are discussed briefly in a final section that summarizes the effort and provides some concluding remarks.

2.0 BASIC INTERFEROMETER THEORY

This section presents the basic principles underlying multielement phase interferometers. Initial attention is directed to the concept of characterizing arrays by two-integer sets. This generalized array concept emphasizes that the susceptibility of interferometers to providing ambiguous (actually, grossly erroneous) estimates of angle of arrival is a function of two integers and two associated channel-pair phase errors.

This method of characterizing an interferometer is compatible with either three-element or four-element arrays. For the former, a portion of the channel-pair phase errors reside in a "common-channel" phase error, whereas for the latter case, phase errors in one pair of channels are independent of phase errors in the other pair of channels.

There has been some confusion in the literature concerning the apparent superiority of one configuration of three-element array with respect to another array configuration as regards susceptibility to ambiguities for a given value of channel-pair phase error; as in Kendall [12] and Margerum [13]. Apparently, Kendall's efforts in generalizing three-element array theory to embrace arbitrary ratios, i.e., arrays whose spacings were *not* relatively prime integers--obscured the fact that if one particular configuration of three-element array is ambiguous (due to some set of channel-pair phase errors), then the other configurations must also be ambiguous. The proof is trivial and is given in Sec. 2.4.

Margerum analyzed a midphase three-element array, but neglected to consider the effects of "common-channel" phase. Consequently, the ambiguity constraints he derived were actually those for the four-channel (independent) two-integer set array. However, Margerum's use of the ambiguity-plane method of illustrating ambiguity boundary relationships seems to predate its employment by others. As will be seen in Sec. 2.3, the ambiguity plane is a valuable concept for understanding the mechanism underlying ambiguities in multielement interferometers.

2.1 Two-Integer Set Interferometer Fundamentals

Consider the linear array shown in Fig. 2-1 where the physical spacing between antennas 1 and 2 is d_L, and the spacing between antennas 3 and 4 is d_S. As depicted,

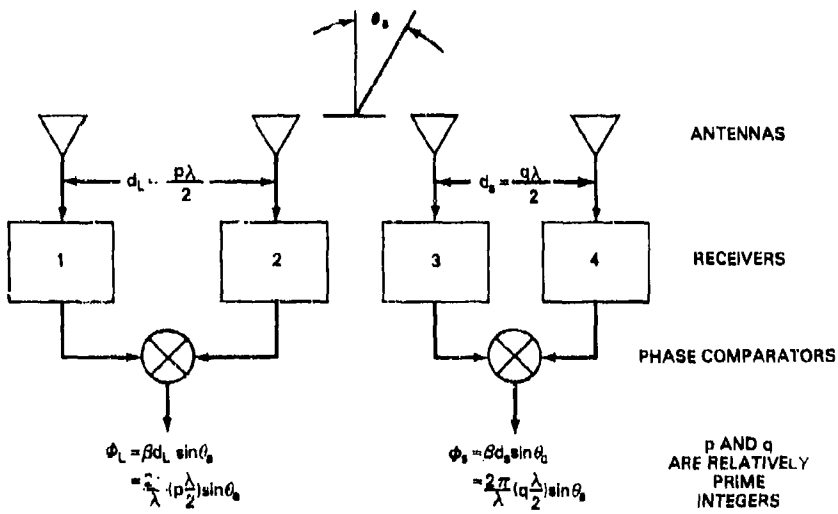

Fig. 2-1—One form of two-integer set interferometer

spatial angles of arrival are defined with respect to the normal to the baseline. With no loss in generality as far as interferometer ambiguities are concerned, the sources of distant signals are assumed to lie in the horizontal plane. It is further assumed that these spatial angles of arrival are restricted to $|\theta_a| \leq 90°$ or that other means have been employed to resolve the gross front-to-back ambiguity inherent in phase interferometers using antenna elements with little directivity.

The electrical phase differences between the signals in the two sets of antennas for radio-frequency (RF) energy arriving from angle θ_a are

Elements 1 and 2

$$\Phi_L = \beta d_L \sin\theta_a$$

$$= \frac{2\pi}{\lambda} d_L \sin\theta_a . \tag{2-1a}$$

Elements 3 and 4

$$\Phi_S = \beta d_S \sin\theta_a$$

$$= \frac{2\pi}{\lambda} d_S \sin\theta_a . \tag{2-1b}$$

These phase differences can be determined by applying the antenna outputs to phase-tracked receiver channels incorporating hard limiters (to remove amplitude fluctuations) and terminating in phase comparators. As is well known, in an elemental two-element

phase interferometer that does not have any available supplemental amplitude information from the antennas for use in resolving ambiguities, the maximum spacing between antenna phase centers is restricted to

$$d_{\max} = \frac{\pi - (-\pi)}{\frac{2\pi}{\lambda}\left[\sin(90^\circ) - \sin(-90^\circ)\right]}$$

$$= \frac{\lambda}{2}. \tag{2-2}$$

In interferometers providing two or more phase differences, it is possible to resolve ambiguities even though one or more spacings exceed a half-wavelength at the operating frequency.

Suppose d_L and d_S in the array of Fig. 2-1 are in the ratio of small integers, as

$$\Re = \frac{d_L}{d_S} = \frac{p}{q}, \tag{2-3}$$

where p and q are relatively prime.

If

$$d_L = \frac{p\lambda}{2}, \quad d_S = \frac{q\lambda}{2},$$

p complete cycles of 2π-rad phase change will occur between the output signals of antennas 1 and 2 and q complete cycles of 2π-rad phase change will occur between the output signals of antennas 3 and 4 as θ_a varies between -90° and $+90^\circ$.

Electrical phase angles can be determined only (mod 2π); hence, the true phase differences Φ_L and Φ_S must be expressed as

$$\Phi_L = \varphi_{L\text{-}pc} \pmod{2\pi} + 2\pi y \tag{2-4a}$$

and

$$\Phi_S = \varphi_{S\text{-}pc} \pmod{2\pi} + 2\pi x, \tag{2-4b}$$

where

subscript pc = voltages available at the output of a phase comparator defining angles,

x, y = pair of integers which must be determined so that Φ_L and Φ_S of Eq. (2-4) are equivalent to those of Eq. (2-1).

Determination of integers for x and y is basic to any vernier-resolving problem (e.g., distance measurement applications in which phase differences between sidetones displaced from a carrier are used to resolve range ambiguities) and is readily achieved. Noting that

$$\Phi_L = \frac{p}{q}\,\Phi_S\,, \tag{2-5}$$

and equating Eq. (2-4a) to (2-4b) yield

$$q[\varphi_{L-pc} \,(\text{mod } 2\pi) + 2\pi y] = p[\varphi_{S-pc} \,(\text{mod } 2\pi) + 2\pi x]\,. \tag{2-6}$$

An equivalent form is

$$p\varphi_S - q\varphi_L + 2\pi(px - qy) = 0\,, \tag{2-7}$$

where the *pc* subscripts and the (mod 2π) notations have been suppressed for clarity.

One method of solving Eq. (2-7) is to doubly iterate through the allowable sets of x and y until the set giving equality is found. As will be shown in Sec. 3.0, the best strategy in a system with phase errors is to accept the x_i, y_j that result in

$$|f(\varphi_L, \varphi_S, x_i, y_j)| \leq \pi\,. \tag{2-8}$$

2.2 Interferometer Array Classification

Figure 2-2 shows the four array configurations capable of providing two electrical phase differences for estimating spatial angle of arrival. Only antennas and the associated phase comparators are depicted; it is understood that receiving channels with phase deviations (as contrasted to ideal channels) are interposed.

Figure 2-2a, b, and c illustrate the three possible ways of obtaining two phase differences using three antennas, a consequence of the fact that the number of combinations of three elements taken two at a time = $3!/2!(3-2)! = 3$. Fig. 2-2d shows an array using four elements.

The arrays may be classified according to the channel used for phase reference. Thus, in Fig. 2-2a, channel 1 is the reference; the array is called End-phase Left. Similarly, in Fig. 2-2c, channel 3 is the reference; the configuration is called End-phase Right. Finally, in Fig. 2-2b, channel 2 is the reference; this array is called Midphase.

Obviously, for the array configuration in Fig. 2-2d, φ_S is unaffected by phase errors in channels 1 and 2. Hence, this four-channel interferometer is called Independent.

Suppose that for each of the three-element interferometers of Fig. 2-2, the element-to-element spacings (normalized to half-wavelengths at the operating frequency) are p between elements 1 and 2, and q between elements 2 and 3. Then, the interferometer ratios in terms of electrical angles and spacing integers are

End-phase Left $\qquad \mathcal{R}_L = \dfrac{\Phi_{L+S}}{\Phi_L} = \dfrac{p+q}{p}$

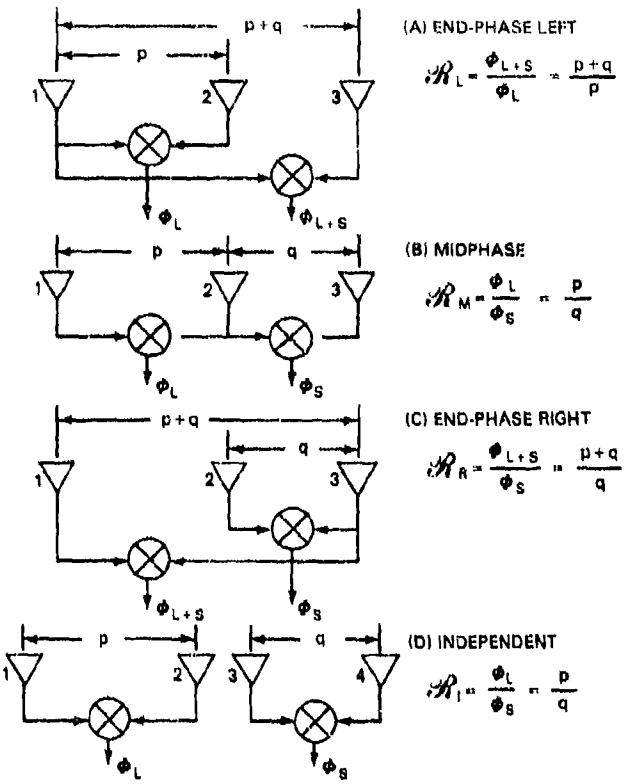

Fig. 2-2—Simplified block diagrams of the four possible two-integer set interferometers

$$\text{Midphase} \qquad \mathcal{R}_M = \frac{\Phi_L}{\Phi_S} = \frac{p}{q}$$

$$\text{End-phase Right} \qquad \mathcal{R}_R = \frac{\Phi_{L+S}}{\Phi_S} = \frac{p+q}{q},$$

where

$$\Phi_{L+S} = \frac{2\pi}{\lambda}(d_L + d_S)\sin\theta_a,$$

$$\Phi_L = \frac{2\pi}{\lambda} d_L \sin\theta_a,$$

$$\Phi_S = \frac{2\pi}{\lambda} d_S \sin\theta_a.$$

For the four-element interferometer, the analogous quantities are

Independent

$$\Re_I = \frac{\Phi_L}{\Phi_S} = \frac{p}{q}.$$

A complete classification should include consideration of phase-error parameters so as to account for unequal channel electrical lengths. Table 2-1 lists the channel-pair phase error parameters appropriate to the four-interferometer array configurations, in accord with the notation of Fig. 2-2. Expression of deviations from some nominal channel phase length in terms of channel-pair errors will be useful in establishing ambiguity constraints for the various interferometer configurations. In following sections, a channel-pair phase error formulation will be useful in deriving analytic expressions for probability of ambiguity in three- and four-element arrays.

2.3 Ambiguity Constraints for Two-Integer Set Interferometers

The constraints on channel-pair phase errors that preclude erroneous determination of the spatial AOA (because of ambiguities) will now be derived for two-integer set interferometers.

Consider an interferometer in which d_L and d_S are in the ratio $m{:}n$. The integers m and n are used to emphasize that a generalized interferometer, rather than one of the specific four configurations introduced earlier, is being discussed. The maximum allowable spacings for the ratio $\Re = m/n$ are, of course, $d_L = m\lambda/2$, and $d_S = n\lambda/2$. Otherwise, more than one θ_a within the $-90°$ to $+90°$ field of view (FOV) will produce a specific (mod 2π) Φ_L, Φ_S set. If $m = 3$, $n = 2$, $d_L = (3/2)\lambda$, $d_S = \lambda$, then

$$\left|\Phi_{L\text{-max}}\right| = \left|\pm\frac{2\pi}{\lambda}\cdot\frac{3}{2}\lambda = \pm 3\pi = \pm m\pi\right|,$$

$$\left|\Phi_{S\text{-max}}\right| = \left|\pm\frac{2\pi}{\lambda}\cdot\lambda = \pm 2\pi = \pm n\pi\right|.$$

If it were possible to measure Φ_L and Φ_S unambiguously over their ranges, a phase-plane plot of Φ_L vs Φ_S would appear as shown in Fig. 2-3a, in a form due to Margerum [13]. A more convenient representation is Fig. 2-3b, which is centered on $\theta_a = \pm 90°$ rather than on $\theta_a = 0°$. The expressions for Φ_L and Φ_S are thus modified to

$$\left.\begin{aligned}\Phi'_L &= \beta d_L \sin\theta_a \\ \Phi'_S &= \beta d_S \sin\theta_a\end{aligned}\right\} 0° \leq \theta < 90°, \qquad (2\text{-}9a)$$

and

$$\left.\begin{aligned}\Phi'_L &= \beta d_L(2 + \sin\theta_a) \\ \Phi'_S &= \beta d_S(2 + \sin\theta_a)\end{aligned}\right\} -90° \leq \theta_a < 0°. \qquad (2\text{-}9b)$$

Table 2-1—Spacings, Related Integers, and Phase-detector Output Voltages for Various Array Configurations

Array Configuration	Array Spacings and Integers		Phase-detector Voltages	
	Large	Small	Large	Small
End-phase left	$d_L + d_S$ $(p+q)$	d_L (p)	$\begin{matrix}\cos\\ \sin\end{matrix}(\Phi_{L+S} + \Delta\varphi_1 - \Delta\varphi_3)$	$\begin{matrix}\cos\\ \sin\end{matrix}(\Phi_L + \Delta\varphi_1 - \Delta\varphi_2)$
Midphase	d_L (p)	d_S (q)	$\begin{matrix}\cos\\ \sin\end{matrix}(\Phi_L - \Delta\varphi_2 + \Delta\varphi_1)$	$\begin{matrix}\cos\\ \sin\end{matrix}(\Phi_S + \Delta\varphi_2 - \Delta\varphi_3)$
End-phase right	$d_L + d_S$ $(p+q)$	d_S (q)	$\begin{matrix}\cos\\ \sin\end{matrix}(\Phi_{L+S} + \Delta\varphi_3 - \Delta\varphi_1)$	$\begin{matrix}\cos\\ \sin\end{matrix}(\Phi_S + \Delta\varphi_3 - \Delta\varphi_2)$
Independent	d_L (p)	d_S (q)	$\begin{matrix}\cos\\ \sin\end{matrix}(\Phi_L + \Delta\varphi_1 - \Delta\varphi_2)$	$\begin{matrix}\cos\\ \sin\end{matrix}(\Phi_S + \Delta\varphi_3 - \Delta\varphi_4)$

$$\Phi_{L+S} = \beta(d_L + d_S)\sin\theta_a = \frac{2\pi}{\lambda}\,\frac{(p+q)\lambda}{2}\sin\theta_a$$

$$\Phi_L = \beta d_L \sin\theta_a = \frac{2\pi}{\lambda}\,\frac{p\lambda}{2}\sin\theta_a$$

$$\Phi_S = \beta d_S \sin\theta_a = \frac{2\pi}{\lambda}\,\frac{q\lambda}{2}\sin\theta_a$$

$\Delta\varphi_i$, i = 1 to 4 are deviations of channel i electrical phase from nominal

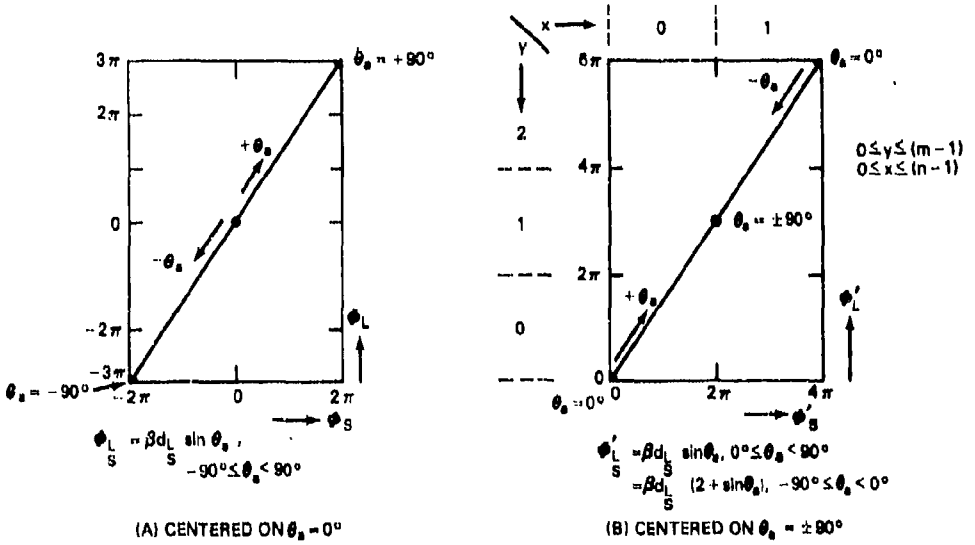

Fig. 2-3—Phase-plane diagrams for $m:n = 3:2$

Since Φ'_L and Φ'_S can be known only to within 2π rad at the outputs of phase comparators, the phase-plane plot must be collapsed to a square 2π rad on a side, as shown in Fig. 2-4. In this diagram, the intersections of the Φ'_L vs Φ'_S trajectories on the φ_L axis are spaced $2\pi/n$ $(=\pi)$. The φ_S axis intersections are spaced $2\pi/m$ $(=2\pi/3)$.

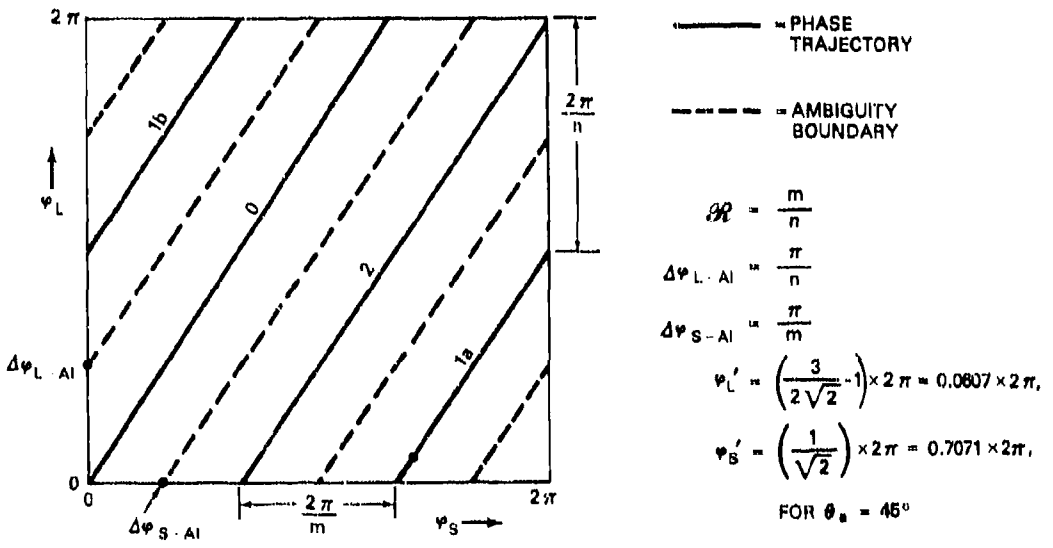

Fig. 2-4—Ambiguity diagram for $m:n = 3:2$

Suppose $\theta_a = 45°$. Then

$$\Phi'_L = 2\pi \times 3/2 \times 1/\sqrt{2},$$

and

$$\varphi'_L = \Phi'_L \pmod{2\pi} = 2\pi(3/2\sqrt{2} - 1).$$

Also,

$$\Phi'_S = 2\pi \times 1 \times 1/\sqrt{2}; \quad \varphi'_S = 2\pi/\sqrt{2}.$$

From Eq. (2-7), we have

$$m\varphi'_S - n\varphi'_L + 2\pi(mx - ny) = 0.$$

Substituting for φ'_L and φ'_S and dividing by 2π yields a trajectory-establishing equation of the form

$$3x + 2 = 2y. \tag{2-10}$$

The only solution of Eq. (2-10) subject to constraints $0 \leq x \leq (n-1)$ and $0 \leq y \leq (m-1)$ is $x = 0$, $y = 1$. (Note: The Fig. 2-3b formulation of the ambiguity plane leads only to positive solutions of Eq. (2-10) and is much less cumbersome than an approach based on Fig. 2-3a.) Thus,

$$\Phi'_L = \varphi_L + 2\pi(1)$$

$$= 2\pi\left(\frac{3}{2\sqrt{2}} - 1\right) + 2\pi = 2\pi \times \frac{3}{2\sqrt{2}}$$

and

$$\Phi'_S = \varphi_S + 2\pi(0)$$

$$= \frac{2\pi}{\sqrt{2}}.$$

The spatial angle of arrival θ_a can be recovered, for example, from the expression

$$\theta_a = \sin^{-1}\left[\frac{\Phi'_L}{\Phi'_{L\text{-max}}}\right] = \sin^{-1}\left[\frac{2\pi \times \frac{3}{2} \times \frac{1}{\sqrt{2}}}{2\pi \times \frac{3}{2}}\right] = 45°.$$

Errors in the channel-pair signals sent to the phase comparators will move the φ_L, φ_S set off the phase trajectories (solid lines 0, 1a, 1b, or 2) in Fig. 2-4. For simplicity, the prime notation on Φ_L, Φ_S and φ_L, φ_S will be dropped henceforth.

If any Φ_L, Φ_S set is in error because of channel deviations, then the (mod 2π) representation at the phase-comparator output is also in error. The *actual* phase differences (including errors) compared to the phase differences made available by the instrumentation are as follows:

Actual Electrical Phase Differences

$$\Phi_{L_{act}} = \frac{2\pi}{\lambda} d_L \sin\theta_a + \Delta\varphi_L = \Phi_L + \Delta\varphi_L \tag{2-11a}$$

$$\Phi_{S_{act}} = \frac{2\pi}{\lambda} d_S \sin\theta_a + \Delta\varphi_S = \Phi_S + \Delta\varphi_S . \tag{2-11b}$$

Available Electrical Phase Differences

$$\varphi_{L_{av}} = [\Phi_L + \Delta\varphi_L] \,(\text{mod } 2\pi) \tag{2-12a}$$

$$\varphi_{S_{av}} = [\Phi_S + \Delta\varphi_S] \,(\text{mod } 2\pi) . \tag{2-12b}$$

The geometry of Fig. 2-4 shows that to equalize the possibility of incurring ambiguities over the −90° to +90° FOV, the dashed boundaries separating the region around one trajectory from the region around another should be located parallel to, and equidistant from, adjacent phase trajectories. The ambiguity boundary directly above trajectory '0' intersects the φ_L axis at

$$\Delta\varphi_{L\text{-}AI} = \frac{\pi}{n}, \tag{2-13a}$$

and the boundary directly below trajectory '0' intersects the φ_S axis at

$$\Delta\varphi_{S\text{-}AI} = \frac{\pi}{m}. \tag{2-13b}$$

In attempting to generalize the conditions for obtaining minimum tendency toward ambiguities over the field of view, Kendall [12] considered ratios $\Re = m/n$ (or n/m) in which m and n were *not* restricted to relatively prime integers. He employed a needlessly complex analytical formulation, whereas, with just the previously used geometric arguments, it is easy to show that m and n must be relatively prime integers, as in the following example.

Figure 2-5 shows a phase-plane plot of the trajectories for $\Re = \sqrt{11}/2 = 3.3166/2$, subject to the element spacing associated with m equal to $\sqrt{11}/2$ wavelengths. The solid trajectories in the figure thus terminate with 3a, at a φ_L value of $0.3166 \times 2\pi$. This indicates, of course, that over a 180° range on θ_a, Φ_L sweeps through $3.3166 \times 2\pi$ rad, and Φ_S sweeps through 2π rad. Since $\Re$ is irrational, one can, in theory, extend the array length indefinitely without encountering a condition where multiple θ_a give rise to the same φ_L, φ_S set. As more trajectories are added to Fig. 2-5 (implying increased array length), the spacing between trajectories, and hence, the tolerance to ambiguities, decreases.

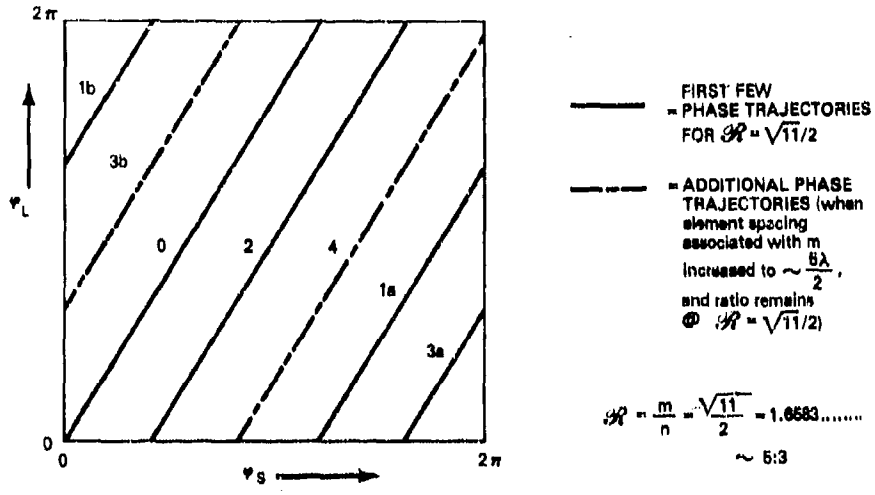

Fig. 2-5—Ambiguity diagram for $\mathcal{R} = \sqrt{11}/2$

Of the additional trajectories 3b and 4 (shown dashed in Fig. 2-5), 4 terminates near the point $\varphi_L, \varphi_S = 2\pi, 2\pi$. This might have been anticipated by noting that the integer-set ratio nearest $\mathcal{R} = \sqrt{11}/2$ is $\mathcal{R} = 5{:}3$. For the latter ratio, there would be five *equally spaced* trajectory intersections on the horizontal axis of the phase plane and three intersections on the vertical axis. Because $\sqrt{11}/2$ is irrational, however, there is no way of drawing ambiguity boundaries to equalize their spacing from adjacent trajectories, thereby making the tendency toward ambiguities implicitly independent of θ_a. Consequently, ratios formed by relatively prime integers are preferable.

All phase trajectories and ambiguity boundaries in phase-plane plots intersect the φ_S axis at an angle $\gamma = \tan^{-1}[(2\pi/n)/(2\pi/m)] = \tan^{-1}[(m/n) = \mathcal{R}]$. For any θ_a, it is easy to show that the two ambiguity constraints are

$$\Delta\varphi_L > \mathcal{R}\Delta\varphi_S + \Delta\varphi_{L-\mathrm{AI}}, \tag{2-14a}$$

and

$$\Delta\varphi_L < \mathcal{R}\Delta\varphi_S - \Delta\varphi_{L-\mathrm{AI}}, \tag{2-14b}$$

for $\mathcal{R} = m/n$, with m and n relatively prime integers.

If the upper inequality is satisfied, the ambiguity boundary *above* a given trajectory has been crossed; an analogous statement holds for the lower inequality.

An expression equivalent to Eq. (2-14a, b) which makes use of $\mathcal{R} = m/n$ and $\Delta\varphi_{L-\mathrm{AI}} = \pi/n$ is

$$|n\Delta\varphi_L - m\Delta\varphi_S| \gtrless \pi, \tag{2-15}$$

where > implies an ambiguity, and < implies no ambiguity.

Equation (2-15) is the ambiguity constraint for any two-integer set interferometer, provided that the channel-pair phase error terms $\Delta\varphi_L$ and $\Delta\varphi_S$ are defined properly with respect to the particular array configuration being analyzed.

2.4 Ambiguity Constraints for Specific Array Configurations

The ambiguity constraints for the four possible two-integer set interferometer configurations are now obtained by making use of the constraint just presented for a generalized interferometer.

Equation (2-15) is expressed in terms of generalized array integers m and n and channel-pair error parameters $\Delta\varphi_L$ and $\Delta\varphi_S$. The array ratios (from Sec. 2.2) and the channel-pair error parameters (from Table 2-1) for each of the array configurations are

End-phase Left

$$\mathcal{R}_L = \frac{m}{n} = \frac{p+q}{p}; \qquad \begin{aligned} \Delta\varphi_L &= \Delta\varphi_1 - \Delta\varphi_3 \\ \Delta\varphi_S &= \Delta\varphi_1 - \Delta\varphi_2 \end{aligned}, \tag{2-16a}$$

Midphase

$$\mathcal{R}_M = \frac{m}{n} = \frac{p}{q}; \qquad \begin{aligned} \Delta\varphi_L &= -\Delta\varphi_2 + \Delta\varphi_1 \\ \Delta\varphi_S &= \Delta\varphi_2 - \Delta\varphi_3 \end{aligned}, \tag{2-16b}$$

End-phase Right

$$\mathcal{R}_R = \frac{m}{n} = \frac{p+q}{q}; \qquad \begin{aligned} \Delta\varphi_L &= \Delta\varphi_3 - \Delta\varphi_1 \\ \Delta\varphi_S &= \Delta\varphi_3 - \Delta\varphi_2 \end{aligned}, \tag{2-16c}$$

Independent

$$\mathcal{R}_I = \frac{m}{n} = \frac{p}{q}; \qquad \begin{aligned} \Delta\varphi_L &= \Delta\varphi_1 - \Delta\varphi_2 \\ \Delta\varphi_S &= \Delta\varphi_3 - \Delta\varphi_4 \end{aligned}. \tag{2-16d}$$

Making the appropriate substitutions into Eq. (2-15) yields

End-phase Left

$$|p(\Delta\varphi_1 - \Delta\varphi_3) - (p+q)(\Delta\varphi_1 - \Delta\varphi_2)| \gtrless \pi, \tag{2-17a}$$

Midphase

$$|q(-\Delta\varphi_2 + \Delta\varphi_1) - p(\Delta\varphi_2 - \Delta\varphi_3)| \gtrless \pi, \tag{2-17b}$$

End-phase Right

$$|q(\Delta\varphi_3 - \Delta\varphi_1) - (p+q)(\Delta\varphi_3 - \Delta\varphi_2)| \gtrless \pi\,, \tag{2-17c}$$

Independent

$$|q(\Delta\varphi_1 - \Delta\varphi_2) - p(\Delta\varphi_3 - \Delta\varphi_4)| \gtrless \pi\,. \tag{2-17d}$$

It is easily shown that Eq. (2-17a, 2-17b, and 2-17c) are all equivalent to the following equation.

Three-element Interferometer

Ambiquity Constraint

$$|q\Delta\varphi_1 - (p+q)\Delta\varphi_2 + p\Delta\varphi_3| \gtrless \pi\,. \tag{2-18}$$

Equation (2-18) is, of course, a consequence of the fact that the channel-pair error parameters in a three-element interferometer are related by

$$a + c = b\,, \tag{2-19}$$

where

$a = \Delta\varphi_1 - \Delta\varphi_2$, on φ_L,

$c = \Delta\varphi_2 - \Delta\varphi_3$, on φ_S,

$b = \Delta\varphi_1 - \Delta\varphi_3$, on φ_{L+S}.

The results of Sec. 2.0 are the basis for correcting past misconceptions concerning the tendency toward ambiguities for various configurations of three-element interferometers. Kendall [12] argued that the end-phase configuration is superior to the midphase configuration. Margerum [13] analyzed only the midphase configuration, giving actually an expression for the probability of ambiguity for the independent four-element configuration. This left the impression, perhaps by omission, that the end-phase array configuration is inferior to the midphase configuration.

The correct statement for the ambiguity constraints in three-element interferometers, based on the development given here, is the following: *Any* configuration of three-element interferometer defined by spacing integers p and q (implying identical overall array length, regardless of configuration) has the same tendency toward ambiguity, regardless of the channel employed as the phase reference.

3.0 PERFORMANCE OF TWO-INTEGER SET INTERFEROMETERS

For many applications, the performance obtainable with two-integer set interferometers, either three- or four-element, is adequate. For example, a three-element array 8 half-wavelengths long at the frequency of operation with channel-pair phase errors of

10 electrical degrees rms can achieve a boresight angular accuracy of 0.40 spatial degrees, and a probability of ambiguity of 1.01%. Performance such as this can satisfy those requirements which do not need the "super" accuracy obtainable with multielement arrays that have longer overall baselines. The primary reason for presenting a comprehensive theory of two-integer set arrays is that they are the basic subarrays that can be cascaded to form longer arrays of four or more elements. In Secs. 4 and 5, examples of the dramatically improved performance that can be achieved with these arrays will be given.

This section discusses error sources, carefully distinguishing between a "channel" error description and a more convenient formulation for design and analysis purposes—the "channel-pair" description of error sources.

A channel-pair error correlation coefficient is introduced and defined for the end-phase, midphase and independent array configurations. Although it is not mandatory to use a channel-pair error and correlation coefficient formulation, this approach to derivation of probability of ambiguity facilitates the development of an exact expression for it in four-element three-integer set arrays in Sec. 5.

A recurrence relationship for generating the optimum spacings for three-element arrays of arbitrary length is given next. It is interesting that the full tabulation of allowable spacings, i.e., nonredundant, for arrays of various lengths has a counterpart in the Farey sequences of rational fractions from number theory. Travers [14] points out, however, that propagation anomalies in the HF band (3 to 30 MHz) may constrain the "small-spaced channel-pair" spacing to one half-wavelength rather than the optimum "small-spaced channel-pair" spacing for the overall array being used, resulting in fewer ambiguities.

The section concludes with a tabulation of probability of ambiguity vs array length (with channel-pair phase error as a parameter) for both three-element (end-phase or midphase) and four-element (independent) two-integer set array configurations. Historically, two-integer set interferometer arrays seem to have been implemented first in the independent configuration as in Bailey and Moller [15]. Watters, Rees, and Enstrom, [16] have reported on a two-frequency technique equivalent to the independent configuration. Later, as the theory of arrays improved and the component art advanced, the three-element, two-integer set arrays became much more prevalent. A recent example of a commercially oriented three-element array is reported by Watanabe, et al. [17]. Many current military surveillance systems also employ the three-element array.

3.1 Interferometer Channel-Pair Errors

In an actual interferometer, the electrical length φ_i of a given channel may be many thousands of electrical degrees. This length may vary because of changes in operating frequency, as a function of temperature, or with input signal power level (AM-to-PM conversion). The length φ_i can be represented (as in Sec. 2.0) by

$$\varphi_i = \varphi_{\text{nominal}} + \Delta\varphi_i \tag{3-1}$$

where $\Delta\varphi_i$ is the deviation of channel i in phase length from φ_{nominal}.

Individual channel errors $\Delta\varphi_i$ are accessible only by measurement to some standard. However, channel-pair errors

$$\begin{aligned}\Delta\varphi_{i,j} &\equiv \varphi_i - \varphi_j \\ &= (\varphi_{\text{nominal}} + \Delta\varphi_i) - (\varphi_{\text{nominal}} + \Delta\varphi_j) \\ &= \Delta\varphi_i - \Delta\varphi_j \end{aligned} \tag{3-2}$$

are manifested in the outputs of phase comparators connected between pairs of channels.

It is convenient to define interferometer performance in terms of channel-pair phase errors, rather than channel errors, for the following reason. The individual components that constitute a channel are usually more readily specified in terms of their deviations with respect to a corresponding component in another channel, rather than in terms of their deviations from nominal (but not conveniently measured) electrical lengths.

The variance of channel-pair phase error between ith and jth channels for the kth component in an n-element cascade is

$$\begin{aligned}\sigma^2_{i,j;k} &= E\{\Delta\varphi^2_{i;k}\} + E\{\Delta\varphi^2_{j;k}\} \\ &= \sigma^2_{i;k} + \sigma^2_{j;k} \end{aligned} \tag{3-3}$$

assuming that $\Delta\varphi_{i;k}$, $\Delta\varphi_{j;k}$ are independent and have zero-mean deviation from $\varphi_{\text{nominal-}k}$ over applicable parameters (RF frequency, power levels, supply voltage, angle of arrival, etc.).

The overall channel-pair error variance, summing over n components, is then

$$\sigma^2_{i,j} = \sum_{k=1}^{n} \sigma^2_{i,j;k} = \sigma^2_i + \sigma^2_j \,. \tag{3-4}$$

For a large number of cascaded components, all of whose variances are comparable, the channel-pair phase error distribution tends toward Gaussian (central-limit theorem). Statistical analyses of channel-pair errors obtained on actual multichannel systems support this contention.

Figure 3-1 is a block diagram of one channel of a multichannel interferometer showing the principal contributors to channel-pair electrical phase error. The direct output from phase comparators is analog. That is, $\Phi_{i,j}(\theta_a)$ is defined by $\sin^{-1}(v_{i,j;s}/v_{\max})$ and $\cos^{-1}(v_{i,j;c}/v_{\max})$, where $v_{i,j;s}$ and $v_{i,j;c}$ are voltages from the sine and cosine phase detectors, respectively, of the phase comparator and $v_{\max}$ is the maximum phase detector output voltage.

In automatic systems, it is convenient to perform ambiguity elimination and other calculations digitally. Hence, additional contributions to channel-pair phase error are

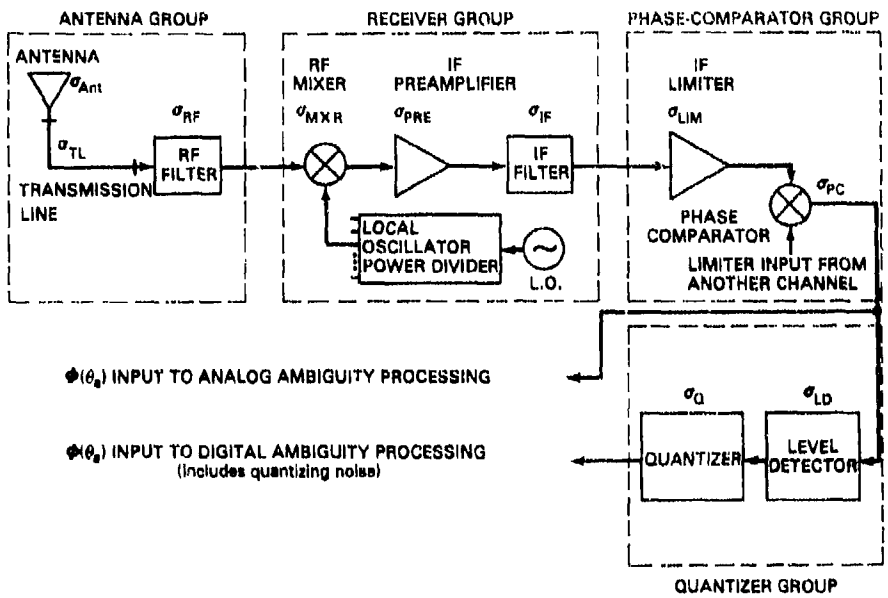

Fig. 3-1—Interferometer error sources

$\Delta\varphi_{LD}$ due to multivoltage level detector nonlinearities, and $\Delta\varphi_Q$ due to the quantization of electrical phase over 2π rad. Detailed consideration of the effects of $\Delta\varphi_{LD}$ and $\Delta\varphi_Q$ on probability of ambiguity is beyond the scope of this report.

Table 3-1 lists typical values of the major contributors to channel-pair phase error. It is assumed that the individual channel-pair errors are uniformly distributed between the limits shown. Phase errors due to finite signal-to-noise ratio (SNR) are not specifically included, but can be readily added with the aid of the relation $\sigma_\phi = 180°/\pi\sqrt{SNR}$, where SNR is in terms of power. The associated standard deviation of channel-pair phase error is $|\Delta\varphi_{X-max}|/\sqrt{3}$ where $\Delta\varphi_{X-max}$ is the peak value of phase error for component-pair X. Two values of phase "noise" due to quantizing are given. These represent upper and lower bounds on the degree of quantizing typically employed in interferometer systems of the type described in Sec. 1.0.

Table 3-1 shows that the phase error due to the quantizer group is more than half the overall phase error on a root-sum-square basis for 4-bit quantizing. On the other hand, quantizing-phase noise is negligible for 7-bit encoding. In general, higher-speed decoding (and possibly less complexity in the ambiguity algorithms) can be achieved with low degrees of quantizing. Conversely, systems employing higher degrees of quantizing perform closer to the theoretical probability of ambiguity for an analog processing system.

Radio-frequency calibration can be employed in interferometer systems to reduce the magnitude of channel-pair phase errors. Alternatively, by the use of calibration techniques, low-quality components (poor phase tracking) can provide performance comparable to that achieved in uncalibrated systems using high-quality components. Calibration signals are usually introduced into the channels directly behind the antennas.

Table 3-1—One-Sigma Channel-Pair Phase Error*
No Calibration

Group	Limits on $\Delta\varphi_{i,j}$†	Standard Deviation
Antenna Group:		
Antenna	= ± 8°	σ_{ANT} = 4.619°
Transmission line	= ± 4°	σ_{TL} = 2.309°
RF filter	= ± 5°	σ_{RF} = 2.887°
		Root-Sum-Square = 5.916°
Receiver Group:		
RF mixer and LO power divider	= ±10°	σ_{MXR} = 5.774°
IF preamplifier	= ± 3°	σ_{PRE} = 1.732°
IF filter	= ± 4°	σ_{IF} = 2.309°
		RSS = 6.455°
Phase Comparator Group:		
IF limiter	= ± 7°	σ_{lim} = 4.041°
Phase comparator	= ± 3°	σ_{PC} = 1.732°
		RSS = 4.397°
Quantizer Group:		
Level detector	= ± 1°	σ_{LD} = 0.577°
Quantizer, 7 bit	= ± 1.406°	σ_{Q} = 0.812°
Quantizer (4 bit)	(= ± 11.25°)	(σ_{Q} = 6.495°)
		RSS = 0.996° (6.521°)
Overall channel-pair phase error =		9.848° rms (11.769° rms)

*"Strong-signal" conditions. †Uniform distribution assumed.
Note: Present technology, wideband systems.

The use of calibration signals whose frequencies are equal to signals of interest makes possible, in principle, the removal of channel-pair phase errors due to RF and IF filters, RF mixer and local oscillator power divider, IF preamplifier, and phase comparator (see Fig. 3-1). Since the power level of an incoming signal within the system dynamic range is arbitrary relative to a fixed-level calibration signal, only a portion of the channel-pair phase error from the IF limiters can be removed. Also, the signal angle of arrival is arbitrary with respect to the fixed angle of arrival synthetically introduced into the system during the calibration mode. Thus, quantizing group errors must be accounted for twice: First, during the signal reception mode; and second, during the calibration mode.

The list of error sources and their magnitudes, typical of a system employing calibration, is given in Table 3-2. The independence of these errors during the two modes of operation is assumed.

Table 3-2—One-Sigma Channel-Pair Phase Error*
With RF Calibration

Component	Limits on $\Delta\varphi_{i,j}$†	Standard Deviation
ANALOG PROCESSING		
Antenna	= ±8°	σ_{ANT} = 4.619°
RF calibration network	= ±3°	σ_{CAL} = 1.732°
IF limiter	= ±3°	σ_{LIM} = 1.732°
		Root-Sum-Square = 5.228°
DIGITAL PROCESSING		
Antenna	= ±8°	σ_{ANT} = 4.619°
RF calibration network	= ±3°	σ_{CAL} = 1.732°
IF limiter	= ±3°	σ_{LIM} = 1.732°
Level detector (signal)	= ±1°	$\sigma_{LD\text{-}SIG}$ = 0.577°
Level detector (calibration)	= ±1°	$\sigma_{LD\text{-}CAL}$ = 0.577°
Quantizer, 7-bit (signal)	= ±1.406°	$\sigma_{Q\text{-}SIG}$ = 0.812°
Quantizer, 7-bit (calibration)	= ±1.406°	$\sigma_{Q\text{-}CAL}$ = 0.812°
		Root-Sum-Square = 5.415°

*"Strong-signal" conditions.
†Uniform distribution assumed.
Note: Present technology, wideband systems.

3.2 Probability of Ambiguity for Two-Integer Set Interferometers

The ambiguity constraints for the three-element interferometer configurations of Sec. 2.4 are

End-phase Left

$$|p(\Delta\varphi_1 - \Delta\varphi_3) - (p+q)(\Delta\varphi_1 - \Delta\varphi_2)| \gtrless \pi \tag{3-5a}$$

where

$$\Delta\varphi_1 - \Delta\varphi_3 \equiv \Delta\varphi_L, \quad \Delta\varphi_1 - \Delta\varphi_2 \equiv \Delta\varphi_S$$

$$\mathcal{R}_L = \frac{m}{n} = \frac{p+q}{p},$$

Midphase

$$|q(-\Delta\varphi_2 + \Delta\varphi_1) - p(\Delta\varphi_2 - \Delta\varphi_3)| \gtrless \pi \tag{3-5b}$$

where

$$-\Delta\varphi_2 + \Delta\varphi_1 \equiv \Delta\varphi_L, \quad \Delta\varphi_2 - \Delta\varphi_3 \equiv \Delta\varphi_S$$

$$\mathcal{R}_M = \frac{m}{n} = \frac{p}{q},$$

End-phase Right

$$|q(\Delta\varphi_3 - \Delta\varphi_1) - (p+q)(\Delta\varphi_3 - \Delta\varphi_2)| \gtrless \pi \tag{3-5c}$$

where

$$\Delta\varphi_3 - \Delta\varphi_1 \equiv \Delta\varphi_L, \quad \Delta\varphi_3 - \Delta\varphi_2 \equiv \Delta\varphi_S$$

$$\mathcal{R}_R = \frac{m}{n} = \frac{p+q}{q}.$$

In Sec. 2.4, it was shown that Eq. (2-17a, b, and c), repeated above for convenience, are equivalent to a single ambiguity constraint

$$|q\Delta\varphi_1 - (p+q)\Delta\varphi_2 + p\Delta\varphi_3| \gtrless \pi. \tag{3-5d}$$

In this section, an expression for the probability of ambiguity of a generalized two-integer set interferometer will be derived, starting from Eq. (3-5a, b, and c) rather than from Eq. (3-5d), as could be readily accomplished. The motive for this indirect derivation is to focus attention on channel-*pair* errors and channel-*pair* error correlation coefficients. A formulation of the probability of ambiguity in terms of these parameters

which simplifies the derivation of an exact expression for the probability of ambiguity in four-element interferometers will be seen later (in Sec. 5).

Expressions for the channel-pair error correlation coefficient will be required. For two zero-mean random variables $\mathfrak{A}$ and $\mathfrak{B}$, the correlation coefficient between them is defined [18] by

$$\rho \equiv \frac{E\{\mathfrak{A}\mathfrak{B}\}}{\sigma_A \sigma_B}, \tag{3-6}$$

where $E[x]$ = expected value of x.

From Eq. (3-5a), for the end-phase left configuration, is derived

$$\begin{aligned} \rho_e &= \frac{E\{(\Delta\varphi_1 - \Delta\varphi_3)(\Delta\varphi_1 - \Delta\varphi_2)\}}{\sqrt{\sigma_1^2 + \sigma_3^2}\ \sqrt{\sigma_1^2 + \sigma_2^2}} \\ &= \frac{\sigma_1^2}{\sigma_L \sigma_S} \\ &= +0.5, \quad \text{all } \sigma_i \text{ equal.} \end{aligned} \tag{3-7}$$

Measurements on the joint statistics of σ_L and σ_S are necessary to define ρ_e; separate measurements of σ_L and σ_S in Eq. (3-7) are insufficient. For array design purposes, the assumption that

$$\sigma_1^2 = \sigma_2^2 = \sigma_3^2 = \frac{1}{2}\sigma_S^2 = \frac{1}{2}\sigma_L^2$$

is a reasonable one.

It is readily shown that $\rho_e = +0.5$, all σ_i equal, for the end-phase right configuration as well.

From Eq. (3-5b), for the midphase configuration, is derived

$$\begin{aligned} \rho_m &\equiv \frac{E\{(-\Delta\varphi_2 + \Delta\varphi_1)(\Delta\varphi_2 - \Delta\varphi_3)\}}{\sqrt{\sigma_2^2 + \sigma_1^2}\ \sqrt{\sigma_2^2 + \sigma_3^2}} \\ &= \frac{-\sigma_2^2}{\sigma_L \sigma_S} \\ &= -0.5, \quad \text{all } \sigma_i \text{ equal.} \end{aligned} \tag{3-8}$$

The variance of the left side of Eq. (3-5a), the end-phase left configuration, is

$$\sigma_e^2 = p^2(\sigma_1^2 + \sigma_3^2) - 2p(p+q)E\{(\Delta\varphi_1 - \Delta\varphi_3)(\Delta\varphi_1 - \Delta\varphi_2)\} + (p+q)^2(\sigma_1^2 + \sigma_2^2) . \quad (3\text{-}9)$$

Substituting $p = n$, $p + q = m$, $\sigma_1^2 + \sigma_3^2 = \sigma_L^2$, and $\sigma_1^2 + \sigma_2^2 = \sigma_S^2$ yields

$$\sigma_e^2 = m^2\sigma_S^2 - 2mnE\{(\Delta\varphi_1 - \Delta\varphi_3)(\Delta\varphi_1 - \Delta\varphi_2)\} + n^2\sigma_L^2 . \quad (3\text{-}10)$$

Since, from Eq. (3-7)

$$E\{(\Delta\varphi_1 - \Delta\varphi_3)(\Delta\varphi_1 - \Delta\varphi_2)\} = \sigma_1^2 = \rho_e\sigma_L\sigma_S ,$$

Eq. (3-10) becomes, for the end-phase configuration,

$$\sigma_e^2 = m^2\sigma_S^2 - 2\rho_e mn\sigma_L\sigma_S + n^2\sigma_L^2 , \quad (3\text{-}11)$$

where

$m = p + q$, σ_L = channel-pair phase error standard deviation, channels 1 and 3
$n = p$, σ_S = channel-pair phase error standard deviation, channels 1 and 2
$\rho_e = \sigma_1^2/\sigma_L\sigma_S$
$= +0.5$, all σ_i equal.

The variance of the left side of Eq. (3-5b), the midphase configuration, is

$$\sigma_m^2 \stackrel{f}{=} q^2(\sigma_2^2 + \sigma_1^2) - 2pqE\{(-\Delta\varphi_2 + \Delta\varphi_1)(\Delta\varphi_2 - \Delta\varphi_3)\} + p^2(\sigma_2^2 + \sigma_3^2) . \quad (3\text{-}12)$$

Substituting $p = m$, $q = n$, $\sigma_1^2 + \sigma_2^2 = \sigma_L^2$, and $\sigma_2^2 + \sigma_3^2 = \sigma_S^2$ yields

$$\sigma_m^2 = m^2\sigma_S^2 - 2mnE\{(-\Delta\varphi_2 + \Delta\varphi_1)(\Delta\varphi_2 - \Delta\varphi_3)\} + n^2\sigma_L . \quad (3\text{-}13)$$

Since, from Eq. (3-8), we have

$$E\{(-\Delta\varphi_2 + \Delta\varphi_1)(\Delta\varphi_2 - \Delta\varphi_3)\} = -\sigma_2^2 = \rho_m\sigma_L\sigma_S ,$$

Eq. (3-13) becomes, for the midphase configuration,

$$\sigma_m^2 = m^2\sigma_S^2 - 2\rho_m mn\sigma_L\sigma_S + n^2\sigma_L^2 , \quad (3\text{-}14)$$

where

$m = p$, σ_L = channel-pair phase error standard deviation, channels 1 and 2

$n = q$, σ_S = channel-pair phase error standard deviation, channels 2 and 3

$$\rho_m = \frac{-\sigma_2^2}{\sigma_L \sigma_S}$$

$$= -0.5, \text{ all } \sigma_i \text{ equal.}$$

Equations (3-11) and (3-14) have the same functional form; hence a single relation suffices provided m, n, σ_L, σ_S, and ρ (ρ_e or ρ_m) are properly defined. In fact, if we refer to Eq. (2-17d), Sec. 2.4, for the four-element independent interferometer, it is apparent that

$$\rho_i = \frac{E\{(\Delta\varphi_1 - \Delta\varphi_2)(\Delta\varphi_3 - \Delta\varphi_4)\}}{\sigma_L \sigma_S} = 0 , \tag{3-15a}$$

and

$$\sigma_L^2 = \sigma_1^2 + \sigma_2^2 , \quad \sigma_S^2 = \sigma_3^2 + \sigma_4^2 . \tag{3-15b}$$

Thus, the variance of the ambiguity variable is

$$\sigma_\phi^2 = m^2\sigma_S^2 - 2\rho mn\sigma_L\sigma_S + n^2\sigma_L^2 , \tag{3-16}$$

where

$\rho = +0.5$, end-phase
$= 0$, independent
$= -0.5$, midphase

} all σ_i equal.

An alternate expression for σ_ϕ^2 is

$$\sigma_\phi^2 = \sigma_{\text{CH-PR}}^2[(m\Sigma)^2 - 2\rho m\Sigma n\Lambda + (n\Lambda)^2] , \tag{3-17}$$

where

$\sigma_{\text{CH-PR}}$ = a nominal, or design, value for channel-pair rms phase error

$\Lambda \equiv \sigma_L/\sigma_{\text{CH-PR}}$

$\Sigma \equiv \sigma_S/\sigma_{\text{CH-PR}}$.

For design purposes, all σ_i are usually specified equal, implying that $\sigma_L = \sigma_S = \sigma_{\text{CH-PR}} = \sqrt{2}\,\sigma_i$. Thus $\Sigma = \Lambda =$ unity, and a simplified form of σ_ϕ^2 is

$$\sigma_\phi^2 = \sigma_{\text{CH-PR}}^2[m^2 - 2\rho mn + n^2] . \tag{3-18}$$

The probability of correct resolution, that is, the probability that the left sides of Eq. (3-5a, b, or c) will not exceed $\pm\pi$ rad, is

$$p_c = \frac{1}{\sqrt{2\pi}} \int_{-\pi/\sigma_\phi}^{\pi/\sigma_\phi} \exp(-t'^2/2)\, dt' . \tag{3-19}$$

Setting $t' = \sqrt{2}\, t$, $dt' = \sqrt{2}\, dt$ and changing the limits of integration gives

$$p_c = \frac{2}{\sqrt{\pi}} \int_0^{\pi/\sqrt{2}\,\sigma_\phi} \exp(-t^2)\, dt$$

$$\equiv \operatorname{erf}\left(\frac{\pi}{\sqrt{2}\,\sigma_\phi}\right). \tag{3-20}$$

Thus, the probability of ambiguity (the probability that the left sides of Eqs. (3-5a, b, or c) will exceed $\pm\pi$ rad) is

$$p_a = 1 - p_c$$

$$\equiv \operatorname{erfc}\left(\frac{\pi}{\sqrt{2}\,\sigma_\phi}\right), \tag{3-21}$$

where

$$\sigma_\phi = \sigma_{\text{CH-PR}}[(m\Sigma)^2 - 2\rho m\Sigma n\Lambda + (n\Lambda)^2]^{1/2} ,$$

m = integer associated with large spacing ($m \geq n$),

n = integer associated with small spacing,

σ_L, σ_S = standard deviations of channel-pair phase errors for large and small spacings, respectively,

$\rho = E\{\delta\delta\}/\sigma_L\sigma_S$, correlation coefficient between large and small channel-pair phase errors,

$\sigma_{\text{CH-PR}}$ = design, or nominal, value for channel-pair phase error,

$\Sigma = \sigma_S/\sigma_{\text{CH-PR}}$, $\Lambda = \sigma_L/\sigma_{\text{CH-PR}}$.

An asymptotic expression for erfc (t) is [19]

$$\operatorname{erfc}(t) \approx \frac{e^{-t^2}}{t\sqrt{\pi}} \left\{ 1 - \frac{1}{2t^2} + \frac{1\cdot 3}{(2t^2)^2} - \frac{1\cdot 3\cdot 5}{(2t^2)^3} + \ldots \right\}. \tag{3-22}$$

If the first two terms above are utilized, p_a is bounded by

$$\sqrt{\frac{2}{\pi}}\,\frac{1}{\left(\frac{\pi}{\sigma_\phi}\right)}\,\exp\left(-\frac{\pi^2}{2\sigma_\phi^2}\right)\left[1-\frac{1}{\left(\frac{\pi}{\sigma_\phi}\right)^2}\right] < p_a < \sqrt{\frac{2}{\pi}}\,\frac{1}{\left(\frac{\pi}{\sigma_\phi}\right)}\,\exp\left(-\frac{\pi^2}{2\sigma_\phi^2}\right). \qquad (3\text{-}23)$$

3.3 Optimum Array Ratios in Three-Element Interferometers

The argument of the complementary error function defining probability of ambiguity Eq. (3-21), with the simplified form of σ_ϕ, is

$$\frac{\pi}{\sigma_{\text{CH-PR}}\sqrt{m^2 - 2\rho mn + n^2}}.$$

For three-element arrays of length $\ell = p + q$ (in half-wavelengths at the operating frequency), regardless of which element is phase reference, the quadratic form within the radical in the denominator of the expression above can be written as

$$p^2 + pq + q^2, \quad p \geq q$$

where

p = integer related to the channel 1—channel 2 baseline,

q = integer related to the channel 2—channel 3 baseline.

To determine which sets of integers p, q are optimum—in the sense of providing arrays having the lowest probability of ambiguity for given ℓ—subject to the constraint $p + q$ = constant = ℓ, it suffices to determine

$$\frac{\partial}{\partial p}\left[p^2 + p(\ell - p) + (\ell - p)^2\right] = 0,$$

which reduces to

$$\frac{\partial}{\partial p}\left[p^2 - \ell p + \ell^2\right] = 0.$$

For no restrictions on p and q, the solution is, of course, $p = q = \ell/2$. To form an allowable interferometer ratio $\mathcal{R}_m = p/q$ or q/p, however, the two parameters must be relatively prime integers.

Thus $p = q$ (=1) only for $\ell = 2$. The optimum p, q for $\ell = 2, 3, 4$ are

$\ell = 2$;	$p = 1$,	$q = 1$	
$= 3$;	$= 2$,	$= 1$	
$= 4$;	$= 3$,	$= 1$	($p = q = 2$ is not allowable since it is a degenerate form of $p = q = 1$).

For $\ell = 5$ through 10, the optimum sets of p, q are

$$
\begin{aligned}
\ell = \ 5; \quad & p = 3, \quad q = 2 \\
= \ 6; \quad & = 5, \quad = 1 \\
= \ 7; \quad & = 4, \quad = 3 \\
= \ 8; \quad & = 5, \quad = 3 \\
= \ 9; \quad & = 5, \quad = 4 \\
= 10; \quad & = 7, \quad = 3.
\end{aligned}
$$

Functions generated by induction for p and q, given $\ell = p + q$, are

$$
\begin{aligned}
p_{i,-1} &= 2i, & q_{i,-1} &= 2i - 1; & \ell_{i,-1} &= 4i - 1 \\
p_{i,0} &= 2i + 1, & q_{i,0} &= 2i - 1; & \ell_{i,0} &= 4i \\
p_{i,1} &= 2i + 1, & q_{i,1} &= 2i; & \ell_{i,1} &= 4i + 1
\end{aligned}
$$

and

$$
p_{i,2} = 2i + 3, \quad q_{i,2} = 2i - 1; \quad \ell_{i,2} = 4i + 2. \tag{3-24}
$$

Table 3-3 lists the optimum p, q and associated end-phase and midphase array ratios vs overall array length $\ell (2 \leq \ell \leq 26)$.

It can be readily deduced from the argument of the probability of ambiguity function for independent arrays,

$$
\frac{\pi}{\sigma_{\text{CH-PR}} \sqrt{m^2 + n^2}},
$$

that the optimum p, q vs array length are just

$$
\left.
\begin{aligned}
m &= p = \ell \\
n &= q = 1
\end{aligned}
\right\} \text{ independent.}
$$

Table 3-4 lists all possible p, q sets (including the optimum set defined above) for three-element arrays of length $\ell = 2$ to 26. It is interesting to note that the ratio entries for p fixed have their counterparts in a table of Farey sequences (arrays of rational fractions between 0 and 1) in number theory as shown by Niven and Zuckerman [20].

3.4 Tabulated Probability of Ambiguity for Three- and Four-Element Two-Integer Set Arrays

Based on Eq. (3-21) from Sec. 3.2, p_a for three-element arrays are listed in Table 3-5 for $\sigma_{\text{CH-PR}} = 5°$, 10°, 12°, 15° and 20°. Table 3-6 provides the same information for four-element (independent) arrays.

Table 3-3—Optimum Midphase and End-phase Ratios vs Array Length ℓ ($2 \leq \ell \leq 26$) for Three-element Interferometers

Array Length, ℓ	$\mathcal{R}_m = \frac{p}{q}$	$\mathcal{R}_E = \frac{p+q}{q}, \frac{p+q}{p}$
2	1:1	2:1 , 2:1
3	2:1	3:1 , 3:2
4	3:1	4:1 , 4:3
5	3:2	5:2 , 5:3
6	5:1	6:1 , 6:5
7	4:3	7:3 , 7:4
8	5:3	8:3 , 8:5
9	5:4	9:4 , 9:5
10	7:3	10:3 , 10:7
11	6:5	11:5 , 11:6
12	7:5	12:5 , 12:7
13	7:6	13:6 , 13:7
14	9:5	14:5 , 14:9
15	8:7	15:7 , 15:8
16	9:7	16:7 , 16:9
17	9:8	17:8 , 17:9
18	11:7	18:7 , 18:11
19	10:9	19:9 , 19:10
20	11:9	20:9 , 20:11
21	11:10	21:10 , 21:11
22	13:9	22:9 , 22:13
23	12:11	23:11 , 23:12
24	13:11	24:11 , 24:13
25	13:12	25:12 , 25:13
26	15:11	26:11 , 26:15

Table 3-4—Allowable p:q vs $\ell = p + q$ $(2 \leqslant \ell \leqslant 26)$ in Three-element Arrays

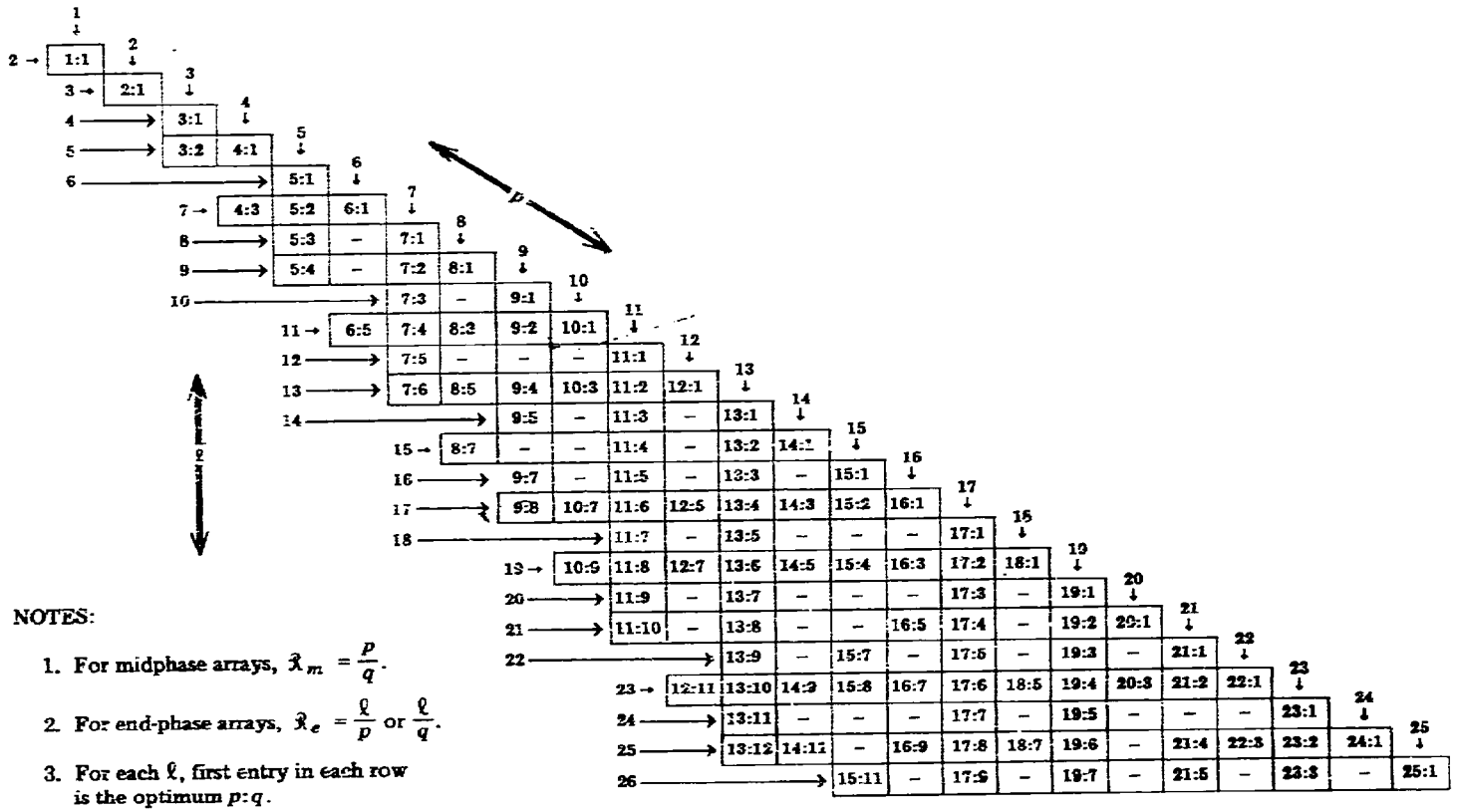

ℓ	1	2	3	4	5	6	7	8	9	10	11	12	13	14	15	16	17	18	19	20	21	22	23	24	25
2	1:1																								
3	2:1																								
4	3:1																								
5	3:2	4:1																							
6	5:1																								
7	4:3	5:2	6:1																						
8	5:3	–	7:1																						
9	5:4	–	7:2	8:1																					
10	7:3	–	9:1																						
11	6:5	7:4	8:2	9:2	10:1																				
12	7:5	–	–	–	11:1																				
13	7:6	8:5	9:4	10:3	11:2	12:1																			
14	9:5	–	11:3	–	13:1																				
15	8:7	–	–	11:4	–	13:2	14:1																		
16	9:7	–	11:5	–	13:3	–	15:1																		
17	9:8	10:7	11:6	12:5	13:4	14:3	15:2	16:1																	
18	11:7	–	13:5	–	–	–	17:1																		
19	10:9	11:8	12:7	13:6	14:5	15:4	16:3	17:2	18:1																
20	11:9	–	13:7	–	–	–	17:3	–	19:1																
21	11:10	–	13:8	–	–	16:5	17:4	–	19:2	20:1															
22	13:9	–	15:7	–	17:5	–	19:3	–	21:1																
23	12:11	13:10	14:9	15:8	16:7	17:6	18:5	19:4	20:3	21:2	22:1														
24	13:11	–	–	–	17:7	–	19:5	–	–	–	23:1														
25	13:12	14:11	–	16:9	17:8	18:7	19:6	–	21:4	22:3	23:2	24:1													
26	15:11	–	17:9	–	19:7	–	21:5	–	23:3	–	25:1														

NOTES:

1. For midphase arrays, $\Re_m = \frac{p}{q}$.
2. For end-phase arrays, $\Re_e = \frac{\ell}{p}$ or $\frac{\ell}{q}$.
3. For each ℓ, first entry in each row is the optimum p:q.

Table 3-5—Probability of Ambiguity vs Channel-pair Phase Error for Three-element Interferometers

Array Length, ℓ	$\mathcal{R}_M = \frac{p}{q}$	$\mathcal{R}_E = \frac{p+q}{q}, \frac{p+q}{p}$	Probability of Ambiguity for Given $\sigma_{CH\text{-}PR}$				
			$\sigma = 5°$	$\sigma = 10°$	$\sigma = 12°$	$\sigma = 15°$	$\sigma = 20°$
3	2:1*	3:1 , 3:2	–†	–	<1E-7	<6E-6	6.70E-4
4	3:1*	4:1 , 4:3	–	<6E-7	3.18E-5	8.74E-4	0.0126
5	3:2*	5:2 , 5:3	–	3.63E-5	5.79E-4	5.91E-3	0.0389
	4:1	5:1 , 5:4	–	8.57E-5	1.06E-3	8.83E-3	0.0495
6	5:1*	6:1 , 6:5	–	1.23E-3	7.06E-3	0.0311	0.106
7	4:3*	7:3 , 7:4	<1E-8	3.09E-3	0.0137	0.0485	0.139
	5:2	7:2 , 7:5	<1E-8	3.95E-3	0.0163	0.0547	0.150
	6:1	7:1 , 7:6	<1E-7	6.05E-3	0.0222	0.0673	0.170
8	5:3*	8:3 , 8:5	<3E-7	0.0101	0.0321	0.0865	0.199
	7:1	8:1 , 8:7	<2E-6	0.0171	0.0469	0.112	0.233
9	5:4*	9:4 , 9:5	4E-6	0.0212	0.0548	0.124	0.249
	7:2	9:2 , 9:7	1.1E-5	0.0279	0.0669	0.143	0.271
	8:1	9:1 , 9:8	2.5E-5	0.0351	0.0791	0.160	0.292
10	7:3*	10:3 , 10:7	5.1E-5	0.0429	0.0915	0.177	0.311
	9:1	10:1 , 10:9	1.61E-4	0.0592	0.116	0.208	0.345
11	6:5*	11:5 , 11:6	1.61E-4	0.0592	0.116	0.208	0.345
	7:4	11:4 , 11:7	1.89E-4	0.0620	0.120	0.213	0.351
	8:3	11:3 , 11:8	2.57E-4	0.0676	0.128	0.223	0.361
	9:2	11:2 , 11:9	3.89E-4	0.0761	0.139	0.237	0.375
	10:1	11:1 , 11:10	6.33E-4	0.0875	0.154	0.255	0.393
12	7:5*	12:5 , 12:7	5.64E-4	0.0847	0.151	0.250	0.389
	11:1	12:1 , 12:11	1.80E-3	0.119	0.193	0.298	0.435

*→ optimum ratio for given ℓ.
† – = p_a < 1E-10.

Table 3-6--Probability of Ambiguity vs Channel-pair Phase Error for Two-integer Set Four-element Interferometers

Maximum Spacing, ℓ	$\mathcal{R}_I = \frac{p}{q}$	Probability of Ambiguity for Given $\sigma_{CH\text{-}PR}$				
		$\sigma = 5°$	$\sigma = 10°$	$\sigma = 12°$	$\sigma = 15°$	$\sigma = 20°$
3	3:1	-*	<1E-7	2E-6	1.48E-4	4.43E-3
4	4:1	-	1.3E-5	2.75E-4	3.61E-3	0.0290
5	5:1	-	4.15E-4	3.26E-3	0.0186	0.0776
6	6:1	<1E-8	3.08E-3	0.0137	0.0485	0.139
7	7:1	<1E-6	0.0109	0.0339	0.0897	0.203
8	8:1	8E-6	0.0256	0.0628	0.137	0.264
9	9:1	7.0E-5	0.0468	0.0976	0.185	0.320
10	10:1	3.41E-4	0.0733	0.136	0.232	0.371
11	11:1	1.12E-3	0.103	0.174	0.277	0.415
12	12:1	2.79E-3	0.135	0.213	0.319	0.455

*- = p_a < 1E-10.

As mentioned previously in Sec. 3.2, $\sigma_{CH\text{-}PR}$ in the range 10° to 12° is typical of present technology for wideband microwave systems--2 to 3 octaves of frequency coverage--with lower and upper absolute limits of 500 MHz and 18 GHz. $\sigma_{CH\text{-}PR}$ on the order of 5° typifies the channel-pair errors in the same category of systems utilizing RF calibration. The probability of ambiguity for $\sigma_{CH\text{-}PR}$ = 15° and 20° has been included as an admittedly crude estimate of the performance that might be experienced with an interferometer operating in a severe multipath situation.

A p_a criterion of 0.01 to 1 percent maximum ambiguity is often set by designers of systems to be used for location by triangulation with multiple DF cuts. As Fig. 3-2 shows, with $\sigma_{CH\text{-}PR}$ in the range 10° to 12°, the maximum allowable array length is between 8 to 6 half-wavelengths.

The angular accuracies of systems with baselines this short may be unacceptable. This is the basic reason for synthesizing and employing arrays with additional elements. In Sec. 5 it will be shown that the optimum four-element array of length ℓ = 25 half-wavelengths has p_a = 0.115 percent for $\sigma_{CH\text{-}PR}$ = 12°, and p_a = 1.17 percent for $\sigma_{CH\text{-}PR}$ = 15°.

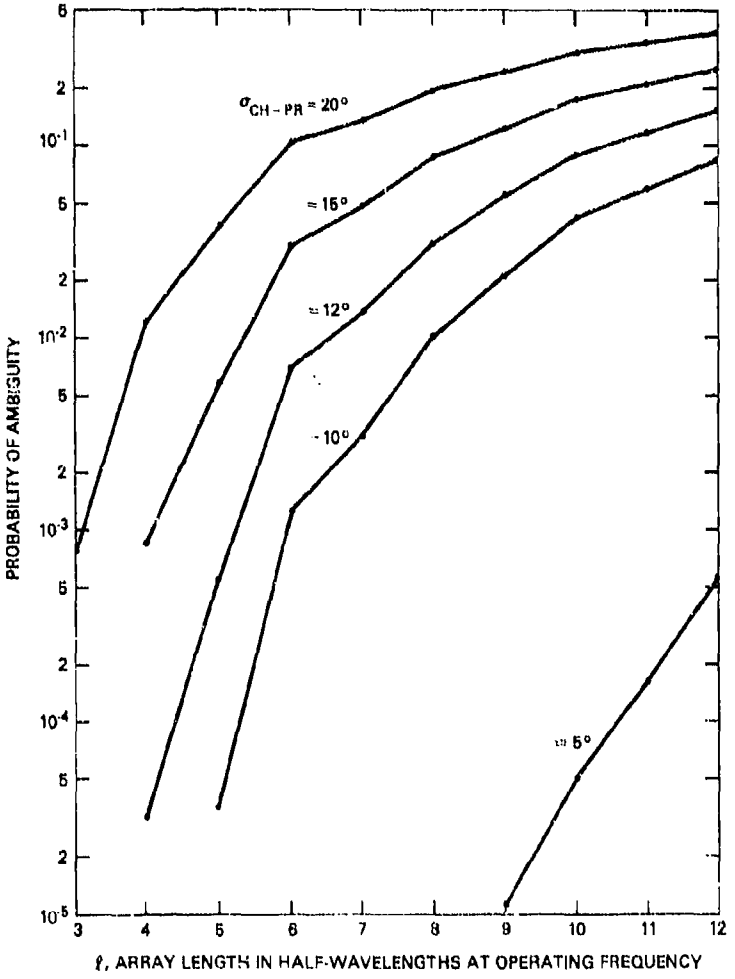

Fig. 3-2—Probability of ambiguity vs σ_{CH-PR} for optimum three-element interferometers

4.0 FUNDAMENTALS OF FOUR-ELEMENT THREE-INTEGER SET INTERFEROMETERS

The theory of three-element interferometers in fairly well known (disregarding some minor inconsistencies in the work referenced in Sec. 3.0). There does not appear to be any corresponding body of theory available for four-element arrays, especially with regard to the question concerning the existence of an optimum four-element array configuration. With an understanding of the material presented in this section, the ESM designer will be prepared for the exposition of the array synthesis techniques of Sec. 5.0, and he will be able to apply them without difficulty.

A four-element interferometer can be characterized by 4 antenna/receiver channels, $4 - 1 = 3$ available channel-pair phase differences (necessary and sufficient for ambiguity resolution of the overall array), and $4 - 2 = 2$ subarrays formed by channels considered three at a time. Section 4.0 introduces several four-element array configurations (some of which are not optimum) which have been widely used in the past. These configurations are compared mainly on the basis of how efficiently the signal processing and mathematical operations needed in ambiguity resolution can be mechanized.

A discussion of resolvable and unresolvable ambiguities in the two three-element subarrays that constitute a four-element array emphasizes that there is no need for either of the two subarrays to be nonredundant. That is, there is no requirement that either of the subarrays be capable of unambiguous operation as a distinct three-element array—as long as the three spacing integers defining the overall array are relatively prime.

Each subarray is characterized by a subarray ratio $\mathcal{R}_i = m_i/n_i$. One member of the subarray ratio $\mathcal{R}_1$ (either m_1 or n_1) contains a factor common to one member of subarray ratio $\mathcal{R}_2$ (either m_2 or n_2), dependent on the overall array configuration. This highest common factor α is introduced, and the manner in which the ambiguity tolerance of subarray 2 is increased because of this factor α is fully explored.

The section closes with a development on canonical array configurations in four-element arrays. It is shown that the cascaded end-phase configuration of four-element interferometers is optimum from considerations of efficiency of hardware usage and probability of ambiguity. This is believed to be a new result, and it was obtained without recourse to the analytical artifice of a fictitious off-axis fifth channel used by Hanson [21].

4.1 Three-Integer Set Interferometers

Interferometers whose performance could be specified as a function of the two spacing integers p and q were classified in Sec. 2.2 according to which channel was designated the phase reference. For arrays formed with the number of channels $n = 4$ and $n = 3$, classification can be done on the basis of the channel (or channels) used as phase reference. The number of possible array configurations increases rapidly with n. It will be shown later (in Sec. 4.4) that in four-element interferometers, the probability of ambiguity is dependent on the *array configuration* as well as on array spacing integers p, q, and r—in contrast to three-element interferometers.

Figure 4-1 illustrates several configurations possible in four-element arrays. Parameters for these arrays of interest to a system designer are given in Table 4-1.

One array comparison parameter is the number of phase comparisons utilized in resolving the overall array ambiguities. The number of these ambiguities is $\ell = p + q + r$, for θ_a within $-90°$ to $+90°$; and p, q, and r represent the element spacings in half-wavelengths at the operating frequency. The minimum possible number of these comparisons is obviously $(n - 1)$, since the use of less than $(n - 1)$ phase comparisons implies that the phase information from one or more channels has been discarded. The cascaded midphase array requires four comparisons in resolving $p + q + r = \ell$ ambiguities. All of the other array configurations require $(n - 1) = 3$ comparisons.

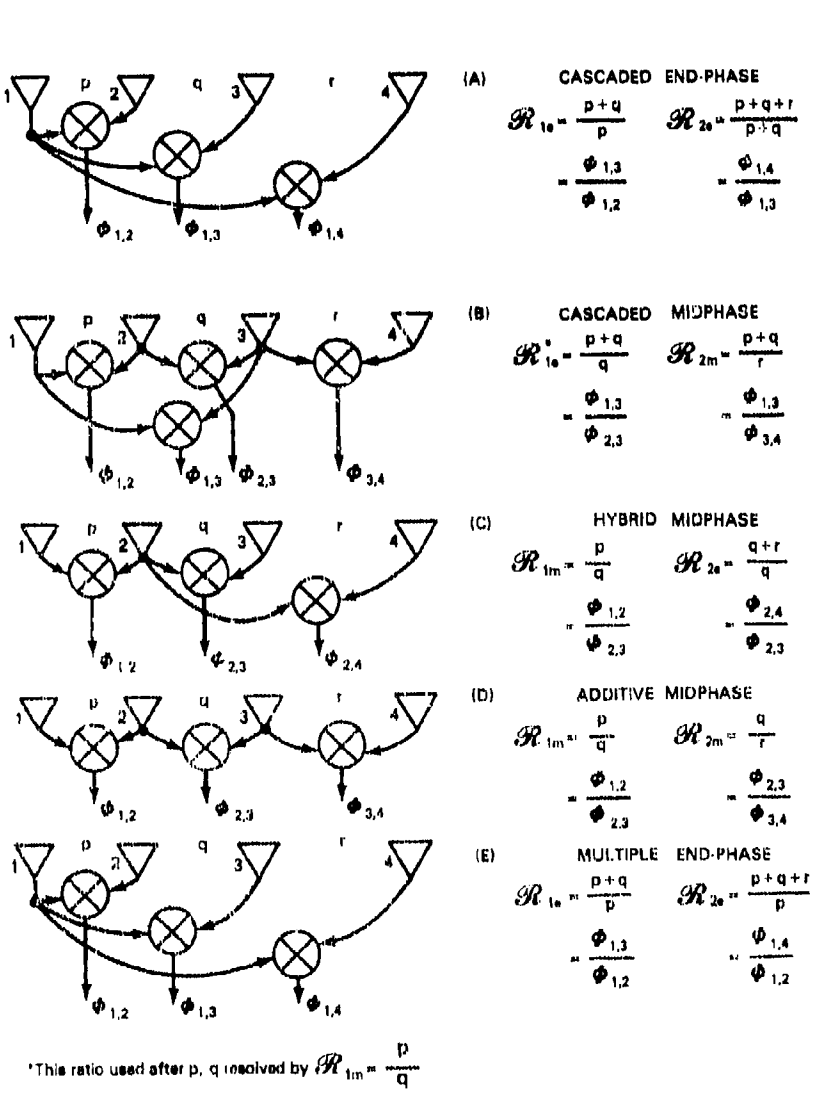

Fig. 4-1 — Various configurations for four-element arrays

Table 4-1—Comparison Parameters for Various Four-element Arrays

Array Type	Illustrated in Figure Number	Subarray Ratios (for ambiguity resolution)		Common Spacing	Number of Phase References	Number of Phase Comparisons	Is $(p + q + r)$ Directly Resolved?
		Ratio $\mathfrak{R}_1$	Ratio $\mathfrak{R}_2$				
Cascaded end-phase	4-1(a)	$\mathfrak{R}_{1e} = \frac{p+q}{p}$	$\mathfrak{R}_{2e} = \frac{p+q+r}{p+q}$	$p + q$	1	3	Yes
Cascaded midphase	4-1(b)	$^*\mathfrak{R}_{1e} = \frac{p+q}{q}$	$\mathfrak{R}_{2m} = \frac{p+q}{r}$	$p + q$	2	4	No
Hybrid midphase	4-1(c)	$\mathfrak{R}_{1m} = \frac{p}{q}$	$\mathfrak{R}_{2e} = \frac{q+r}{q}$	q	1	3	No
Additive midphase	4-1(d)	$\mathfrak{R}_{1m} = \frac{p}{q}$	$\mathfrak{R}_{2m} = \frac{q}{r}$	q	2	3	No
Multiple end-phase	4-1(e)	$\mathfrak{R}_{1e} = \frac{p+q}{p}$	$\mathfrak{R}_{2e} = \frac{p+q+r}{p}$	p	1	3	Yes

*This ratio is used after p, q are resolved by $\mathfrak{R}_{1m} = p/q$.

Note: For the "infinite-resolution" phase-measurement systems considered here, implementation of other comparisons in addition to some minimum set is easily accomplished. Thus, the phase difference $\Phi_{1,3}$ is equal (formally) to $\Phi_{1,2} + \Phi_{2,3}$, including any errors. In quantized-phase systems, the direct representation of $\Phi_{1,3}$ may differ from $\Phi_{1,3}$ obtained by summing quantized representations of $\Phi_{1,2}$ and $\Phi_{2,3}$. Hence, depending on the degree of quantizing implemented, the system designer might be advised to obtain $\Phi_{1,3}$ directly by use of the additional phase comparator.

A second array-configuration comparison parameter is the number of phase references needed to implement a particular array. The number of high-level input signals that must be provided is equal to the number of phase references. Minimizing this number is desirable, since the analog phase comparators in widespread use in present wideband receiving systems usually require a drive level on one of the input ports to be at least 10 dB stronger than the other to facilitate accurate recovery of $\sin\varphi$ and $\cos\varphi$, the quadrature components defining phase difference.

Another array-configuration comparison parameter is whether or not the $\ell = p + q + r$ ambiguities associated with the overall array length are resolved directly as a consequence of the ambiguity-resolution process. If not, additional operations and calculations will be needed. Table 4-1 shows, for $n = 4$, that only the cascaded end-phase and multiple end-phase array configurations meet this criterion.

A final array-configuration comparison parameter is the subarray spacing length common to each of the two ratios characterizing the arrays shown in Fig. 4-1. The subarray spacing length common to the two ratios influences the order of the ratio. An example is a comparison between the midphase configuration and the cascaded end-phase configuration for $p = 3$, $q = 1$, and $r = 7$ half-wavelengths.

Midphase

$$\mathcal{R}_{1m} = \frac{p}{q} = \frac{3}{1}$$

$$\mathcal{R}_{2m} = \frac{q}{r} = \frac{1}{7}$$

Common spacing: $q = 1$,

Cascaded End-phase

$$\mathcal{R}_{1e} = \frac{p + q}{p} = \frac{4}{3}$$

$$\mathcal{R}_{2e} = \frac{p + q + r}{p + q} = \frac{11}{4}$$

Common spacing: $p + q = 4$.

Previous analyses into the theory of multiple-element ambiguity resolution have proceeded on the assumption that composite arrays having low probability of ambiguity could only be achieved by combining subarrays of low order. Thus, inordinate interest has been placed on the hybrid midphase and additive midphase configurations. It will be shown

later in this section that the cascaded end-phase and cascaded midphase configurations exhibit the lowest probability of ambiguity for given p, q, and r because they have the largest common spacing $p + q$, as the arrays are configured in Fig. 4-1. It will also be shown that if the subarrays are redefined properly, all array configurations in Fig. 4-1 are equivalent except the multiple end-phase configuration. This is a new result in the theory of four-element interferometers.

In summary, the four-element cascaded end-phase configuration

- Employs the minimum possible number of phase comparisons—3
- Requires the smallest number of phase references—1
- Resolves the overall length $p + q + r = \ell$ directly as a consequence of the ambiguity resolution process
- Exhibits the largest spacing common to the two subarrays constituting the overall array—$p + q$.

4.2 Resolvable and Unresolvable Ambiguities in Subarrays of Three Elements

In this section, the distinction between resolvable and unresolvable ambiguities in subarrays will be defined. The material will be useful in understanding the discussion on ambiguity constraints in the section following.

For a four-element cascaded end-phase array, as shown in Table 4-1, the two subarrays are defined by

$$\Re_{1e} = \frac{p + q}{p} = \frac{m_1}{n_1} \tag{4-1a}$$

and

$$\Re_{2e} = \frac{p + q + r}{p + q} = \frac{m_2}{n_2}. \tag{4-1b}$$

Analogous to the requirements for an end-phase three-element interferometer, each of the numbers m_i and n_i ($i = 1, 2$) associated with the two subarrays must meet the criterion for a realizable interferometer. That is, m_i and n_i must be relatively prime integers. There is a corresponding restriction that the spacing integers p, $p + q$, and $p + q + r$ be relatively prime, as will be shown in the next section on ambiguity constraints.

As an example, consider the cascaded end-phase array defined by $p = 3$, $q = 3$, and $r = 10$ half-wavelengths at the operating frequency. The subarray parameters are

Subarray 1

$$\frac{p + q}{p} = \frac{3 + 3}{3} = \frac{6}{3}; \quad \Re_{1e} = \frac{m_1}{n_1} = \frac{2}{1},$$

Subarray 2

$$\frac{p+q+r}{p+q} = \frac{3+3+10}{3+3} = \frac{16}{6}; \qquad \mathcal{R}_{2e} = \frac{m_2}{n_2} = \frac{8}{3}.$$

The individual three-element interferometers are respectively "three-times ambiguous" $[(p+q)/m_1 = p/n_1 = 3]$, and "two-times ambiguous" $[(p+q+r)/m_2 = (p+q)/n_2 = 2]$. The overall array, as well as the individual subarrays, can be resolved, however, because the four-element array was synthesized from two realizable ratios. An equivalent way of stating this is to say that a four-element array is resolvable provided at least two of the three spacing integers are relatively prime. Thus, the array formed by $p = 3$, $q = 3$, $r = 9$ is not resolvable, whereas the array formed by removing the common factor 3, $p' = 1$, $q' = 1$, $r' = 3$, resolvable.

In the above example involving subarray 1 with $p = q = 3$ half-wavelengths, there are $p + q = 6$ angles of arrival over a $-90°$ to $+90°$ field of view that will give rise to the same phase code $\varphi_{1,3\text{-available}} = \Phi_{1,3} \pmod{2\pi}$. This is, of course, a restatement of the principle that a three-element array of length $\ell = p + q$ (in half-wavelengths) cannot exceed m_1 $\lambda/2$ wavelengths; otherwise there will exist ambiguities beyond the capability of the channel-pair spaced p half-wavelengths to resolve.

Subarrays which have no unresolvable ambiguities over the field of view are called "unambiguous." Subarrays which exhibit one or more unresolvable ambiguities over the field of view are therefore called "ambiguous."

Table 4-2 lists all possible four-element arrays of length $\ell = p + q + r = 16$ half-wavelengths, with the associated subarray ratios $\mathcal{R}_{1e}$ and $\mathcal{R}_{2e}$ for the cascaded end-phase configuration (subject to an example constraint of $p = 3$). The purpose of the listing is to illustrate the conditions unambiguous and ambiguous.

The number of unresolvable ambiguities for each subarray are

$$\text{subarray 1} \quad A_1 = (p+q) - m_1 \tag{4-2a}$$

$$\text{subarray 2} \quad A_2 = (p+q+r) - m_2 . \tag{4-2b}$$

Of the entries in Table 4-2, only 4 out of 12 have both subarrays 1 and 2 unambiguous. It is stressed, however, that the usual impetus for implementing arrays of four or more elements is to achieve the higher angular resolution implied by larger overall spacings (with an acceptably low probability of ambiguity). Thus, the array designer is normally indifferent to employing angular estimates from any spacings except the overall array spacing ℓ. An exception to this statement occurs if all of the array spacings are used to form an estimate of the angle of arrival, e.g., as in perhaps maximum-likelihood processing of the electrical phases from the appropriate channel-pairs.

4.3 Ambiguity Constraints and Probability of Ambiguity for the Four-element Cascaded End-phase Array

Explicit relations for the ambiguity constraints in the cascaded end-phase configuration of a four-element array will be derived in this section. The derivations for the other array configurations given in Sec. 4.1 are similar.

Table 4-2—Parameters of Four-element Arrays of Length $\ell = p + q + r = 16$ (subject to the constraint $p = 3$)

Spacing Integers $p - q - r$	$\mathcal{R}_1 = (p+q):p$	$\mathcal{R}_2 = (p+q+r):(p+q)$	Number of Unresolvable Ambiguities, A_i in $\mathcal{R}_i$	
			A_1	A_2
3 - 2 - 11	5:3	16: 5	U	U
3 - 4 - 9	7:3	16: 7	U	U
3 - 8 - 5	11:3	16:11	U	U
3 - 10 - 3	13:3	16:13	U	U
3 - 1 - 12	4:3	4: 1	U	12
3 - 5 - 8	8:3	2: 1	U	14
3 - 7 - 6	10:3	8: 5	U	8
3 - 11 - 2	14:3	8: 7	U	8
3 - 6 - 7	3:1	16: 9	6	U
3 - 12 - 1	5:1	16:15	10	U
3 - 3 - 10	2:1	8: 3	4	8
3 - 9 - 4	4:1	4: 3	8	12

Notes:
1. $U \Rightarrow$ unambiguous (no unresolvable ambiguities).
2. A_1, number of unresolvable ambiguities $= (p+q) - m_1$, in $\mathcal{R}_1$.
3. A_2, number of unresolvable ambiguities $= (p+q+r) - m_2$, in $\mathcal{R}_2$.

It will be convenient to introduce expressions for the array spacings in terms of the subarray ratios $\mathcal{R}_{1e}$ and $\mathcal{R}_{2e}$.

Consider a four-element cascaded end-phase array (see Fig. 4-1a). The two subarray ratios, with the subscript e dropped for brevity, are

$$\mathcal{R}_1 = \frac{m_1}{n_1} = \frac{\alpha m_1'}{n_1} = \frac{p+q}{p}, \tag{4-3a}$$

and

$$\mathcal{R}_2 = \frac{m_2}{n_2} = \frac{m_2}{\alpha n_2'} = \frac{p+q+r}{p+q}, \tag{4-3b}$$

with α an integer introduced for generality, to account for possible common factors in m_1 and n_2 (common factors in n_1 and m_2 are irrelevant). Another ratio $\mathcal{R}_0$, the product of $\mathcal{R}_1$ and $\mathcal{R}_2$, may be defined as

$$\mathcal{R}_0 = \frac{m_1 m_2}{n_1 n_2} = \frac{\alpha m_1' m_2}{n_1 \alpha n_2'} = \frac{m_0}{n_0},$$

$$= \frac{p+q}{p}\,\frac{p+q+r}{p+q} = \frac{p+q+r}{p}. \tag{4-3c}$$

Identifying like terms in the denominators of the two forms for $\mathcal{R}_0$ provides

$$p = n_1 n_2' = \frac{n_1 n_2}{\alpha}. \tag{4-4}$$

Substituting this value for p into Eq. (4-3a) gives

$$\frac{p+q}{p} = \frac{\frac{n_1 n_2}{\alpha} + q}{\frac{n_1 n_2}{\alpha}} = \frac{m_1}{n_1},$$

and solving for q,

$$q = \frac{n_2}{\alpha}(m_1 - n_1). \tag{4-5}$$

Adding Eq. (4-4) to Eq. (4-5) gives

$$p + q = \frac{m_1 n_2}{\alpha}. \tag{4-6}$$

Substituting this value for $(p+q)$ into Eq. (4-3b) gives

$$\frac{p+q+r}{p+q} = \frac{\frac{m_1 n_2}{\alpha} + r}{m_1 n_2} = \frac{m_2}{n_2},$$

and solving for r,

$$r = \frac{m_1}{\alpha}(m_2 - n_2). \tag{4-7}$$

Summarizing, we have

$$\left.\begin{aligned} p &= \frac{n_1 n_2}{\alpha} \\ q &= \frac{n_2}{\alpha}(m_1 - n_1) \\ r &= \frac{m_1}{\alpha}(m_2 - n_2) \end{aligned}\right\} \quad \begin{aligned} \ell &= p + q + r \\ &= \frac{m_1 m_2}{\alpha}; \end{aligned} \tag{4-8}$$

where

$$\mathcal{R}_1 = \frac{m_1}{n_1} = \frac{p+q}{p}; \quad \mathcal{R}_2 = \frac{m_2}{n_2} = \frac{p+q+r}{p+q},$$

α = factor common to m_1 and n_2.

With the aid of subarray ambiguity diagrams, the ambiguity constraints for a four-element cascaded end-phase array will now be derived.

Figure 4-2 shows the subarray ambiguity diagrams for the array ratios $\mathcal{R}_1 = m_1/n_1 = 4{:}3$; $\mathcal{R}_2 = m_2/n_2 = 11{:}4$. Since $m_1 = n_2 = 4$, the common factor α in Eq. (4-8) is 4, and p, q, and r are given by

$$\left.\begin{aligned} p &= \frac{3\times 4}{4} = 3 \\ q &= \frac{4}{4}(4-3) = 1 \\ r &= \frac{4}{4}(11-4) = 7 \end{aligned}\right\} \quad \ell = p+q+r = \frac{4\times 11}{4} = 11.$$

The ambiguity diagram for subarray 2, unresolved by subarray 1, has ambiguity intercepts of

$$\Delta\varphi_{1,4\text{-AI}} = \frac{\pi}{n_2} = \frac{\pi}{4}(45^\circ),$$

$$\Delta\varphi_{1,3\text{-AI}} = \frac{\pi}{m_2} = \frac{\pi}{11}(16.36^\circ).$$

Similarly, the ambiguity diagram for subarray 1 has ambiguity intercepts of

$$\Delta\varphi_{1,3\text{-AI}} = \frac{\pi}{n_1} = \frac{\pi}{3}(60^\circ),$$

$$\Delta\varphi_{1,2\text{-AI}} = \frac{\pi}{m_1} = \frac{\pi}{4}(45^\circ).$$

It will be noted that the trajectories for subarray 1 are labelled with unprimed numerals *below* the trajectories of slope 4:3, whereas the primed numerals *above* the trajectories show parametrically the equivalent trajectory for subarray 2. This dual labelling reflects the fact that as θ_a varies from -90° to $+90^\circ$, the channel pair spaced $(p+q)$ half-wavelengths manifests $4\times 2\pi$ rad phase change, whereas the channel-pair spaced $(p+q+r)$ half-wavelengths manifests $11\times 2\pi$ rad phase change.

The spacing integers $p = 3$, $q = 1$, and $r = 7$ for this example have been chosen so that both subarray 1 and subarray 2 are unambiguous in the sense of the development of Sec. 4.2. That is, the appropriate processing of each of the subarray phase-comparator

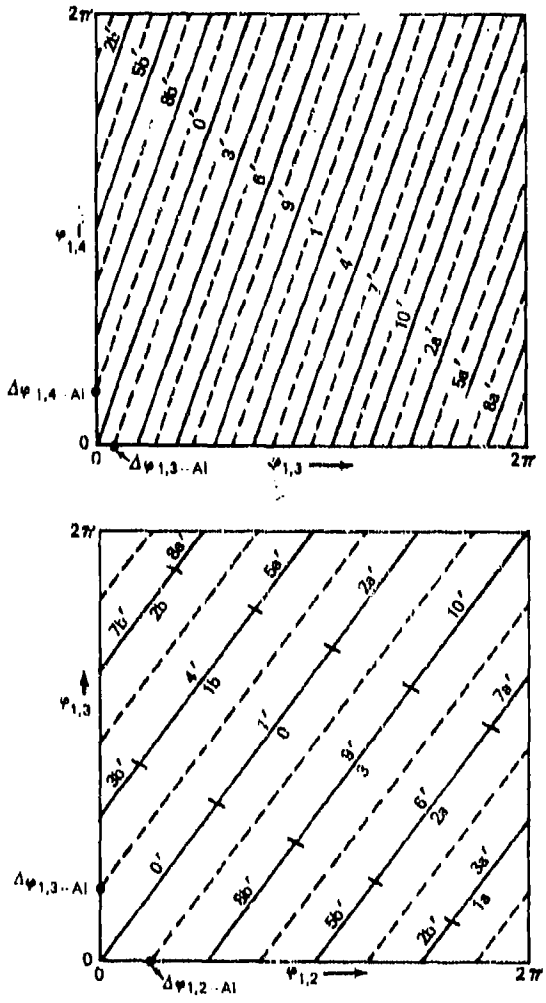

Fig. 4-2—Ambiguity diagrams for unresolved four-element interferometer ($\Re_1 = m_1:n_1 = 4:3 \oplus \Re_2 = m_2:n_2 = 11:4$)

outputs can provide a single (though inexact) estimate of θ_a for sufficiently small phase errors.

The channel-pair errors for the two subarrays are

Subarray 1

$$\Delta\varphi_{S_1} = \Delta\varphi_1 - \Delta\varphi_2 = \Delta\varphi_{1,2}$$

$$\Delta\varphi_{L_1} = \Delta\varphi_1 - \Delta\varphi_3 = \Delta\varphi_{1,3} . \tag{4-9a}$$

Subarray 2

$$\Delta\varphi_{S_2} = \Delta\varphi_1 - \Delta\varphi_3 = \Delta\varphi_{1,3}$$

$$\Delta\varphi_{L_2} = \Delta\varphi_1 - \Delta\varphi_4 = \Delta\varphi_{1,4} , \tag{4-9b}$$

where S_i, L_i ➡ small and large spacings for subarray i. For zero-mean channel phase errors, the associated standard deviations of channel-pair phase error are

Subarray 1

$$\sigma_{S_1} = [\sigma_1^2 + \sigma_2^2]^{1/2} = \sigma_{1,2}$$

$$\sigma_{L_1} = [\sigma_1^2 + \sigma_3^2]^{1/2} = \sigma_{1,3} , \tag{4-10a}$$

and

Subarray 2

$$\sigma_{S_2} = [\sigma_1^2 + \sigma_3^2]^{1/2} = \sigma_{1,3}$$

$$\sigma_{L_2} = [\sigma_1^2 + \sigma_4^2]^{1/2} = \sigma_{1,4} . \tag{4-10b}$$

For all $\sigma_{1,j} = \sigma_{\text{CH-PR}}$, $j = 2$ to 4, the ambiguity variable in Eq. (3-18) for each of the two subarrays is given by

$$\sigma_{\phi_i} = \sigma_{\text{CH-PR}}[m_i^2 - 2\rho_e m_i n_i + n_i^2]^{1/2}$$

$$= \sigma_{\text{CH-PR}}[m_i^2 - m_i n_i + n_i^2]^{1/2} , \tag{4-11}$$

since $\rho_e = +0.5$ for end-phase arrays. Consequently,

$$\sigma_{\phi_1} = \sigma_{\text{CH-PR}} \sqrt{4^2 - 4 \cdot 3 + 3^2}$$

$$= \sigma_{\text{CH-PR}} \sqrt{13} \qquad \text{for subarray 1,}$$

and

$$\sigma_{\phi_2} = \sigma_{\text{CH-PR}} \sqrt{11^2 - 11 \cdot 4 + 4^2}$$

$$= \sigma_{\text{CH-PR}} \sqrt{93} \qquad \text{for subarray 2.}$$

Suppose that the rms electrical phase error between channel pairs $\sigma_{\text{CH-PR}} = 12.5°$. Then,

$$\sigma_{\phi_1} = 12.5° \sqrt{13} = 45.07°,$$

and

$$\sigma_{\phi_2} = 12.5° \sqrt{93} = 120.55°.$$

The integration limits in Eq. (3-19) are

$$\text{Subarray 1:} \quad \pm \frac{180°}{\sigma_{\phi_1}} = \pm 3.994,$$

$$\text{Subarray 2:} \quad \pm \frac{180°}{\sigma_{\phi_2}} = \pm 1.493.$$

When Eq. (3-21) is used, the probability of ambiguity of the individual subarrays is

$$\text{Subarray 1:} \quad p_a = \text{erfc}\left(\frac{180°}{\sqrt{2}\,\sigma_{\phi_1}}\right) = 6.497 \times 10^{-5},$$

$$\text{Subarray 2:} \quad p_a = \text{erfc}\left(\frac{180°}{\sqrt{2}\,\sigma_{\phi_2}}\right) = 0.1354.$$

The p_a for subarray 2 is over three orders of magnitude larger than for subarray 1. This dramatically illustrates the desirability of utilizing the information from channels 1-2-3 (subarray 1) to improve the ambiguity performance of subarray 2, composed of channels 1-3-4.

The ambiguity diagrams for the two subarrays illustrate how this may be accomplished. Suppose that $\theta_a = 0°$ and that $\Delta\varphi_{1,2} = 36.818°$, $\Delta\varphi_{1,3} = 49.091°$, and $\Delta\varphi_{1,4} = 45°$. (Note: These error sets have been chosen to place the error sets $(\Delta\varphi_{1,2}, \Delta\varphi_{1,3})$ as well as $(\Delta\varphi_{1,3}, \Delta\varphi_{1,4})$ directly on ambiguity-plane trajectories, but this assumption is not essential to the following development.) Now, the error set $(\Delta\varphi_{1,2}, \Delta\varphi_{1,3})$ lies on trajectory 0 for subarray 1 (lower diagram in Fig. 4-2), whereas the error set $(\Delta\varphi_{1,3}, \Delta\varphi_{1,4})$ lies on trajectory 3′ for subarray 2 (upper diagram in Fig. 4-2).

If the phase-comparator output from only the larger baseline in each of the two subarrays was used separately to form an estimate of the angle of arrival, the results would be as follows

Subarray 1:

$$\hat{\theta}_{a_1} = \sin^{-1}\left[\frac{0 \times 360^\circ + 49.091^\circ}{\frac{4}{2} \times 360^\circ}\right] = 3.91^\circ ,$$

Subarray 2:

$$\hat{\theta}_{a_2} = \sin^{-1}\left[\frac{3 \times 360^\circ + 45^\circ}{\frac{11}{2} \times 360^\circ}\right] = 34.62^\circ .$$

Thus, although the channel-pair phase errors are comparable in magnitude, since trajectory 3′ for subarray 2 is *not* the true trajectory, using the phase information from subarray 2 *alone* provides a grossly incorrect angle-of-arrival estimate.

Given that the error set $(\Delta\varphi_{1,2}, \Delta\varphi_{1,3})$ for subarray 1 lies within the boundaries around the trajectory associated with the true angle of arrival, the following items may be noted

- The true trajectory for subarray 1 is 0,
- The true trajectory for subarray 2 is 0′,
- The *contiguous* subarray 2 trajectories (plotted on the trajectories for subarray 1) are 1′ for θ_a (+) and 10′ for θ_a (−),
- The *adjacent* ambiguous trajectories for subarray 2 in Fig. 4-2a are 3′ and 8′, which are $n_2 - 1 = 3$ greater or less than (mod 11) 0′: (0 + 3 = 3; 11 − 3 = 8),
- Trajectories 6′ $(3 + n_2 - 1 = 6)$ and 5′ $(8 - n_2 + 1 = 5)$ lie midway between trajectories 0′ and 1′, and 0′ and 10′, respectively.

The p_a calculations made above show that it is almost a certainty that the true trajectory for subarray 1 is 0 for the given example, subject to channel-pair errors of 12.5° rms, with Gaussian distribution. The only subarray 2 trajectories possible, given trajectory 0 on subarray 1, are 0′, 1′, and 2a′. Trajectory 3′ in Fig. 4-2a for subarray 2 is adjacent to trajectory 0′, whereas trajectories 1′ and 2′ are four trajectories to the right and left, respectively, of trajectory 0′. Hence, the true trajectory for subarray 2 is 0′, to a very high probability.

Subarray 1, in effect, increases the width of the ambiguity boundaries around the phase trajectories for subarray 2 by the factor $m_1 = 4$. This is shown in Fig. 4-3, the ambiguity diagram for $\mathcal{R}_2 = m_2 : n_2 = 11:4$, resolved by m_1 in $\mathcal{R}_1 = m_1 : n_1 = 4:3$. Rather than a square 2π on each side, the ambiguity-plane surface is now 2π long on the m_2 axis,

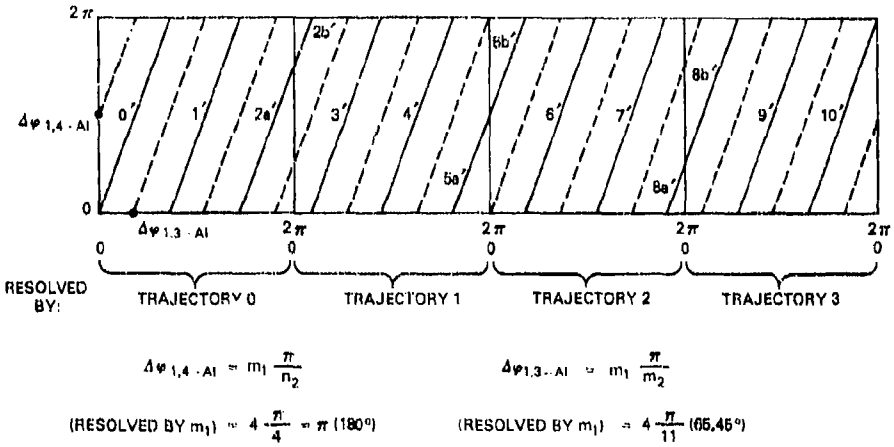

Fig. 4-3—Ambiguity diagram for $\Re_2 = m_2{:}n_2 = 11{:}4$ resolved by m_1 in $\Re_1 = m_1{:}n_1 = 4{:}3$

but is increased to $4 \times 2\pi$ long on the n_2 axis. It is readily seen that as trajectory $2'$ pierces the first 2π ordinate to the right of $\Delta\varphi_{1,3} = 0$, there is no need to translate this intersection point back to the ordinate at $\Delta\varphi_{1,3} = 0$. The new ambiguity boundary between trajectory $0'$ and $1'$ (in reality trajectory $6'$ in the previous illustration) is two times the distance between trajectories $0'$ and $3'$ in Fig. 4-2a.

In this modified ambiguity diagram for subarray 2, resolved by subarray 1, the ambiguity intercepts are

$$\Delta\varphi_{1,4\text{-AI}} = m_1 \frac{\pi}{n_2} = 4 \frac{\pi}{4} = \pi\ (180^\circ)\,,$$

$$\Delta\varphi_{1,3\text{-AI}} = m_1 \frac{\pi}{m_2} = 4 \frac{\pi}{11}\ (65.45^\circ)\,.$$

The new integration limits in Eq. (3-19) for subarray 2 are

$$\pm \frac{m_1\ 180^\circ}{\sigma_{\phi_2}} = \pm \frac{4 \times 180^\circ}{120.55^\circ} = \pm 5.973\,.$$

Thus, the p_a for subarray 2, resolved by subarray 1, is

$$p_a = \operatorname{erfc}\left(\frac{m_1\ 180^\circ}{\sqrt{2}\,\sigma_{\phi_2}}\right) \leqslant 2.3 \times 10^{-9}\,.$$

If independence between ambiguities in subarray 2 and subarray 1 is assumed, the overall array p_a is given by

$$p_{a\text{-overall}} = 1 - (1 - p_{a_1})(1 - p_{a_2}) . \tag{4-12}$$

For the example above,

$$p_{a\text{-overall}} = 1 - (1 - 6.497 \times 10^{-5})(1 - 2.3 \times 10^{-9})$$

$$= 6.49723 \times 10^{-5} .$$

This is a negligible increase from the p_a for subarray 1 alone. However, the overall array has a length $\ell = 11$ half-wavelengths, whereas subarray 1 has a length $p + q = 4$ half-wavelengths. Thus, the accuracy of angle of arrival estimates using the whole array is almost three times (11/4) better than for subarray 1 alone.

The geometric arguments above illustrate how the ambiguity boundaries for subarray 2 in a four-element cascaded end-phase interferometer are extended by a factor related to the m_1 spacing integer in subarray 1. This ambiguity constraint relaxation on subarray 2 can also be developed analytically, as shown below.

The ambiguity constraints for the two subarrays (considered as isolated three-element arrays) can be written in several forms

Array Ratio Form

$$\text{Subarray 1} \quad |n_1 \Delta\varphi_{1,3} - m_1 \Delta\varphi_{1,2}| \gtrless \pi \tag{4-13a}$$

$$\text{Subarray 2} \quad |n_2 \Delta\varphi_{1,4} - m_2 \Delta\varphi_{1,3}| \gtrless \pi , \tag{4-13b}$$

Spacing Integer Form

$$\text{Subarray 1} \quad |p \Delta\varphi_{1,3} - (p + q) \Delta\varphi_{1,2}| \gtrless \pi \tag{4-14a}$$

$$\text{Subarray 2} \quad |(p + q) \Delta\varphi_{1,4} - (p + q + r) \Delta\varphi_{1,3}| \gtrless \pi , \tag{4-14b}$$

Spacing Integer-Channel Error Form

$$\text{Subarray 1} \quad |-q \Delta\varphi_1 + (p + q) \Delta\varphi_2 - p \Delta\varphi_3| \gtrless \pi \tag{4-15a}$$

$$\text{Subarray 2} \quad |-r \Delta\varphi_1 + (p + q + r) \Delta\varphi_3 - (p + q) \Delta\varphi_4| \gtrless \pi \tag{4-15b}$$

where

$$p = \frac{n_1 n_2}{\alpha} \qquad p + q = \frac{m_1 n_2}{\alpha}$$

$$q = \frac{n_2}{\alpha} (m_1 - n_1) \qquad p + q + r = \frac{m_1 m_2}{\alpha} = \ell$$

$$r = \frac{m_1}{\alpha} (m_2 - n_2)$$

α = factor common to m_1 and n_2.

If the subarray ratio-integer forms for the spacing integers p, q, r, ... are used, and if subarray 2 is resolved by subarray 1, the ambiguity constraint Eq. (4-15b) becomes

$$\left|-\frac{m_1}{\alpha}(m_2-n_2)\Delta\varphi_1+\frac{m_1m_2}{\alpha}\Delta\varphi_3-\frac{m_1n_2}{\alpha}\Delta\varphi_4\right| \gtrless m_1\pi\,. \tag{4-16}$$

Multiplying both sides of the inequality above by α/m_1 yields

$$|-(m_2-n_2)\Delta\varphi_1+m_2\Delta\varphi_3-n_2\Delta\varphi_4| \gtrless \alpha\pi\,,$$

which simplifies to

$$\left.|n_2\Delta\varphi_{1,4}-m_2\Delta\varphi_{1,3}| \gtrless \alpha\pi\right\} \quad \begin{array}{l}\text{Ambiguity constraint for subarray 2}\\ \text{resolved by subarray 1}\end{array} \tag{4-17}$$

using

$$\Delta\varphi_1-\Delta\varphi_4 \equiv \Delta\varphi_{1,4}, \Delta\varphi_1-\Delta\varphi_3 \equiv \Delta\varphi_{1,3}\,.$$

The ambiguity constraint discussion in this section culminating in Eq. (4-17) can be summarized for the four-element cascaded end-phase interferometer as follows

Four-Element Cascaded End-phase Interferometer

- Array Constants

Ratios:
$$\Re_1=\frac{m_1}{n_1}=\frac{p+q}{p} \tag{4-18a}$$

$$\Re_2=\frac{m_2}{n_2}=\frac{p+q+r}{p+q} \tag{4-18b}$$

Spacing Integers:
$$p=\frac{n_1n_2}{\alpha},\quad q=\frac{n_2}{\alpha}(m_1-n_1),\quad r=\frac{m_1}{\alpha}(m_2-n_2)$$

$$p+q+r=\ell=\frac{m_1m_2}{\alpha} \tag{4-18c}$$

α = factor common to m_1 and n_2

- Ambiguity Constraints (each subarray considered separately)

Subarray 1:
$$|n_1\Delta\varphi_{1,3}-m_1\Delta\varphi_{1,2}| \gtrless \pi \tag{4-18d}$$

Subarray 2:
$$|n_2\Delta\varphi_{1,4}-m_2\Delta\varphi_{1,3}| \gtrless \pi \tag{4-18e}$$

- Ambiguity Variables

$$\sigma_{\phi_1} = \sigma_{\text{CH-PR}}[m_1^2 - 2\rho_{e_1} m_1 n_1 + n_1^2]^{1/2} \tag{4-18f}$$

$$\sigma_{\phi_2} = \sigma_{\text{CH-PR}}[m_2^2 - 2\rho_{e_2} m_2 n_2 + n_2^2]^{1/2} \tag{4-18g}$$

- Integration Limits

$$\text{Subarray 1:} \quad \pm \frac{180^\circ}{\sigma_{\phi_1}} \tag{4-18h}$$

$$\text{Subarray 2:} \quad \pm \frac{\alpha 180^\circ}{\sigma_{\phi_2}} \tag{4-18i}$$

- Probability of Ambiguity

$$p_{a_1} = \text{erfc}\left(\frac{180^\circ}{\sqrt{2}\,\sigma_{\phi_1}}\right) \tag{4-18j}$$

$$p_{a_2} = \text{erfc}\left(\frac{\alpha 180^\circ}{\sqrt{2}\,\sigma_{\phi_2}}\right) \tag{4-18k}$$

The relations above were derived analytically and hold for all four-element cascaded end-phase arrays, regardless of whether the individual subarrays are unambiguous or ambiguous in the sense of Table 4-2 in Sec. 4-2.

Table 4-3 shows examples of cascaded end-phase arrays falling into two classes:

Class A $\quad \ell = p + q + r$ is expressible directly as m_2,

Class B $\quad \ell$ can only be expressed as $m_1 m_2/\alpha$.

Note: The meaning of the terms in parentheses will be explained below.

It should be apparent from Fig. 4-3 that α is the factor by which the width of the ambiguity diagram for subarray 2 is increased. Even though for the Class B, $\mathcal{R}_1 = 4{:}1$, $\mathcal{R}_2 = 3{:}1$ example, α is only unity, it should not be assumed that this is an array with poor tolerance to ambiguities.

The ambiguity diagram for this array (Fig. 4-4) shows why this is so. Since $(p + q + r)/(p + q) = 3$, the trajectories 3′, 4′, and 5′ overlay respectively the trajectories 0′, 1′ and 2′. In the terminology of Sec. 4.2, subarray 2 is ambiguous-resolvable. The factor α is unity (the common factor between $m_1 = 4$ and $n_2 = 1$ is 1); consequently, even with the information from subarray 1, the ambiguity diagram for subarray 2 cannot be extended, as was the case in the previous example. There is no need to do this, however, because subarray 2

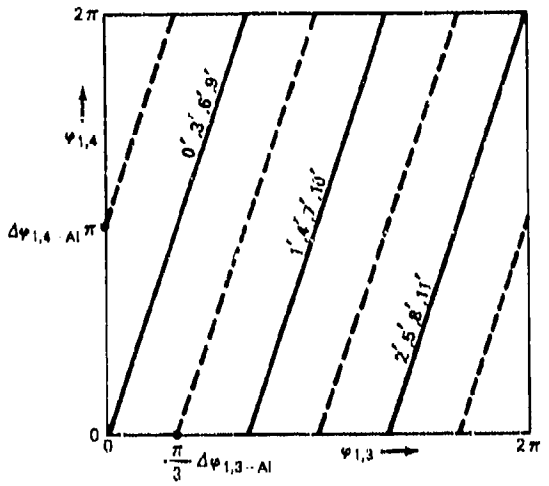

SUBARRAY 2

$\mathscr{R}_2$ = 3:1

$= \frac{p+q+r}{p+q} = \frac{m_2}{n_2}$

p = 1

q = 3

r = 8

$l = p+q+r = 12$

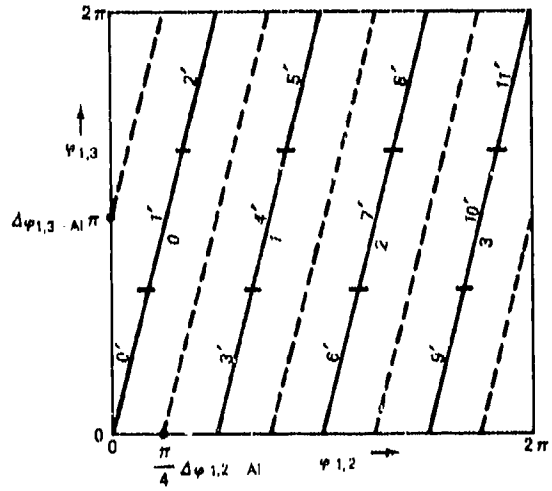

SUBARRAY 1

$\mathscr{R}_1$ = 4:1

$= \frac{p+q}{p} = \frac{m_1}{n_1}$

Fig. 4-4—Ambiguity diagrams for four-element array, cascaded end-phase: $\mathscr{R}_1$ = 4:1 ⊕ $\mathscr{R}_2$ = 3:1

Table 4-3—Examples of the Two Classes of Four-element Cascaded End-phase Arrays

Array Class	Subarray Ratios		α	Array Spacing Integers			
	$\mathcal{R}_1 = m_1:n_1$	$\mathcal{R}_2 = m_2:n_2$		p	q	r	ℓ
A	4:3	11:4	4	3	1	7	11
A	3:2	11:6	3	4	2	5	11
B	4:3	7:2 (14:4)	2 (4)	3	1	10	14
B	4:1	3:1 (12:4)	1 (4)	1	3	8	12

Notes:
1. α = factor common to m_1 and n_2.
2. $p = \frac{n_1 n_2}{\alpha}$, $q = \frac{n_2}{\alpha}(m_1 - n_1)$, $r = \frac{m_1}{\alpha}(m_2 - n_2)$; $\ell = p + q + r = \frac{m_1 m_2}{\alpha}$.

is expressed in a form which already is "reduced" from an ambiguous higher-order form. This can be illustrated as follows.

Suppose that subarray 2 is expressed as $\mathcal{R}_2 = m_2:n_2 = 12:4$, such that m_2 must equal ℓ (disregarding any common factors in m_2 and n_2). Then $\alpha = 4$. Direct application of the spacing integer equations will provide the *same* spacing integers p, q, and r as long as the factor α appropriate to the m_2, n_2 set under consideration is used. This is indicated in Table 4-3 by listing, where necessary, a second set of parameters within parentheses for the Class B entries.

Now, from Eq. (4-18g),

$$\sigma_{\phi_2} = \sigma_{\text{CH-PR}}[12^2 - 12 \cdot 4 + 4^2]^{1/2}$$

$$= \sigma_{\text{CH-PR}}(4\sqrt{7}), \quad \text{or } 132.29^\circ, \quad \text{for } \sigma_{\text{CH-PR}} = 12.5^\circ.$$

The integration limits for subarray 2 (with $m_2 = 12$, $n_2 = 4$, $\alpha = 4$), using Eq. (4-18i), are

$$\pm\frac{\alpha 180^\circ}{\sigma_{\phi_2}} = \pm\frac{4 \times 180^\circ}{12.5^\circ \times 4 \times \sqrt{7}} = \pm 5.443.$$

But, these are precisely the same integration limits that result with $\mathcal{R}_2 = 3:1$, $\alpha = 1$, as

$$\sigma_{\phi_2} = \sigma_{\text{CH-PR}}[3^2 - 3{\cdot}1 + 1^2]^{1/2} = 33.07^\circ, \quad \text{for } \sigma_{\text{CH-PR}} = 12.5^\circ;$$

$$\pm\frac{\alpha 180^\circ}{\sigma_{\phi_2}} = \pm\frac{1 \times 180^\circ}{33.07^\circ} = \pm 5.443.$$

It is apparent that one form of expressing $\mathcal{R}_2$ for Class B arrays exhibits m_2 and n_2 *without* common factors, and with $\alpha \neq m_1$. But the second form manifests m_2 and n_2 *with* $\ell = m_2$, and *with* a common factor $\alpha \equiv m_1$. Thus, if m_2 and n_2 are expressed in a form that preserves any common factors, and if the appropriate modification is made in α, the distinctions between Class A and B disappear.

In Sec. 5.5, the tabulated results of an array synthesis procedure developed earlier in that section will be presented. It will be seen that consistent expression of m_2 and n_2 directly as $m_2 \equiv p + q + r = \ell$, and $n_2 \equiv p + q$, with $\alpha \equiv m_1$ highlights the importance of basing a four-element array synthesis procedure on the subarray 1 integer m_1. It is also stressed that the subarray 2 ambiguity constraint development ending in Eq. (4-17) holds no matter in what form m_2 and n_2 are expressed, provided α is correctly defined.

4.4 Ambiguity Constraints and p_a for Four-element Arrays of Various Configurations

The theory developed in Sec. 4.3 for the ambiguity constraints and p_a associated with the cascaded end-phase array will now be extended to other four-element array configurations. Attention will be concentrated initially on the other four configurations of Fig. 4-1 (see Sec. 4.1). Later, the development will be generalized to all possible array configurations using three phase differences—the minimum number required to resolve the ambiguities in a four-element array.

Subarray ratios $\mathcal{R}_1$ and $\mathcal{R}_2$ for the remaining four configurations of Fig. 4-1 can be expressed in terms of the ratio numerators and denominators by carrying out analyses similar to those appearing in Eq. (4-3) through Eq. (4-8) of Sec. 4.3. The results of such analyses are given in Table 4-4, which, for convenience of reference, also lists the appropriate parameters for cascaded end-phase arrays.

Consider the hybrid midphase configuration, as shown in Fig. 4-1c as an example of how the ambiguity constraints, coupled with the factor α—the greatest factor common to the two subarray integers associated with the common spacing—lead to the p_a function. The derivations of the ambiguity constraints are similar to those for the cascaded end-phase configuration in Sec. 4.3, Eqs. (4-13) through (4-17). Since the derivations are similar and are based on the same kind of geometric arguments, it will be convenient to express the parameters for the hybrid midphase configuration in the same format as the summary for the cascaded end-phase configuration following Eq. (4-17) in Sec. 4.3.

Table 4-4—Common Spacing, Factor α, and Spacing Integers for Various Configurations of Four-element Arrays

Array Type	Subarray Ratios		Common Spacing	α Common to:	Array Spacing Integers			
	$\Re_1$	$\Re_2$			p	q	r	ℓ
Cascaded end-phase	$\Re_{1e} = \frac{m_1}{n_1} = \frac{\alpha m_1'}{n_1}$	$\Re_{2e} = \frac{m_2}{n_2} = \frac{m_2}{\alpha n_2'}$	$p + q$	m_1 and n_2	$\frac{n_1 n_2}{\alpha}$	$\frac{(m_1 - n_1)n_2}{\alpha}$	$\frac{m_1(m_2 - n_2)}{\alpha}$	$\frac{m_1 m_2}{\alpha}$
Cascaded midphase	$\Re_{1c} = \frac{x_1}{y_1} = \frac{\alpha x_1'}{y_1}$	$\Re_{2m} = \frac{x_2}{y_2} = \frac{\alpha x_2'}{y_2}$	$p + q$	x_1 and x_2	$\frac{(x_1 - y_1)x_2}{\alpha}$	$\frac{y_1 x_2}{\alpha}$	$\frac{x_1 y_2}{\alpha}$	$\frac{x_1(x_2 + y_2)}{\alpha}$
Hybrid midphase	$\Re_{1m} = \frac{e_1}{f_1} = \frac{e_1}{\alpha f_1'}$	$\Re_{2e} = \frac{e_2}{f_2} = \frac{e_2}{\alpha f_2'}$	q	f_1 and f_2	$\frac{e_1 f_2}{\alpha}$	$\frac{f_1 f_2}{\alpha}$	$\frac{f_1(e_2 - f_2)}{\alpha}$	$\frac{e_1 f_2 + f_1 e_2}{\alpha}$
Additive midphase	$\Re_{1m} = \frac{c_1}{d_1} = \frac{c_1}{\alpha d_1'}$	$\Re_{2m} = \frac{c_2}{d_2} = \frac{\alpha c_2'}{d_2}$	q	d_1 and c_2	$\frac{c_1 c_2}{\alpha}$	$\frac{d_1 c_2}{\alpha}$	$\frac{d_1 d_2}{\alpha}$	$[c_1 c_2 + d_1 c_2 + d_1 d_2] \div \alpha$
Multiple end-phase	$\Re_{1e} = \frac{g_1}{h_1} = \frac{g_1}{\alpha h_1'}$	$\Re_{2e} = \frac{g_2}{h_2} = \frac{g_2}{\alpha h_2'}$	p	h_1 and h_2	$\frac{h_1 h_2}{\alpha}$	$\frac{(g_1 - h_1)h_2}{\alpha}$	$[h_1 g_2 - g_1 h_2] \div \alpha$	$\frac{h_1 g_2}{\alpha}$

Note: Array configurations are illustrated in Fig. 4-1.

Four-element Hybrid Midphase Interferometer

- Array Constants

Ratios: $$R_{1m} = \frac{e_1}{f_1} = \frac{p}{q} \tag{4-19a}$$

$$R_{2e} = \frac{e_2}{f_2} = \frac{q + r}{q} \tag{4-19b}$$

Spacing Integers: $$p = \frac{e_1 f_2}{\alpha}, \quad q = \frac{f_1 f_2}{\alpha}, \quad r = \frac{f_1(e_2 - f_2)}{\alpha}$$

$$p + q + r = \ell = \frac{e_1 f_2 + f_1 e_2}{\alpha} \tag{4-19c}$$

α = factor common to f_1 and f_2

- Ambiguity Constraints (each subarray considered separately)

Subarray 1: $$|f_1 \Delta\varphi_{1,2} - e_1 \Delta\varphi_{2,3}| \gtrless \pi \tag{4-19d}$$

Subarray 2: $$|f_2 \Delta\varphi_{2,4} - e_2 \Delta\varphi_{2,3}| \gtrless \pi \tag{4-19e}$$

- Ambiguity Variables

$$\sigma_{\varphi_1} = \sigma_{\text{CH-PR}}[e_1^2 - 2\rho_m e_1 f_1 + f_1^2]^{1/2} \tag{4-19f}$$

$$\sigma_{\varphi_2} = \sigma_{\text{CH-PR}}[e_2^2 - 2\rho_e e_2 f_2 + f_2^2]^{1/2} \tag{4-19g}$$

- Integration Limits

Subarray 1: $$\pm \frac{180^\circ}{\sigma_{\varphi_1}} \tag{4-19h}$$

Subarray 2: $$\pm \frac{\alpha 180^\circ}{\sigma_{\varphi_2}} \tag{4-19i}$$

- Probability of Ambiguity

$$p_{a_1} = \text{erfc}\left(\frac{180^\circ}{\sqrt{2}\,\sigma_{\varphi_1}}\right) \tag{4-19j}$$

$$p_{a_2} = \text{erfc}\left(\frac{\alpha 180^\circ}{\sqrt{2}\,\sigma_{\varphi_2}}\right) \tag{4-19k}$$

With the information from Fig. 4-1 and Table 4-4, similar summaries can readily be generated for the remaining array configurations--cascade midphase, additive midphase, and multiple midphase.

Calculated p_a are given for all array configurations in Table 4-5, with either $p = 6$, $q = 4$, $r = 11$ or $p = 4$, $q = 6$, $r = 11$, subject to $\sigma_{CH\text{-}PR} = 12.5°$, thus lending insight into the importance of the factor α on overall array performance. The overall array length $\ell = p + q + r = 21$ half-wavelengths.

In the p_a calculations, it has been assumed that ambiguities in subarray 2 (resolved by subarray 1) are independent of ambiguities in subarray 1. [Note: Later, in Sec. 5, an exact expression involving integration of a bivariate Gaussian density function will be given for four-element arrays. It will be seen that for most cases of practical interest, the assumption of subarray independence causes negligible error in overall array p_a.]

Table 4-5 shows that all array configurations are characterized by identical subarray 1 p_a. This results, of course, from the fact that any configuration of three-element array, end-phase left, midphase, or end-phase right, has the same p_a for given p, q, and $\sigma_{CH\text{-}PR}$.

The factor α for the five configurations varies from a maximum of 5 to a minimum of 1. In addition, although it is not shown explicitly in the table, the subarray 2 ambiguity variable also varies. Consequently, the p_a of subarray 2 ranges widely. The tabulation of overall p_a shows that the multiple end-phase configuration is clearly inferior to the others for $p = 4$, $q = 6$, $r = 11$. For these spacings, multiple end-phase exhibits p_a two orders of magnitude inferior to cascaded end-phase.

It might be conjectured that hybrid and additive midphase arrays cannot achieve as low an overall p_a as cascaded end-phase and cascaded midphase arrays. This conjecture is incorrect, as the following development will show.

Consider the hybrid midphase configuration. Suppose that

1. the array spacings are transformed according to the rules

$$r \rightarrow p' \ (=11)$$
$$q \rightarrow q' \ (=4)$$
$$p \rightarrow r' \ (=6),$$

but that

2. the location of the phase reference at channel 2 remains unchanged.

Now, by redefining

$$\mathcal{R}_{1e} = \frac{r' + q'}{q'} = \frac{u_1}{v_1} = \frac{\alpha u_1'}{v_1}$$

$$\left(= \frac{6 + 4}{4} = 5{:}2\right),$$

and

Table 4-5—Ambiguity Probability for Various Configurations of Four-element Arrays with $p = 6$, $q = 4$, $r = 11$, or $p = 4$, $q = 6$, $r = 11$; and $\sigma_{CH\text{-}PR} = 12.5°$

Array Type	Array Spacings				Subarray Ratios		α	Integration Limits (±)		Ambiguity Probabilities		
	p	q	r	ℓ	$\Re_1$	$\Re_2$		Number 1	Number 2	Number 1	Number 2	Overall
Cascaded end-phase	6	4	11	21	5:3	21:10	5	3.304	3.957	9.532×10^{-4}	7.59×10^{-5}	1.029×10^{-3}
	4	6	11	21	5:2	21:10	5	3.304	3.957	9.532×10^{-4}	7.59×10^{-5}	1.029×10^{-3}
Cascaded midphase	6	4	11	21	5:2	10:11	5	3.304	3.957	9.532×10^{-4}	7.59×10^{-5}	1.029×10^{-3}
	4	6	11	21	5:3	10:11	5	3.304	3.957	9.532×10^{-4}	7.59×10^{-5}	1.029×10^{-3}
Hybrid midphase	6	4	11	21	3:2	15:4	2	3.304	2.141	9.532×10^{-4}	3.227×10^{-2}	3.320×10^{-2}
	4	6	11	21	2:3	17:6	3	3.304	2.893	9.532×10^{-4}	3.815×10^{-3}	4.765×10^{-3}
Additive midphase	6	4	11	21	3:2	4:11	2	3.304	2.141	9.532×10^{-4}	3.227×10^{-2}	3.320×10^{-2}
	4	6	11	21	2:3	6:11	3	3.304	2.893	9.532×10^{-4}	3.816×10^{-3}	4.765×10^{-3}
Multiple end-phase	6	4	11	21	5:3	7:2	1	3.304	2.306	9.532×10^{-4}	2.111×10^{-2}	2.204×10^{-2}
	4	6	11	21	5:2	21:4	2	3.304	1.491	9.532×10^{-4}	0.13596	0.13678

Notes:

1. $\sigma_{CH\text{-}PR} = 12.5°$, for calculations of integration limits and probabilities.
2. $p_{c\text{-overall}} = 1 - (1 - p_{c_1})(1 - p_{c_2})$; i.e., independence assumed.

$$\mathcal{R}_{2m} = \frac{p'}{r' + q'} = \frac{u_2}{v_2} = \frac{u_2}{\alpha v_2'}$$

$$\left(= \frac{11}{6 + 4} = 11{:}10\right),$$

we can easily show that

$$\alpha = \text{factor common to } u_1 \text{ and } v_2$$

$$= 5.$$

Figure 4-5 shows the original, as well as the transformed, array.

It can be seen, by referring to Table 4-5, that the parameters for the transformed array are identical to those of the original cascaded midphase array, which in turn has a p_a equivalent to the cascaded end-phase array. Thus, by redefining the spacing integers and the directions in which the subarrays expand, it has been shown that hybrid midphase arrays are equivalent to cascaded midphase, and ultimately, to cascaded end-phase arrays.

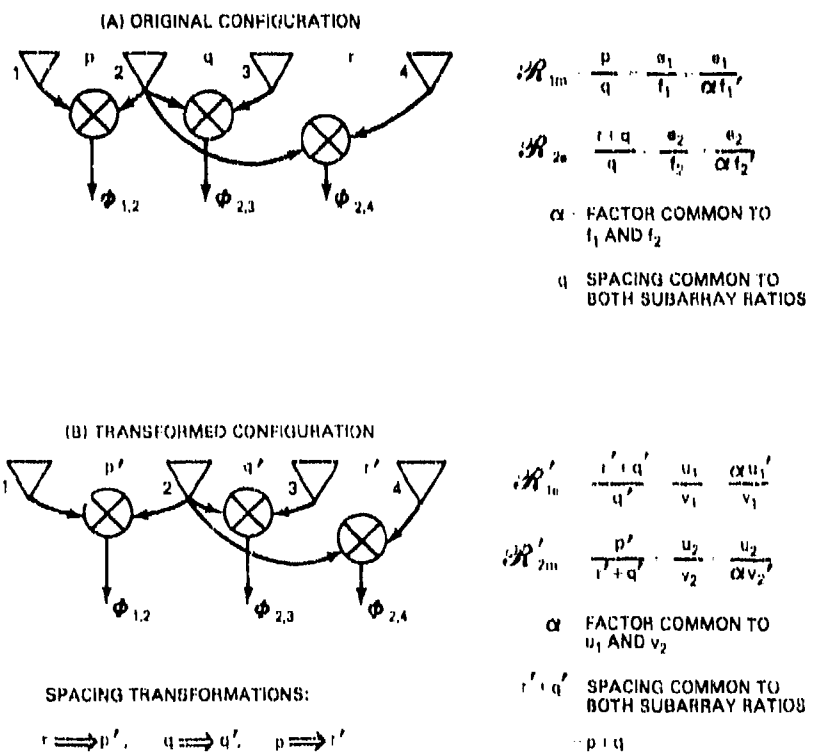

Fig. 4-5—Original and transformed four-element hybrid midphase arrays

4.5 Canonical Configurations for Four-element Arrays

Canonical array configurations may be defined as those for which

- The minimum number of phase comparisons are implemented.
- The overall p_a is the lowest achievable for specific array spacing integers $p, q, r, \ldots$.

In Sec. 4.5, intuitive arguments showed that the cascaded end-phase configuration was optimum. This optimality of the cascaded end-phase configuration will now be proved. It will be convenient to precede the specific development for $n = 4$ by some observations on arrays using an arbitrary number of elements.

Consider an n-element array where (as shown in Fig. 4-1 for some four-element configurations) the antenna receiver channels are numbered from the left as $i = 1, 2, \ldots, j, \ldots, n$. Adopt the convention that for any electrical phase angle $\Phi_{j,k}$ provided by instrumentation associated with these channels, channel j is denoted the phase reference. Thus,

$$\Phi_{j,k} = \frac{2\pi}{\lambda} d_{j,k} \sin \theta_a$$

$$= \frac{2\pi}{\lambda} (x_k - x_j) \sin \theta_a ; \quad \left.\begin{matrix} +, k > j \\ -, k < j \end{matrix}\right\} \theta_a(+) , \tag{4-20}$$

where x_k is the spacing of antenna k from antenna 1, $x_1 = 0$.

Obviously, by definition $\Phi_{i,i} = 0$. Further, $\Phi_{j,k} = -\Phi_{k,j}$. For $n = 2$, 3, or 4, matrix representations for the channel-pair phase variables are

$n = 2$:

$$\tilde{\Phi}_2 = \begin{bmatrix} 0 & \Phi_{1,2} \\ -\Phi_{1,2} & 0 \end{bmatrix} = \Phi \begin{bmatrix} 0 & p \\ -p & 0 \end{bmatrix} \tag{4-21a}$$

$n = 3$:

$$\tilde{\Phi}_3 = \begin{bmatrix} 0 & \Phi_{1,2} & \Phi_{1,3} \\ -\Phi_{1,2} & 0 & \Phi_{2,3} \\ -\Phi_{1,3} & -\Phi_{2,3} & 0 \end{bmatrix} = \Phi \begin{bmatrix} 0 & p & (p+q) \\ -p & 0 & q \\ -(p+q) & -q & 0 \end{bmatrix} \tag{4-21b}$$

$n = 4$:

$$\tilde{\Phi}_4 = \begin{bmatrix} 0 & \Phi_{1,2} & \Phi_{1,3} & \Phi_{1,4} \\ -\Phi_{1,2} & 0 & \Phi_{2,3} & \Phi_{2,4} \\ -\Phi_{1,3} & -\Phi_{2,3} & 0 & \Phi_{3,4} \\ -\Phi_{1,4} & -\Phi_{2,4} & -\Phi_{3,4} & 0 \end{bmatrix} = \Phi \begin{bmatrix} 0 & p & (p+q) & (p+q+r) \\ -p & 0 & q & (q+r) \\ -(p+q) & -q & 0 & r \\ -(p+q+r) & -(q+r) & -r & 0 \end{bmatrix} \tag{4-21c}$$

with $\Phi = \frac{2\pi}{\lambda} \frac{\lambda}{2} \sin \theta_a = \pi \sin \theta_a$.

Extension of this channel-pair phase matrix to $n \geq 5$ should be obvious. It is emphasized that these matrices list all possible channel-pair differences, but that usually, a particular set of $(n-1)$ p' se differences are the only ones implemented in an array of a given configuration.

By inspection, it can be seen that the n^2 elements in these matrices are apportioned as

- number of comparisons $\Phi_{i,j} = n(n-1)/2$
- number of comparisons $\Phi_{j,i} = n(n-1)/2$
- number of comparisons $\Phi_{i,i} = n$

total $= n^2$

Eliminating the phase differences $\Phi_{i,i}$ which are not functions of the angle of arrival in the systems under consideration in this report leaves only $n(n-1)/2$ different comparisons (excluding negatives) possible in an n-element interferometer. The number n_φ of these comparisons for $2 \leq n \leq 7$ is

n	n_φ
2	1
3	3
4	6
5	10
6	15
7	21.

It is obviously necessary to implement only $(n-1)$ phase comparisons in an n-element interferometer, if these comparisons make use of the phase information from all n channels. The number N_φ of different sets of $(n-1)$ comparisons is given by the number of combinations of n_φ, taken $(n-1)$ at a time, or

$$N_\varphi = \frac{n_\varphi!}{(n-1)!(n_\varphi - n + 1)!} . \tag{4-22}$$

For $2 \leq n \leq 7$, N_φ is given below.

n	N_φ
2	1
3	3
4	20
5	210
6	3,003
7	54,264

Note: For $n \geq 3$, N_φ includes mirror-image configurations; for strict consistency then, with $n = 2$, N_φ should be equal to 2.

For $n = 3$, the matrix form of Eq. (4-21b) provides an illustration of the physical counterpart of N_φ. The first tow of this matrix defines an end-phase left array, the middle row defines a midphase array, and the bottom row defines an end-phase right array.

For $n = 4$, it is difficult to visualize all 20 possible arrays with just the matrix form of Eq. (4-21c). Therefore, the phase differences defined by the matrix form are used $(n - 1) = 3$ at a time, and the 20 possible array configurations are sketched as in Fig. 4-6.

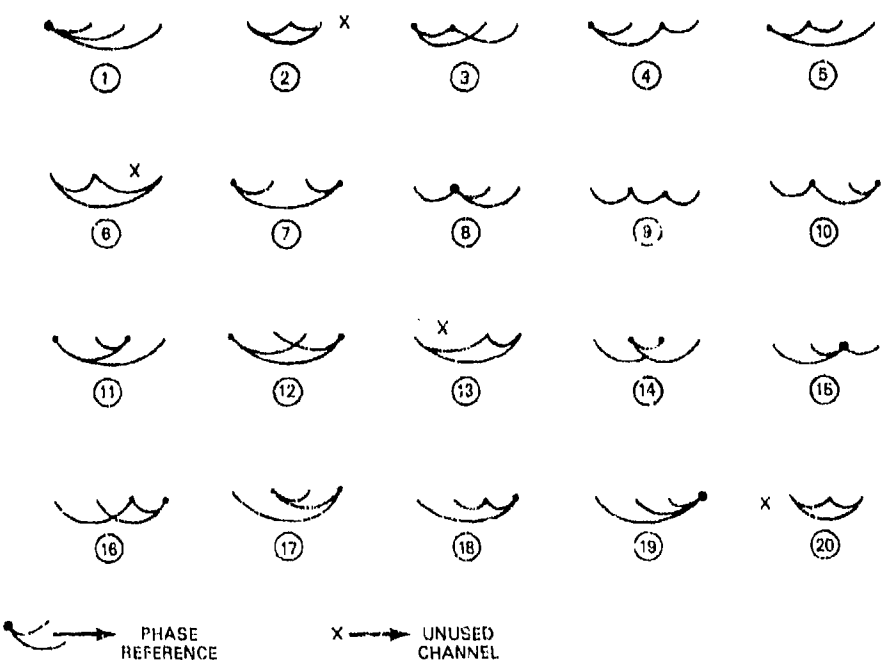

Fig. 4-6—Simplified representations of the twenty possible four-element array configurations using three phase differences

Table 4-6 lists the spacings utilized, the array phase reference(s), and the spacing common to the two subarrays. The arrays numbered 2, 6, 13, and 20 can be immediately removed from further consideration, since they do not employ information from channels 4, 3, 2, or 1, respectively.

Arrays 7 and 12 have spacings of $p + q + r$ common to the two subarrays. Thus, whichever subarray is denoted subarray 2 in each of these four-element arrays has the benefit of a large common factor α in increasing the value of the argument of the ambiguity variable. Unfortunately, the array ratio for subarray 1 will be so large (this subarray ratio also involves $p + q + r$) that the p_a of subarray 1 will be much larger than that obtained with a cascaded end-phase configuration.

Arrays using a single common spacing—p, q, or r—cannot, of course, achieve the performance of those using a double common spacing such as $p + q$ or $q + r$. This was shown in the calculations for p_a in the example arrays of Sec. 4.4. This fact removes from further consideration arrays 3 and 5 (with common spacing p), 9 and 14 (with q), and 16 and 18 (with r).

The remaining arrays share two attributes: (a) the common spacings are either $p + q$ or $q + r$, and (b) four of the arrays are mirror images of the other four. Table 4-7 lists the comparison factors for these eight arrays. Arrays 4 and 11 can be shown with no difficulty (by developments similar to those resulting in Eqs. (4-18a) through (4-18k)) to be identical in p_a performance to array 1. But arrays 4 and 11 do not resolve the overall array length associated with the integers $p + q + r$ as does array 1. Hence array 1 is superior to arrays 4 and 11.

Now, it has already been shown in Sec. 4.4 that the transformed hybrid midphase array is equivalent in p_a performance to the cascaded end-phase array. Once again, however, array 1 is superior to its transformed counterpart, array 15, in the sense that overall length $p + q + r$ is resolved directly.

Each of the four arrays discussed above has its mirror-image counterpart in the remainder of the table. Thus, it should be obvious that with the aid of the transformations $p \rightarrow r'$, $q \rightarrow q'$, and $r \rightarrow p'$, the performance of second group of arrays is identical to the first group, and that a cascaded end-phase configuration is indeed optimum.

In contrast to two-element and three-element arrays, the performance of arbitrary-configuration four-element arrays is dependent both on the configuration and on the array expansion direction.

The preceding development has shown that of the 20 possible (by definition) four-element array configurations, there are four configurations that have particularly simple realizations:

- Array 1—Cascaded end-phase (Reference channel 1)
- Array 8—Transformed hybrid midphase (Reference channel 2)
- Array 15—Transformed hybrid midphase (Reference channel 3)
- Array 19—Cascaded end-phase (Reference channel 4).

Table 4-6—Parameters for the Twenty Possible Four-element Arrays With Three Phase Differences

Array Number	Spacings Utilized						Array Phase Reference	Common Spacing
	p	q	r	$p+q$	$q+r$	$p+q+r$		
1	√			√		√	1	$p+q$
2	√	√		√			–	*Not* a 4-element array; channel 4 not used
3	√			√	√		1, 2	p
4	√		√	√			1, 3	$p+q$
5	√	√				√	1, 2	p
6	√				√	√	–	*Not* a 4-element array; channel 3 not used
7	√		√			√	1, 4	$p+q+r$
8	√	√			√		2	$q+r$
9	√	√	√				2, 3	q

10	√		√		√		2, 4	$q + r$
11		√		√		√	1,3	$p + q$
12				√	√	√	1, 4	$p + q + r$
13			√	√		√	–	*Not* a 4-element array; channel 2 not used
14		√		√	√		2, 3	q
15		√	√	√			3	$p + q$
16			√	√	√		3, 4	r
17		√			√		2, 4	$r + q$
18		√	√			√	3, 4	r
19			√		√	√	4	$r + q$
20		√	√		√	√	–	*Not* a 4-element array; channel 1 not used

Note: Array configurations are illustrated in Fig. 4-6.

Table 4-7—Comparison Factors for Four-element Arrays with Spacings $b + q$ or $q + r$

Array Configuration	Common Spacing	Array Reference(s)	Array Number	'Mirror-image' Array Number
Cascaded end-phase	$p + q$	1	1	19
Equivalent to CE-P	$p + q$	1, 3	4	10
Equivalent to CE-P	$p + q$	1, 3	11	17
Transformed hybrid midphase	$p + q$	3	15	8
Axis of configuration symmetry				
Transformed hybrid midphase	$q + r$	2	8	15
Cascaded end-phase	$q + r$	4	19	1
Equivalent to CE-P	$q + r$	4, 2	10	4
Equivalent to CE-P	$q + r$	4, 2	17	11

Note: Array numbers are defined in Fig. 4-6.

These four array configurations are defined by rows one, two, three, and four in the channel-phase error matrix of Eq. (4-21c).

This development showing that the cascaded end-phase configuration is indeed optimum for $n = 4$, is, as far as the writer can determine, a new result. Although some of the material presented by Hanson [21] for the case of four apertures on a line appears relevant, he neglects to consider the effects of correlation between channel-*pair* phase errors in subarrays. Thus, he is, in effect, formulating judgements on array-configuration suitability based on "independent," i.e., four-element two-integer set subarrays. It is known from Sec. 3.0 that this leads to incorrect conclusions when one deals with three-element subarrays.

This concludes the exposition of the fundamental *analyses* associated with four-element arrays. Sec. 5.0 will address the *synthesis* of four-element arrays and will provide techniques by which the optimum array of any length $\ell = p + q + r$ half-wavelengths can be readily synthesized.

5.0 SYNTHESIS OF OPTIMUM FOUR-ELEMENT ARRAYS

This section provides the theoretical basis for synthesizing the optimum-realizable four-element cascaded end-phase array of arbitrary length $\ell \geq 4$ half-wavelengths. (Note: the case $\ell = 3$ is trivial; the array consists of four channels separated by spacings $p = q = r = 1$ half-wavelength.)

It is shown first that the ideal numerators to employ in the subarray ratios $\mathcal{R}_i = m_i/n_i$ are just $m_i = \sqrt{\ell}$. Of course, this condition can be met only for those cases in which ℓ is a perfect square. Next, an ideal-unrealizable array (achieving the minimum possible p_a) is defined. The only four-element array for which this ideal condition can be met is the one defined by $p = 1$, $q = 1$, and $r = 2$; $\ell = 4$. The performance of an array of any other length can approach, but never equal, the performance of the ideal-unrealizable array for that length. Interestingly, Moffet [22], citing a result due to Arsac, shows that the longest zero-redundancy array in spatial-frequency terms, from the radio-astronomy art, regardless of the number of elements, cannot exceed $\ell = 6$, with $n = 4$ elements.

The concept of the ideal-unrealizable array is quite useful, nevertheless, because it leads to a direct approximate synthesis procedure. This initial procedure assumes independence of subarray ambiguities but achieves the twin objectives of (a) readily visualized physical spacing interpretations, and (b) rapid convergence to a region of low p_a so that an exact-p_a analysis on only a very small set of candidate arrays need be done.

The synthesis procedures given in this section lead to a specification of the channel spacings for the optimum-realizable (minimum physically realizable probability of ambiguity) array of arbitrary length under the assumption of channel-pair phase errors that are Gaussian, zero-mean with equal standard deviations. This assumption simplifies the analysis and subsequent synthesis, and in practice is not too restrictive. This is because the phase errors in channels comprised of several components in cascade (see Sec. 3.1) approach statistical regularity.

For a procedure to be exact, it must of course, take account of possible dependence, or correlation between the ambiguities in subarray 1 and those in subarray 2. This dependence is indicated by the absolute magnitude of an array-to-array correlation coefficient. For equal channel-pair phase errors, the correlation coefficient is a function only of the subarray ratio integers (or equivalently, the array spacing integers). A knowledge of this correlation coefficient, in conjunction with the ambiguity variables previously defined in Sec. 4.0, enables one to define the complete bivariate ambiguity density function (actually, the no-ambiguity density function). Integrating this function between the appropriate limits provides the probability of "no ambiguity," and ultimately, the probability of ambiguity.

For many cases of interest, the array p_a is only a weak function of the array-to-array correlation coefficient. The value of the exact formulation, including the array-to-array correlation coefficient, is that a four-element array of *any* configuration, subject to various channel-pair phase errors, can be precisely characterized. For example, arrays in which more than one antenna are switched sequentially into a common channel (to minimize hardware) can be exactly analyzed upon derivation of the appropriate subarray-to-subarray correlation coefficient.

In the final portions of this section, the array length is characterized for synthesis purposes as falling into one of three classes. These are Class I (ℓ = perfect square), Class II (ℓ = geometric mean between successive square arrays), and Class III (ℓ = any length not falling into Classes I and II). Examples of an optimum-realizable synthesis for each of these array classes are given.

The section closes with tabulated exact p_a (including the effect of array-to-array correlation) for optimum-realizable, four-element cascaded end-phase arrays of various lengths from $\ell = 4$ to 100 half-wavelengths, with channel-pair phase error as a parameter. It may be noted that very early multielement interferometer configurations based on a binary progression of spacings: $p = 1$, $p + q = 2$, $p + q + r = 4$, $p + q + r + s = 8$, etc., [23], inherently have a very high resistance to ambiguities for the usual range of channel-pair phase errors (even when relatively coarse quantizing of electrical phase is done). Thus, based on the phase-tracking performance associated with presently available microwave components, such a multielement design approach represents extreme (and uneconomical) overdesign.

5.1 Optimum Numerators m_i for the Subarray Ratios $\mathcal{R}_i$ in n-Element Arrays

In synthesizing n-element arrays of a given length ℓ, it is desirable to have a procedure for obtaining the particular set (or sets) of subarray ratios $\mathcal{R}_i$, $i = 1, 2, \ldots, n-2$ that will provide the lowest overall p_a, subject to given $\sigma_{\text{CH PR}}$. (The optimum $\mathcal{R}$, for $n = 3$ element arrays, has already been formulated in Sec. 3.0.)

Since the array length $\ell = m_1 m_2/\alpha$ in four-element arrays, it is natural to focus attention on the numerators m_i in the subarray ratios $\mathcal{R}_i = m_i/n_i$. For four-element cascaded end-phase arrays, the optimum (in general, unrealizable) $\mathcal{R}_1$ and $\mathcal{R}_2$ are readily derived. The generalization to $n \geq 5$, i.e., three or more subarray ratios $\mathcal{R}_i$, follows easily.

Making use of Eq. (3-19) and the summary material in Eqs. (4-18a) through (4-18i) results in the overall probability of "no-ambiguity," i.e., probability of "correct," $p_{c\text{-overall}}$, in a four-element cascaded end-phase array, of

$$p_{c\text{-overall}} = (1 - p_{a_1})(1 - p_{a_2})$$

$$= \prod_{i=1}^{2} \left[\frac{1}{\sqrt{2\pi}} \int_{-\alpha_i \pi/\sigma_{\phi_i}}^{\alpha_i \pi/\sigma_{\phi_i}} \exp(-t_i^2/2)\, dt_i \right], \tag{5-1}$$

where

$$\sigma_{\phi_1} = \sigma_{\text{CH-PR}} [m_i^2 - m_i n_i + n_i^2]^{1/2},$$

$$\alpha_i = 1, \quad i = 1,$$

$$= \alpha, \quad i = 2, \quad \alpha = \text{factor common to } m_1 \text{ and } n_2.$$

Equation (5-1a) assumes, of course, that ambiguities in subarray 2 (resolved by subarray 1) are independent of ambiguities in subarray 1. In Sec. 5.4, an additional development will include the effects of correlated subarray ambiguities. It will be seen that optimum subarray ratios are only weak functions of subarray correlation coefficients.

It is convenient to normalize the n_i in Eq. (5-1) to the associated m_i, as

$$\sigma_{\phi_1} = m_1 \sigma_{\text{CH-PR}} \left[1 - \frac{n_1}{m_1} + \left(\frac{n_1}{m_1} \right)^2 \right]^{1/2}$$

$$= m_1 \sigma_{\text{CH-PR}} \left[1 - a + a^2 \right]^{1/2}, \quad a = n_1/m_1, \quad 0 < a < 1, \tag{5-2a}$$

and

$$\sigma_{\phi_2} = m_2 \sigma_{\text{CH-PR}} \left[1 - b + b^2 \right]^{1/2}, \quad b = n_2/m_2, \quad 0 < b < 1. \tag{5-2b}$$

From Eq. (4-18c), the array length ℓ is

$$\ell = p + q + r = \frac{m_1 m_2}{\alpha}.$$

For ℓ constant, and with subarray ratio optimization carried out with respect to m_1 (for convenience), m_2 is given by

$$m_2 = \frac{\alpha \ell}{m_1}. \tag{5-3}$$

Thus, with Eq. (5-3), the integration limits ($\pm$) in the integral forms of p_{c_i} in Eq. (5-1a) become

$$\text{Subarray 1} \quad \frac{\pi}{\sigma_{\phi_1}} = \frac{\frac{\pi}{\sigma_{\text{CH-PR}}}}{m_1 (1 - a + a^2)^{1/2}}, \tag{5-4a}$$

and

$$\text{Subarray 2} \quad \frac{\alpha\pi}{\sigma_{\phi_2}} = \frac{\frac{\alpha\pi}{\sigma_{\text{CH-PR}}}}{m_2 (1 - b + b^2)^{1/2}}$$

$$= \frac{m_1 \frac{\pi}{\sigma_{\text{CH-PH}}}}{\ell (1 - b + b^2)^{1/2}}. \tag{5-4b}$$

Functions of the form $(1 - x + x^2)^{1/2}$, $0 < x < 1$, have a single minimum of $\sqrt{0.75} = 0.866$, at $x = 0.5$, compared to end point values of 1.000 at $x = 0, 1$. Independent selection of $a = n_1/m_1$ and $b = n_2/m_2$ is, in general, not possible because m_1 and n_2 are both related to the same array spacing $p + q$. But, to establish optimum realizable m_i, we can

assume that a and $b = 0$ or 1, with negligible error. The integration limits of Eq. (5-4a, b) are now approximated by

$$\text{Subarray 1} \qquad \frac{\pi}{\sigma_{\phi_1}} \approx \frac{\pi}{\frac{\sigma_{\text{CH-PR}}}{m_1}}$$

$$\approx \frac{k_0}{m_1}\,, \tag{5-5a}$$

and

$$\text{Subarray 2} \qquad \frac{\alpha\pi}{\sigma_{\phi_2}} \approx \frac{m_1 k_0}{\ell}\,, \tag{5-5b}$$

where

$$k_0 \equiv \frac{\pi}{\sigma_{\text{CH-PR}}}\,.$$

If $m_1 = \sqrt{\ell}$, both integration limits in Eq. (5-5) are equal, and $p_{c\text{-overall}} = p_{c_1}^2 = p_{c_2}^2$.

As in numerous related problems in communications technology in which there is freedom to vary parameters to minimize overall probability of error, a value of $\sqrt{\ell}$ is readily shown by assuming that $m_1' = m_{1\text{-OPT}} + \Delta m_1$ is actually the optimum value and then proving the converse.

Assume that $\Delta m_1/m_1 = \delta << 1$. Then, in Eq. (5-5), the integration limits are

$$\text{Subarray 1} \qquad \frac{\pi}{\sigma_{\phi_1}} = \frac{k_0}{m_1(1+\delta)} \approx \frac{k_0}{\sqrt{\ell}}\,(1-\delta)\,, \tag{5-6a}$$

and

$$\text{Subarray 2} \qquad \frac{\alpha\pi}{\sigma_{\phi_2}} \approx \frac{k_0}{\sqrt{\ell}}\,(1+\delta)\,. \tag{5-6b}$$

For small changes in integration limits, each p_{c_i} in Eq. (5-1a) can be expressed as

$$p_{c_1} = \Phi\left(\frac{k_0}{\sqrt{\ell}}\right) - \frac{\delta k_0}{\sqrt{\ell}} \cdot \frac{2}{\sqrt{2\pi}} \exp\left(-\frac{k_0}{\sqrt{\ell}}\right) \tag{5-7a}$$

and

$$p_{c_2} = \Phi\left(\frac{k_0}{\sqrt{\ell}}\right) + \frac{\delta k_0}{\sqrt{\ell}} \cdot \frac{2}{\sqrt{2\pi}} \exp\left(-\frac{k_0}{\sqrt{\ell}}\right), \tag{5-7b}$$

where

$$\Phi(x) = \frac{1}{\sqrt{2\pi}} \int_{-x}^{x} \exp\left(\frac{-t^2}{2}\right) dt.$$

The overall p_c thus becomes

$$p_{c\text{-overall}} \approx \Phi^2\left(\frac{k_0}{\sqrt{\ell}}\right) - \left[\frac{\delta k_0}{\sqrt{\ell}} \sqrt{\frac{2}{\pi}} \exp\left(-\frac{k_0}{\sqrt{\ell}}\right)\right]^2. \tag{5-8}$$

The overall probability of correct ambiguity resolution, $p_{c\text{-overall}}$, is maximum when $\delta = 0$, proving that the optimum value for m_1 is

$$m_{1\text{-OPT}} = \sqrt{\ell}, \quad n = 4 \text{ elements}. \tag{5-9}$$

The generalization for arbitrary $n \geq 3$ is obviously

$$m_{1\text{-OPT}} = [\ell]^{1/(n-2)}, \quad n \geq 3 \text{ elements}, \tag{5-10}$$

taking into account that an n-element array defines $(n-1)$ element spacings, and a minimum set (for ambiguity resolution) of $(n-2)$ subarray ratios $\mathcal{R}_l$ and associated m_l.

5.2 Integration Limits in Ideal-Unrealizable and Realizable Arrays

Determination of particular spacings for the lowest p_a in a four-element array of a given length ℓ can be accomplished by exhaustively iterating Eq. (5-1) through all possible m_l and n_l defined by p, q, and r, and selecting the nonredundant array that exhibits the lowest p_a. This determination is not necessary if the concept of the ideal-unrealizable array is utilized.

Consider a four-element array in which the length ℓ, for generality, is not a perfect square. Equation (5-9) from the previous section defines the ideal $m_{1\text{-ID}} = m_{2\text{-ID}}$ as $\sqrt{\ell}$, which is not an integer if $\ell \neq l^2$, $l \geq 2$. If any considerations of multiple ambiguities over the field of view are disregarded (because of common factors in the m_l and n_l subarray ratio integers), the ideal (ID) n_l associated with m_l are just

$$n_{l\text{-ID}} = \frac{m_{l\text{-ID}}}{2} = \frac{\sqrt{\ell}}{2}.$$

Then, the integration limits (IL_l) in Eq. (5-1) for p_c for these subarrays are

$$IL_{1\text{-ID}} = IL_{2\text{-ID}} = \frac{\pi}{\sigma_{CH\text{-}PR}} \frac{1}{[m_{l\text{-ID}}^2 - m_{l\text{-ID}} n_{l\text{-ID}} + n_{l\text{-ID}}^2]^{1/2}}$$

$$= \frac{\pi}{\sigma_{CH\text{-}PR}} \frac{1}{\sqrt{\ell}} \frac{1}{\sqrt{1 - \frac{1}{2} + \frac{1}{4}}}$$

$$= \frac{k_0}{\sqrt{\ell}} \frac{2}{\sqrt{3}}, \tag{5-11}$$

where

$$k_0 \equiv \frac{\pi}{\sigma_{CH\text{-}PR}}.$$

An example of the use of this concept is an array whose length is 12. By definition, $m_{1\text{-ID}} = m_{2\text{-ID}} = \sqrt{12} = 3.4641\ldots$; $n_{1\text{-ID}} = n_{2\text{-ID}} = 1.7321\ldots$. No p, q, and r exist such that $p + q + r = 12$ *and* $(p + q)/p = 2{:}1$, $(p + q + r)/(p + q) = 2{:}1$. If such an array existed, it would exhibit the lowest p_a of all arrays of length 12. Hence, the term ideal-unrealizable array seems appropriate.

Arrays which are realizable, and which approach, but do not necessarily equal, the performance of the ideal array are called "optimum-realizable."

Realizable (RE) arrays have an integration-limit (IL) product given by

$$IL_{l\text{-RE}} = k_0 \frac{\alpha_l}{(m_l^2 - m_l n_l + n_l^2)^{1/2}}, \tag{5-12}$$

where

$\alpha_1 = 1$,

$\alpha_2 =$ factor common to m_1 and n_2,

$k_0 = \frac{\pi}{\sigma_{CH\text{-}PR}}$, as in Eq. (5-11).

Each of the $IL_{l\text{-RE}}$ can be expressed as the sum of $IL_{l\text{-ID}}$ and a deviation from this ideal-unrealizable integration limit, as follows. For $IL_{1\text{-RE}}$, we have

$$IL_{1\text{-RE}} = k_0 \frac{1}{(m_1^2 - m_1 n_1 + n_1^2)^{1/2}} \tag{5-13a}$$

$$= \frac{2k_0}{\sqrt{3\ell}} \left[\frac{\sqrt{3\ell}}{2(m_1^2 - m_1 n_1 + n_1^2)^{1/2}} \right] \tag{5-13b}$$

$$= \frac{2k_0}{\sqrt{3\ell}} [1 + \delta_1]. \tag{5-13c}$$

Equating the terms within the brackets in Eq. (5-13b) and (5-13c) defines

$$\delta_1 = \frac{(3/4 \cdot \ell)^{1/2}}{(m_1^2 - m_1 n_1 + n_1^2)^{1/2}} - 1 . \tag{5-14}$$

If the form $d_1 = 2k_0/\sqrt{3\ell} \cdot \delta_1$ is used in conjunction with Eqs. (5-13) and (5-14), it is easy to express $IL_{1\text{-RE}}$ in the form

$$IL_{1\text{-RE}} = \frac{2k_0}{\sqrt{3\ell}} + k_0 \left[\frac{1}{(m_1^2 - m_1 n_1 + n_1^2)^{1/2}} - \frac{2}{\sqrt{3\ell}} \right]$$

$$= IL_{1\text{-ID}} + d_1 . \tag{5-15}$$

By a similar development, it can be shown that

$$IL_{2\text{-RE}} = \frac{2k_0}{\sqrt{3\ell}} + k_0 \left[\frac{\alpha}{(m_2^2 - m_2 n_2 + n_2^2)^{1/2}} - \frac{2}{\sqrt{3\ell}} \right]$$

$$= IL_{2\text{-ID}} + d_2 . \tag{5-16}$$

The only realizable four-element array for which $IL_{i\text{-RE}} = IL_{i\text{-ID}}$ is the one in which $p = 1$, $q = 1$, $r = 2$; $\ell = 4$. Here, $m_1 = m_2 = 2$, $n_1 = n_2 = 1$, $\alpha = 1$. Thus,

$$d_i = k_0 \left[\frac{1}{(2^2 - 2 \cdot 1 + 1^2 = 3)^{1/2}} - \frac{2}{\sqrt{3 \cdot 4}} \right]$$

$$= k_0 \left[\frac{1}{\sqrt{3}} - \frac{1}{\sqrt{3}} \right] = 0 , \qquad i = 1, 2 ,$$

and hence,

$$IL_{1\text{-RE}} = IL_{2\text{-RE}} = IL_{1\text{-ID}} = IL_{2\text{-ID}} = \frac{2k_0}{\sqrt{3\ell}} = \frac{\pi}{\sqrt{3}\ \sigma_{\text{CH-PR}}} .$$

Other arrays approach, but do not satisfy, the relations $IL_{i\text{-RE}} = IL_{i\text{-ID}}$ because the ratio m_i/n_i can equal 2 only for $\mathcal{R}_i = 2{:}1$. The d_i in Eqs. (5-15) and (5-16) are a measure of how a realizable array differs in performance from an ideal-unrealizable array. Synthesis procedures based on the concept of deviation from the condition of ideal-unrealizability will be given in the next subsection.

5.3 Synthesis of Cascaded End-phase Four-element Arrays

The basis of the synthesis procedures to be discussed involves the subarray 1 numerator m_1 and manipulations of the two realizable integration limits, $IL_{1\text{-}RE}$ and $IL_{2\text{-}RE}$. The standard forms for these two limits are

$$IL_{1\text{-}RE} = k_0 \frac{1}{(m_1^2 - m_1 n_1 + n_1^2)^{1/2}} \tag{5-17a}$$

and

$$IL_{2\text{-}RE} = k_0 \frac{\alpha}{(m_2^2 - m_2 n_2 + n_2^2)^{1/2}} . \tag{5-17b}$$

In this form, the dependence of the integration limits on array length ℓ is implicitly, rather than explicitly, expressed. An equivalent form for $IL_{2\text{-}RE}$ is more suitable for array synthesis.

Use of Eq. (4-18c) from Sec. 4 yields equivalent forms for m_2 and n_2;

$$m_2 = \frac{\ell\alpha}{m_1} \quad \text{and} \quad n_2 = \frac{(p+q)\alpha}{m_1} .$$

When these substitutions are made in Eq. (5-17b), and some simplification is done, the result is

$$IL_{2\text{-}RE} = k_0 \frac{1}{\sqrt{\left(\frac{\ell}{m_1}\right)^2 - \left(\frac{\ell}{m_1}\right)\left(\frac{p+q}{m_1}\right) + \left(\frac{p+q}{m_1}\right)^2}} . \tag{5-18}$$

The channel 1 to channel 3 spacing integer, $p + q$, can be equal only to a multiple of the subarray 1 numerator integer m_1 as,

$$p + q = jm_1 .$$

Furthermore, $p + q$ cannot exceed $\ell = p + q + r$. Thus, the $IL_{1\text{-}RE}$ (in a form suitable for synthesizing realizable arrays) become

$$IL_{1\text{-}RE} = k_0 \frac{1}{(m_1^2 - m_1 n_1 + n_1^2)^{1/2}} , \tag{5-19a}$$

and

$$IL_{2\text{-}RE} = k_0 \frac{m_1}{(\ell^2 - \ell(jm_1) + (jm_1)^2)^{1/2}} , \tag{5-19b}$$

where

$$k_0 = \frac{\pi}{\sigma_{\text{CH-PR}}},$$

$$j = 1, 2, \ldots, \frac{\ell}{m_1}\Bigg], \text{ where } x] \text{ indicates the nearest integer less than } x.$$

So far, nothing more has been accomplished than to express the $\text{IL}_{j\text{-RE}}$ in a slightly different form to emphasize that subarray 2 is more logically thought of as a function of the overall array length ℓ and the subarray 1 numerator integer m_1. If one wanted to establish that a particular set of m_j, n_j is the optimum-realizable for given ℓ, integration of Gaussian error functions (as in Eq. (5-1)) seems necessary. These integrations can be avoided by the use of a simple test function which involves the expansion of the error function about a specific value.

The first step in determining this test function is to express Eq. (5-19b) in the form of Eq. (5-16); that is, as the sum of $\text{IL}_{2\text{-RE}}$ and a term d_2 which represents the deviation of $\text{IL}_{2\text{-RE}}$ from $\text{IL}_{2\text{-ID}}$. This is readily done. The result, with Eq. (5-15) for $\text{IL}_{1\text{-RE}}$ repeated below for ease of comparison, is

$$\text{IL}_{1\text{-RE}} = \frac{2k_0}{\sqrt{3\ell}} + k_0\left[\frac{1}{(m_1^2 - m_1 n_1 + n_1^2)^{1/2}} - \frac{2}{\sqrt{3\ell}}\right]$$

$$= \text{IL}_{1\text{-ID}} + d_1, \tag{5-20a}$$

$$\text{IL}_{2\text{-RE}} = \frac{2k_0}{\sqrt{3\ell}} + k_0\left[\frac{m_1}{[\ell^2 - \ell(jm_1) + (jm_1)^2]^{1/2}} - \frac{2}{\sqrt{3\ell}}\right]$$

$$= \text{IL}_{2\text{-ID}} + d_2. \tag{5-20b}$$

Equation (A-9) of Appendix A gives a three-term Taylor's series expansion of the Gaussian error integral about a specific argument, as

$$A\left(\frac{X + \Delta}{\sigma}\right) \approx A\left(\frac{x}{\sigma}\right) + Z\left(\frac{x}{\sigma}\right)\left[2\left(\frac{\Delta}{\sigma}\right) - \left(\frac{\Delta}{\sigma}\right)^2\left(\frac{x}{\sigma}\right) + \frac{1}{3}\left(\frac{\Delta}{\sigma}\right)^3\left(\frac{x^2}{\sigma^2} - 1\right)\right], \tag{5-21}$$

where

$$A\left(\frac{x}{\sigma}\right) = \frac{1}{\sqrt{2\pi}}\int_{-x/\sigma}^{x/\sigma} e^{-t^2/2}\, dt,$$

$$Z\left(\frac{x}{\sigma}\right) = \frac{1}{\sqrt{2\pi}}\, e^{-x^2/2\sigma^2}.$$

For $x/\sigma = 2.000$ (i.e., the argument of $A(\cdot)$ is set at the 2σ value), $A(x + \Delta/\sigma)$ becomes

$$A\left(2 + \frac{\Delta}{\sigma}\right) \approx A(2) + \frac{e^{-2}}{\sqrt{2\pi}}\left[2\left(\frac{\Delta}{\sigma}\right) - 2\left(\frac{\Delta}{\sigma}\right)^2 + \left(\frac{\Delta}{\sigma}\right)^3\right]. \tag{5-22}$$

Equation (5-22) is an approximation to the Gaussian error integral in the vicinity of an argument set at the 2σ value. Note that $A(2) = 0.9544997$. The corresponding compound p_a (assuming independence) is $1 - A(2)A(2) = 0.08893$ or 8.893%.

Now, k_0 is defined as $\pi/\sigma_{\text{CH-PR}}$. Thus, to force $\text{IL}_{i\text{-ID}}$ to assume the value of 2.000 (strictly for simplicity in generating a useful test function) regardless of array length ℓ, Eq. (5-11) can be set equal to 2.000 and solved for the appropriate value of $\sigma_{\text{CH-PR}}$, as

$$\text{IL}_{i\text{-ID}} = \frac{\frac{2\pi}{\sqrt{3\ell}}}{\sigma_{\text{CH-PR}}} = 2.000,$$

or

$$\sigma_{\text{CH-PR}}\big]_2 = \frac{\pi}{\sqrt{3\ell}}. \tag{5-23}$$

Use of this value of $\sigma_{\text{CH-PR}}$ in Eq. (5-20a) and (5-20b) yields

$$\text{IL}_{1\text{-RE}} = 2 + \left[\sqrt{\frac{3\ell}{m_1^2 - m_1 n_1 + n_1^2}} - 2\right]$$

$$= 2 + \left(\frac{\Delta_1}{\sigma}\right), \tag{5-24a}$$

and

$$\text{IL}_{2\text{-RE}} = 2 + \left[\frac{m_1\sqrt{3\ell}}{\sqrt{\ell^2 - \ell(jm_1) + (jm_1)^2}} - 2\right]$$

$$= 2 + \left(\frac{\Delta_2}{\sigma}\right). \tag{5-24b}$$

The approximate probabilities that subarray 1 and subarray 2 (resolved by subarray 1) are unambiguous are

$$p_{c\cdot 1} \approx 0.9544997 + \frac{1}{\sqrt{2\pi}} e^{-2}\left[2\left(\frac{\Delta_1}{\sigma}\right) - 2\left(\frac{\Delta_1}{\sigma}\right)^2 + \left(\frac{\Delta_1}{\sigma}\right)^3\right] \tag{5-25a}$$

and

$$p_{c\cdot 2} \approx 0.9544997 + \frac{1}{\sqrt{2\pi}} e^{-2}\left[2\left(\frac{\Delta_2}{\sigma}\right) - 2\left(\frac{\Delta_2}{\sigma}\right)^2 + \left(\frac{\Delta_2}{\sigma}\right)^3\right]. \tag{5-25b}$$

The procedure for obtaining an approximate array synthesis, one not taking into consideration subarray-to-subarray correlation of ambiguities, can be summarized as follows.

- Choose a trial m_1 close to $\sqrt{\ell}$

- Choose an appropriate value of q_1 from Table 3-4 of Sec. 3.0.

- $IL_{1\text{-}RE}$ of Eq. (5-24a) is thus defined.

- Compute a set of trial values of $IL_{2\text{-}RE}$ by iterating through Eq. (5-24b) with $j = 1, 2, \ldots, \ell/m_1]$ where $\cdot]$ indicates the nearest integer less than the ratio ℓ/m_1.

- Substitute the trial $IL_{1\text{-}RE}$ and the set of trial $IL_{2\text{-}RE}$ into Eq. (5-25a) and Eq. (5-25b) and compute the overall probability-of-correct product $p_{c_1} p_{c_2}$.

- The trial array achieving the highest $p_{c_1} p_{c_2}$ product is the best array for the particular trial m_1 that was chosen initially.

These steps can be repeated for other trial values of m_1, and the best-performing arrays obtained for each m_1 can then be compared to determine the optimum-realizable array. This approximate procedure does not take into account a possible subarray-to-subarray correlation of ambiguities. Thus, several arrays may be obtained, all of which have the same independent probability of ambiguity. Also, since this approximate procedure is based on an expansion of the normal probability integral (evaluated in the vicinity of argument 2.0000), a slightly different array may actually have a somewhat better p_a at a lower value of $\sigma_{CH\text{-}PR}$ (implying a larger value of the probability function integral argument) than the array found by this procedure. The designer may have to perform an exact analysis at the specific value of $\sigma_{CH\text{-}PR}$ that will be used for a particular application.

Both the procedure outlined above and an exact analytical form for p_a, are easily programmed. For the convenience of the designer, these programs are collected in Appendix B. The use of these programs will be described fully in Sec. 5.5.

In Sec. 5.4, an exact relation—one which considers the effect of subarray-to-subarray correlation of ambiguities—for the p_a in *any* four-element array will be derived. This expression will become the basis for determining the optimum-realizable array (from p_a considerations) in the cascaded end-phase configuration (from the development of Sec. 4.5) of *any* length.

5.4 Exact p_a for Four-element Arrays

In the previous section, a synthesis procedure was given for cascaded end-phase four-element arrays of arbitrary length $\ell \geq 3$ (in half-wavelengths). The procedure was approximate, as the possibility that ambiguities in subarray 1 might be correlated with ambiguities in subarray 2 was ignored. As will be shown in Sec. 5.5, certain arrays having the same length ℓ apparently have the same probability of ambiguity, even though the element spacings p, q, and r are different if correlation is ignored. In actuality, there is a slight dependence of p_a on array arrangement for fixed ℓ.

This dependence is most conveniently expressed in terms of an array-to-array correlation coefficient. This correlation coefficient $\rho_{a_1 a_2}$ will be shown to be a function of the array configuration (e.g., cascaded end-phase, hybrid midphase, etc.) as well as array spacings (e.g., the actual p, q, and r employed).

The ambiguity constraints of a four-element cascaded end-phase array, using modified forms of Eq. (4-18d, e), can be written as

$$\text{Subarray 1} \quad -\pi < [\phi_1 = n_1 \Delta\varphi_{1,3} - m_1 \Delta\varphi_{1,2}] < \pi , \tag{5-26a}$$

and

$$\text{Subarray 2} \quad -\pi < [\phi_2 = n_2 \Delta\varphi_{1,4} - m_2 \Delta\varphi_{1,3}] < \pi . \tag{5-26b}$$

The above two random variables (r.v.) Φ_1 and Φ_2 are Gaussian, since they are linear combinations of various channel-pair phase errors $\Delta\varphi_{1,j} = \Delta\varphi_1 - \Delta\varphi_j (j = 2, 3, 4)$ which are assumed Gaussian, zero mean according to the development in Sec. 3.1. The variances of these ambiguity variables, if Eq. (3-11) is used, are

$$\sigma_{\phi_1}^2 = m_1^2\sigma_{1,2}^2 - 2\rho_{e_1} m_1 n_1 \sigma_{1,2}\sigma_{1,3} + n_1^2\sigma_{1,3}^2 \tag{5-27a}$$

and

$$\sigma_{\phi_2}^2 = m_2^2\sigma_{1,3}^2 - 2\rho_{e_2} m_2 n_2 \sigma_{1,3}\sigma_{1,4} + n_2^2\sigma_{1,4}^2 , \tag{5-27b}$$

$$\left.\begin{aligned} \sigma_{1,2}^2 &= \sigma_1^2 + \sigma_2^2 \\ \sigma_{1,3}^2 &= \sigma_1^2 + \sigma_3^2 \\ \sigma_{1,4}^2 &= \sigma_1^2 + \sigma_4^2 \end{aligned}\right\}$$ These define relations between channel-pair error variances and channel error variances,

$$\rho_{e_1} = \frac{\sigma_1^2}{\sigma_{1,2}\sigma_{1,3}} \quad (=0.5, \text{ all } \sigma_i \text{ equal}) ,$$

$$\rho_{e_2} = \frac{\sigma_1^2}{\sigma_{1,3}\sigma_{1,4}} \quad (=0.5, \text{ all } \sigma_i \text{ equal}) .$$

If we allow for possible correlation between the r.v. Φ_1 and Φ_2, their joint density function is [18]

$$p_{\Phi_1\Phi_2}(\varphi_1\varphi_2) = \frac{1}{2\pi\sigma_{\phi_1}\sigma_{\phi_2}\sqrt{1 - \rho_{a_1,a_2}^2}} \times \exp\left\{-\frac{1}{2\left(1 - \rho_{a_1,a_2}^2\right)}\left[\left(\frac{\varphi_1}{\sigma_{\phi_1}}\right)^2 - 2\rho_{a_1,a_2}\cdot\frac{\varphi_1}{\sigma_{\phi_1}}\cdot\frac{\varphi_2}{\sigma_{\phi_2}} + \left(\frac{\varphi_2}{\sigma_{\phi_2}}\right)^2\right]\right\}. \tag{5-28}$$

The subarray 1-to-subarray 2 correlation coefficient ρ_{a_1,a_2} is defined by

$$\rho_{a_1,a_2} = \frac{E[\Phi_1 \Phi_2]}{\sigma_{\phi_1} \sigma_{\phi_2}} . \tag{5-29}$$

The probability that $|\varphi_1| < \pi$ and $|\varphi_2| = \alpha\pi$, i.e., the probability that array ambiguities will be correctly resolved, is

$$p_{c\text{-overall}} = \int_{-\pi}^{\pi} \int_{-\alpha\pi}^{\alpha\pi} p_{\Phi_1 \Phi_2}(\varphi_1, \varphi_2)\, d\varphi_1\, d\varphi_2 . \tag{5-30}$$

Equation (5-30) becomes just

$$p_{c\text{-overall}} = \int_{-\pi}^{\pi} p_{\Phi_1}(\varphi_1)\, d\varphi_1 \int_{-\alpha\pi}^{\alpha\pi} p_{\Phi_2}(\varphi_2)\, d\varphi_2 , \tag{5-31}$$

for $\rho_{a_1,a_2} = 0$.

In general, $\rho_{a_1,a_2} \neq 0$, and to calculate the exact $p_{c\text{-overall}}$ requires (a) determination of ρ_{a_1,a_2} and (b) integration of the bivariate density function of Eq. (5-28) between the appropriate limits.

The array-to-array correlation coefficient is readily found, if Eq. (5-29) is used with Eq. (5-27a, b). The expected value of $(\Phi_1 \Phi_2)$—is given by

$$\begin{aligned} E[\Phi_1, \Phi_2] &= E[(n_1 \Delta\varphi_{1,3} - m_1 \Delta\varphi_{1,2})(n_2 \Delta\varphi_{1,4} - m_2 \Delta\varphi_{1,3})] \\ &= n_1 n_2 E[(\Delta\varphi_1 - \Delta\varphi_3)(\Delta\varphi_1 - \Delta\varphi_4)] \\ &\quad - m_1 n_2 E[(\Delta\varphi_1 - \Delta\varphi_2)(\Delta\varphi_1 - \Delta\varphi_4)] \\ &\quad - n_1 m_2 E[(\Delta\varphi_1 - \Delta\varphi_3)^2] \\ &\quad + m_1 m_2 E[(\Delta\varphi_1 - \Delta\varphi_2)(\Delta\varphi_1 - \Delta\varphi_3)] . \end{aligned} \tag{5-32}$$

The taking of the expected values of the various cross-products of channel-pair error yields

$$E[\Phi_1 \Phi_2] = n_1 n_2 \sigma_1^2 - m_1 n_2 \sigma_1^2 - n_1 m_2 \left(\sigma_1^2 + \sigma_3^2\right) + m_1 n_2 \sigma_1^2 . \tag{5-33}$$

Equation (5-33) expresses $E[\Phi_1 \Phi_2]$ in channel-error form. An equivalent expression, in channel-pair error form is

$$\begin{aligned} E[\Phi_1 \Phi_2] &= n_1 n_2 \rho_{1,3;1,4} \sigma_{1,3} \sigma_{1,4} - m_1 n_2 \rho_{1,2;1,4} \sigma_{1,4} \\ &\quad - n_1 m_2 \rho_{1,3;1,3} \sigma_{1,3}^2 + m_1 m_2 \rho_{1,2;1,3} \sigma_{1,2} \sigma_{1,3} , \end{aligned} \tag{5-34}$$

where

$$\rho_{1,j;1,k} \equiv \frac{E[(\Delta\varphi_1 - \Delta\varphi_j)(\Delta\varphi_1 - \Delta\varphi_k)]}{\sigma_{1,j}\sigma_{1,k}} .$$

By definition, $\rho_{1,3;1,3} = 1$. Now, if all channel phase errors σ_l are equal, this implies that $\sigma_l^2 = 0.5\,\sigma_{l,j}^2 = 0.5\,\sigma_{\text{CH-PR}}^2$ and that $\rho_{l,j;1,k} = 0.5$, $j \neq k$. For this situation, both forms of $E[\Phi_1\Phi_2]$ become

$$E[\Phi_1\Phi_2] = \frac{1}{2}\,\sigma_{\text{CH-PR}}^2[(n_1n_2 - m_1n_2 + m_1m_2) - 2n_1m_2] , \quad \text{all } \sigma_l^2 = \frac{1}{2}\,\sigma_{\text{CH-PR}}^2 . \tag{5-35}$$

Equation (5-35) can also be expressed as

$$E[\Phi_1\Phi_2] = \frac{1}{2}\,\sigma_{\text{CH-PR}}^2[(m_1 - n_1)(m_2 - n_2) - n_1m_2] , \quad \text{all } \sigma_l^2 = \frac{1}{2}\,\sigma_{\text{CH-PR}}^2 . \tag{5-36}$$

Finally, the use of Eq. (5-36) with Eq. (5-29) yields

$$\rho_{a_1,a_2} = \frac{1}{2}\,\frac{(m_1 - n_1)(m_2 - n_2) - n_1m_2}{(m_1^2 - m_1n_1n_1 + n_1^2)^{1/2}(m_2^2 - m_2n_2 + n_2^2)^{1/2}} , \quad \text{all } \sigma_l^2 = \frac{1}{2}\,\sigma_{\text{CH-PR}}^2 . \tag{5-37}$$

Equation (5-37) is solely a function of the subarray ratio integers for $\sigma_l^2 = 0.5\,\sigma_{\text{CH-PR}}^2$. Furthermore, as with any correlation coefficient, $-1 \leq \rho_{a_1,a_2} \leq 1$.

Array-to-array correlation coefficients for the other four-element array configurations of Fig. 4-1 and Table 4-1 are readily derived. Table 5-1 lists the correlation coefficients for all five array configurations.

It is convenient to define two standardized variables with standard analytical techniques for integrating bivariate density functions, as

$$\mathfrak{X} \equiv \frac{\Phi_1}{\sigma_{\phi_1}} ; \quad \mathfrak{Y} \equiv \frac{\Phi_2}{\sigma_{\phi_2}} .$$

Equation (5-30) is thus transformed into

$$p_{\text{c-overall}} = \int_{-h}^{h} dx \int_{-k}^{k} \frac{1}{2\pi\sqrt{1 - \rho^2}} \exp\left[-\frac{1}{2(1-\rho^2)}\,(x^2 - 2\rho xy + y^2)\right] dy$$

$$= \int_{-h}^{h} dx \int_{-k}^{k} g(x, y, \rho)\, dy , \tag{5-38}$$

where

Table 5-1—Subarray to Subarray Correlation Coefficients for the Four-element Array Configurations of Fig. 4-1

Array Type	Subarray Ratios $\mathcal{R}_1$	Subarray Ratios $\mathcal{R}_2$	Common Spacing	Subarray to Subarray Correlation Coefficient, $\rho_{a,a}$*
Cascaded end-phase	$\mathcal{R}_{1e} = \frac{m_1}{n_1} = \frac{\alpha m_1'}{n_1}$	$\mathcal{R}_{2e} = \frac{m_2}{n_2} = \frac{m_2}{\alpha n_2'}$	$p + q$	$\rho_{a,a} = \frac{1}{2} \frac{(m_1 - n_1)(m_2 - n_2) - n_1 m_2}{(m_1^2 - m_1 n_1 + n_1^2)^{1/2}(m_2^2 - m_2 n_2 + n_2^2)^{1/2}}$
Cascaded midphase	$\mathcal{R}_{1e} = \frac{x_1}{y_1} = \frac{\alpha x_1'}{y_1}$	$\mathcal{R}_{2m} = \frac{x_2}{y_2} = \frac{\alpha x_2'}{y_2}$	$p + q$†	$\rho_{a,a} = -\frac{1}{2} \frac{(x_1 - y_1)(x_2 + y_2) - y_1 y_2}{(x_1^2 - x_1 y_1 + y_1^2)^{1/2}(x_2^2 + x_2 y_2 + y_2^2)^{1/2}}$
Hybrid midphase	$\mathcal{R}_{1m} = \frac{e_1}{f_1} = \frac{e_1}{\alpha f_1'}$	$\mathcal{R}_{2e} = \frac{e_2}{f_2} = \frac{e_2}{\alpha f_2'}$	q	$\rho_{a,a} = \frac{1}{2} \frac{(e_1 + f_1)(e_2 - f_2) + e_1 e_2}{(e_1^2 + e_1 f_1 + f_1^2)^{1/2}(e_2^2 - e_2 f_2 + f_2^2)^{1/2}}$
Additive midphase	$\mathcal{R}_{1m} = \frac{c_1}{d_1} = \frac{c_1}{\alpha d_1'}$	$\mathcal{R}_{2m} = \frac{c_2}{d_2} = \frac{\alpha c_2'}{d_2}$	q	$\rho_{a,a} = -\frac{1}{2} \frac{(c_1 + d_1)c_2 + 2c_1 d_2}{(c_1^2 + c_1 d_1 + d_1^2)^{1/2}(c_2^2 + c_2 d_2 + d_2^2)^{1/2}}$
Multiple end-phase	$\mathcal{R}_{1e} = \frac{g_1}{h_1} = \frac{g_1}{\alpha h_1'}$	$\mathcal{R}_{2e} = \frac{g_2}{h_2} = \frac{g_2}{\alpha h_2'}$	p	$\rho_{a,a} = \frac{1}{2} \frac{(g_1 - h_1)(g_2 - h_2) + g_1 g_2}{(g_1^2 - g_1 h_1 + h_1^2)^{1/2}(g_2^2 - g_2 h_2 + h_2^2)^{1/2}}$

*All $\sigma_i = \frac{1}{2}\sigma_{\text{CH-PR}}$, $i = 1$ to 4. †*After* subarray 1 is resolved and $\Phi_{1,3}$ is determined (see Fig. 4-1).

$$h = \frac{\pi}{\sigma_{\phi_1}},$$

$$k = \frac{\alpha\pi}{\sigma_{\phi_2}},$$

$$\rho = \rho_{a_1,a_2}.$$

Equation (5-38) is the standardized form for the integral of the bivariate Gaussian density function [19,24,25].

An alternate form for $p_{c\text{-overall}}$ which uses the well-known $L(h, k, \rho)$ and $A(x)$ functions [19a]

$$p_{c\text{-overall}} = 2L(h, k, \rho) + 2L(h, k, -\rho) + A(h) + A(k) - 1, \tag{5-39}$$

where

$$L(h, k, \rho) = \int_h^\infty dx \int_k^\infty g(x, y, \rho)\, dx,$$

$$A(h) = \int_{-h}^{h} \frac{1}{\sqrt{2\pi}} e^{-t^2/2}\, dt = \text{Probability of being correct, subarray 1,}$$

$$A(k) = \int_{-k}^{k} \frac{1}{\sqrt{2\pi}} e^{-t^2/2}\, dt = \text{Probability of being correct, subarray 2 (resolved by 1).}$$

Many expressions for calculating $L(h, k, \rho)$ are available; one which is suitable for $h, k \geq 1$ and $|\rho| < 0.95$ as is the case for arrays of interest in this report, is based on the series expansion [19b]

$$L(h, k, \rho) = Q(h)Q(k) + \sum_{n=0}^{\infty} \frac{Z^{(n)}(h)Z^{(n)}(k)}{(n+1)!}\, \rho^{n+1}, \tag{5-40}$$

where

$$Q(x) = \int_x^\infty \frac{1}{\sqrt{2\pi}} e^{-t^2/2}\, dt,$$

$$Z(x) = \frac{1}{\sqrt{2\pi}} e^{-x^2/2},$$

$$Z^{(n)}(x) = \frac{d}{dx^n} Z(x),$$

$$Z^{(n+2)}(x) = -xZ^{(n+1)}(x) - (n+1)Z^{(n)}(x).$$

A special value of $L(h, k, \rho)$ is

$$L(h, k, 0) = Q(h)Q(k)$$

$$= \frac{1}{4}\,[1 - A(h)]\,[1 - A(k)]\,. \tag{5-41}$$

This indicates statistical independence between ambiguities in subarrays 1 and 2, for $\rho = 0$. Thus,

$$p_{c\text{-overall}} = [1 - A(h)][1 - A(k)] + A(h) + A(k) - 1$$

$$= A(h)A(k)\,. \tag{5-42}$$

Obviously, the overall probability of ambiguity, $p_{a\text{-overall}}$ is $1 - p_{c\text{-overall}}$ from Eq. (5-39), and is given by

$$p_{a\text{-overall}} = 2 - [2L(h, k, \rho) + 2L(h, k, -\rho) + A(h) + A(k)] \tag{5-43}$$

where

$$h = \frac{\pi}{\sigma_{\phi_1}}\,,$$

$$k = \frac{\alpha\pi}{\sigma_{\phi_2}}\,,$$

$$\rho = \frac{E[\Phi_1\Phi_2]}{\sigma_{\phi_1}\sigma_{\phi_2}}\,,$$

and the functions $L(h, k, \rho)$, $A(h)$, $A(k)$ are as defined by Eq. (5-39).

The following points may be noted about Eq. (5-43).

- $p_{a\text{-overall}}$ is independent of the arithmetic sign of ρ, since the sum $L(h, k, \rho) + L(h, k, -\rho)$ is independent of the sign of ρ.

- $p_{a\text{-overall}}$ is greatest (other parameters being equal) when ρ is zero, since $L(h, k, \rho) + L(h, k, -\rho) \geq 2L(h, k, 0)$.

- The formula for p_a is general and can be used to calculate the performance of any four-element array, where h, k, and ρ are properly defined.

5.5 Tabulated p_a and Array Spacings for Optimum-Realizable Four-Element Cascaded End-Phase Arrays

In this section, the probability of ambiguity, p_a, the array spacings corresponding to the optimum realizable arrays for $4 \leq \mathcal{L} \leq 42$, and selected lengths from 42 to 100 half-wavelengths will be given for the cascaded end-phase configuration. It was shown in

Sec. 4.5 that the performance of the cascaded end-phase configuration exceeds that of all other four-element array configurations.

It will be convenient to use as the point of departure in obtaining these optimum spacings the fact that if the overall array length ℓ is a perfect square, then the individual subarray numerators are $\sqrt{\ell}$ (Sec. 5.1). An example is $\ell = 16$; here $m_1 = m_2 = 4$. (It will be seen that expression of m_2 as ℓ *without* removing a common factor α, will in general lead to a consistent procedure for classifying arrays in which ℓ is *not* a perfect square.)

After considering the so-called square arrays as those in which ℓ is equal to i^2, $i = 2, 3, 4, \ldots$, it is natural to examine arrays in which ℓ is equal to the product $i(i + 1)$. An example is $\ell = 20$. Here $i = 4$, $i + 1 = 5$. It may also be noted that 20 is the geometric mean of 16 and 25. That is, "mid-square" arrays are those whose overall array lengths are "midway," in a geometric sense, between adjacent "square" arrays.

A final part of this array classification methodology will group into one remaining category those arrays whose overall lengths do not fall into the other two categories.

This array classification may be summarized as follows:

Class I: $\ell = i^2, i = 2, 3, 4, \ldots$

Class II: $\ell = i(i + 1), i = 2, 3, 4, \ldots$

Class III: $\ell =$ *any* length not falling into Classes I or II.

The synthesis procedure is based on the development in Sec. 5.3, and is mechanized as computer program CLSIII (see Appendix B for collected programs). In the remainder of this section, an example of the use of CLSIII for each of the array classes will be given. Then p_a for various array lengths vs $\sigma_{\text{CH-PR}}$ will be tabulated.

Class I

The first example synthesizes the optimum realizable array for $\ell = 25$. The procedure is best described by an examination of a sample printout from CLSIII. Table 5-2a shows the CLSIII printout for $\ell = 25$, when an m_1 value of 5 (known by inspection, because 25 is a perfect square) and a trial value of $n_1 = 1$ is used. Candidate values of n_1 can be obtained from Table 3-4, which provides the allowable $p{:}q$ values for use in synthesizing three-element arrays. It will be remembered from Sec. 4.0 that a cascaded end-phase four-element array can be thought of as two three-element arrays.

CLSIII yields for each trial value of $n_2 = jm_1$ (see Eq. 5-19) the parameters

- Ratio $m_2{:}n_2$
- Spacings: p, q, and r in half-wavelengths
- Subarray 1 to subarray 2 correlation coefficient

Table 5-2a--Program CLSIII Printout for $\ell = 25$, $m_1 = 5$; Trial $n_1 = 1$

```
550 DATA 25,5

CLSIII


SIGMA-CHANNEL-PAIR = 20.7846  ELECTRICAL DEGREES
OVERALL ARRAY LENGTH = 25 HALF-WAVELENGTHS
M1 = 5

THE TRIAL VALUE OF N1 IS   ?1


  M1:N1***M2:N2
ALPHA,LENGTH    P***Q***P     CO.COEFF.        P-AMB        REDUN?
                                               (PCT)


 5 : 1 *** 25 : 5
 5 , 25         1  4  20      0.261905        11.4106        99999


 5 : 1 *** 25 : 10
 5 , 25         2  8  15      0.175219        10.2966        99999


 5 : 1 *** 25 : 15
 5 , 25         3  12  10     7.50239E-2      10.2966        99999


 5 : 1 *** 25 : 20
 5 , 25         4  16  5      -2.38095E-2     11.4106        99999
```

- Overall compound probability of ambiguity (assuming subarray/ambiguities are independent) in percent

- Test of whether the resultant synthesized array is redundant, i.e., whether p, q, and r have common factors.

It is stressed that CLSIII provides a synthesis under the assumption that subarray ambiguities are independent. The correlation coefficient is displayed as an aid to the user to show that among arrays with the same *independent* compound p_a, the array with the largest absolute-value correlation coefficient will have the lowest overall p_a. The effect of subarray-to-subarray ρ is secondary, as pointed out in Sec. 5.4. To establish optimality of a particular array configuration, an exact calculation requires consideration of the array correlation coefficient. Table 5-2a shows, that of all arrays of length 25 based on an $m_1:n_1 = 5:1$ ratio, the array $m_1:n_1 \oplus m_2:n_2$, α; $\rho = 5{:}1 \oplus 25{:}10$, 5; +0.175219 is the best. That is, although both the arrays with p, q, and r spacings of 2, 8, 15 or 3, 12, 10 have the same independent p_a, consideration of the correlation coefficient in a exact analysis will show the 2, 8, 15 array to be better.

Of course, the choice of $m_1:n_1 = 5:1$ is unwise, because Table 3-4 shows that the optimum n_1 for a three-element array when $m_1 = 5$ is either $n_1 = 2$, or 3. Tables 5-2b and c result when CLSIII is rerun for $n_1 = 2$ and 3 respectively. There are four candidate arrays

$$5{:}2 \oplus 25{:}10$$
$$5{:}2 \oplus 25{:}15$$
$$5{:}3 \oplus 25{:}10$$
$$5{:}3 \oplus 25{:}15,$$

all exhibiting the same p_a of 9.17% (due to $\sigma_{\text{CH-PR}} = 20.78$ electrical degrees, as forced by the criterion of Eq. (5-23)). Of these four arrays however, the array defined by $5{:}3 \oplus 25{:}15$ has the largest absolute value of correlation coefficient, $\rho = -0.289373$. Consequently, this array has the lowest overall p_a for given $\sigma_{\text{CH-PR}}$ of arrays of length 25. (Exact calculations of p_a will be deferred until approximate synthesis procedures for the other array classes have been described.)

It is easy to show that in Class I arrays the optimum n_i must be equal to or greater than $m_1/2$. If Eq. (5-37) is taken as a starting point, then expression of n_i as $m_i(1 + \delta_i)/2$, where δ_i is a deviation of n_i from $m_i/2$, the array-to-array correlation coefficient can be put into the form

$$\rho_{a,a} = -\frac{1}{2}\,\frac{1 + 3\delta_1 + \delta_2 - \delta_1\delta_2}{(3 + \delta_1^2)^{1/2}(3 + \delta_2^2)^{1/2}}. \tag{5-44}$$

Table 5-2b—Program CLSIII Printout for $\ell = 25$, $m_1 = 5$; Trial $n_1 = 2$

```
550 DATA 25,5

CLSIII


SIGMA-CHANNEL-PAIR = 20.7846  ELECTRICAL DEGREES
@VERALL ARRAY LENGTH = 25 HALF-WAVELENGTHS
M1 = 5

THE TRIAL VALUE @F N1 IS   ?2

  M1:N1***M2:N2
ALPHA,LENGTH    P***Q***R      C@.C@EFF.          P-AMB          REDUN?
                                                  (PCT)


 5 : 2 *** 25 : 5
 5 , 25          2  3  20      5.00626E-2        10.2966         99999


 5 : 2 *** 25 : 10
 5 , 25          4  6  15      -2.63158E-2       9.16857         99999


 5 : 2 *** 25 : 15
 5 , 25          6  9  10      -0.105263         9.16857         99999  <----


 5 : 2 *** 25 : 20
 5 , 25          8  12  5      -0.175219         10.2966         99999
```

Table 5-2c—Program CLSIII Printout for $\ell = 25$, $m_1 = 5$; Trial $n_1 = 3$

```
550 DATA 25,5

CLSIII


SIGMA-CHANNEL-PAIR = 20.7846  ELECTRICAL DEGREES
OVERALL ARRAY LENGTH = 25 HALF-WAVELENGTHS
M1 = 5

THE TRIAL VALUE OF N1 IS   ?3

  M1:N1***M2:N2
ALPHA,LENGTH    P***Q***R     CO.COEFF.        P-AMB          REDUN?
                                                (PCT)

 5 : 3 *** 25 : 5
 5 , 25          3  2  20     -0.175219        10.2966         99999

 5 : 3 *** 25 : 10
 5 , 25          6  4  15     -0.236342        9.16857         99999

 5 : 3 *** 25 : 15
 5 , 25          9  6  10     -0.289474        9.16857         99999  <-------

 5 : 3 *** 25 : 20
 5 , 25          12  8  5     -0.325407        10.2966         99999
```

The δ_i do not now depend on the size of m_i and n_i, but only on their ratio. Hence, even though m_2 and n_2 might be expressed in CLSIII as 25 and 15 respectively, if the common factor $\alpha = 5$ is suppressed, m_2 and n_2 are functionally equivalent to 5 and 3 respectively. It is obvious that subarrays in which $m_i = 5$ must utilize $n_i = 2$ or 3 in order to minimize their respective subarray ambiguities. But, the values of δ_i that *maximize* the correlation coefficient of Eq. (5-44) must have the same algebraic sign. Hence, the δ_i must be positive, which means that the n_i must be equal, and greater than $m_i/2$.

As a second example of a Class I synthesis, consider $\ell = 16$. Table 5-3 shows the result of running program CLSIII for $\ell = 16$. It is seen that for $m_1{:}n_1 \oplus m_2{:}m_2 = 4{:}3 \oplus 16{:}8$, the array is redundant, as indicated by the figure 2 in the REDUN? column. This is the factor by which $p = 6$, $q = 2$, and $r = 8$ are redundant. Thus, the optimum array for $\ell = 16$ is $4{:}3 \oplus 16{:}12$, with array-to-array correlation coefficient = $-0.423077 = -11/26$.

One further observation in respect to Class I arrays is that the optimum subarray ratios automatically ensure that the spacings $p-q-r$ will be maximized. The array $4{:}3 \oplus 16{:}12$ has minimum spacing $q = 3$, whereas the array $4{:}3 \oplus 16{:}4$ has minimum spacing $p = 1$. Thus, for $\ell = 16$, the optimum array can be operated over a 3:1 bandwidth before the shortest spacing approaches one half-wavelength, whereas in the other two arrays, the shortest spacing is already at one half-wavelength. For separations less than

Table 5-3—Program CLSIII Printout for $\ell = 16$, $m_1 = 4$; Trial $n_1 = 3, 1$

```
550 DATA 16,4

CLSIII


SIGMA-CHANNEL-PAIR = 25.9808  ELECTRICAL DEGREES
OVERALL ARRAY LENGTH = 16 HALF-WAVELENGTHS
M1 = 4

THE TRIAL VALUE OF N1 IS   ?3

  M1:N1***M2:N2
ALPHA,LENGTH    P***Q***R      CO.COEFF.        P-AMB          REDUN?
                                                (PCT)

 4 : 3 *** 16 : 4
 4 , 16          3  1  12      -0.346154        10.6339        99999

 4 : 3 *** 16 : 8
 4 , 16          6  2  8       -0.40032         9.76767        2

 4 : 3 *** 16 : 12
 4 , 16          9  3  4       -0.423077        10.6339        99999 <-------


550 DATA 16,4

CLSIII


SIGMA-CHANNEL-PAIR = 25.9808  ELECTRICAL DEGREES
OVERALL ARRAY LENGTH = 16 HALF-WAVELENGTHS
M1 = 4

THE TRIAL VALUE OF N1 IS   ?1

  M1:N1***M2:N2
ALPHA,LENGTH    P***Q***R      CO.COEFF.        P-AMB          REDUN?
                                                (PCT)

 4 : 1 *** 16 : 4
 4 , 16          1  3  12      0.192308         10.6339        99999

 4 : 1 *** 16 : 8
 4 , 16          2  6  8       8.00641E-2       9.76767        2

 4 : 1 *** 16 : 12
 4 , 16          3  9  4       -3.84615E-2      10.6339        99999
```

one half-wavelength, mutual impedance effects between antenna elements may affect the phase tracking, thus increasing ambiguities.

Class II

The example for a Class II synthesis is for $\ell = 20$. The integer factors of 20 are 4 and 5 (=4 + 1). In the absence of array-to-array correlation it might be speculated that there are eight "optimum" arrays formed by combinations of $m_1{:}n_1 \oplus m_2{:}n_2$ using numerators 4 or 5 and denominators 3 or 1 (with $m_i = 4$) and 3 or 2 (with $m_i = 5$). As in the case of $\ell = 16$, there may be factors common to m_1 and n_2 (even after the common factor has been suppressed), in which case the program CLSIII will indicate the redundant arrays, as before.

Table 5-4a through d show the results of CLSIII for $\ell = 20$. For each listing, the arrow "←" indicates a candidate array. Examination of all four listings shows that the array 4:3 ⊕ 20:12 has the largest array-to-array correlation coefficient, and hence, will exhibit the lowest p_a. The arrays 5:2 ⊕ 20:15 and 5:3 ⊕ 20:15 have p, q, r spacings of 6, 9, 5 and 9, 6, 5, respectively, in contrast to the optimum 4:3 ⊕ 20:12 array which has spacings 9, 3, 8.

Table 5-4a—Program CLSIII Printout for $\ell = 20$, $m_1 = 4$; Trial $n_1 = 3$

```
550 DATA 20,4

CLSIII


SIGMA-CHANNEL-PAIR = 23.2379  ELECTRICAL DEGREES
OVERALL ARRAY LENGTH = 20 HALF-WAVELENGTHS
M1 = 4

THE TRIAL VALUE OF N1 IS   ?3


  M1:N1***M2:N2
ALPHA,LENGTH    P***Q***R     CO.COEFF.        P-AMB          REDUN?
                                                (PCT)


 4 : 3 *** 20 : 4
 4 , 20          3  1  16     -0.332875        11.9703         99999


 4 : 3 *** 20 : 8
 4 , 20          6  2  12     -0.381771        10.483          2


 4 : 3 *** 20 : 12
 4 , 20          9  3  8      -0.413585        10.483          99999  <-------


 4 : 3 *** 20 : 16
 4 , 20          12 4  4      -0.423659        11.9703         4
```

Table 5-4b—Program CLSIII Printout for $\ell = 20$, $m_1 = 4$; Trial $n_1 = 1$

```
550 DATA 20,4

CLSIII


SIGMA-CHANNEL-PAIR = 23.2379  ELECTRICAL DEGREES
ØVERALL ARRAY LENGTH = 20 HALF-WAVELENGTHS
M1 = 4

THE TRIAL VALUE ØF N1 IS   ?1

  M1:N1***M2:N2
ALPHA,LENGTH    P***Q***R     CØ.CØEFF.        P-AMB          REDUN?
                                               (PCT)

 4 : 1 *** 20 : 4
 4 , 20          1  3  16      0.21183         11.9703         99999

 4 : 1 *** 20 : 8
 4 , 20          2  6  12      0.127257        10.483          2

 4 : 1 *** 20 : 12
 4 , 20          3  9  8       3.18142E-2      10.483          99999  <----

 4 : 1 *** 20 : 16
 4 , 20          4  12  4     -6.05228E-2      11.9703         4
```

Table 5-4c—Program CLSIII Printout for $\ell = 20$, $m_1 = 5$; Trial $n_1 = 2$

```
550 DATA 20,5

CLSIII


SIGMA-CHANNEL-PAIR = 23.2379  ELECTRICAL DEGREES
ØVERALL ARRAY LENGTH = 20 HALF-WAVELENGTHS
M1 = 5

THE TRIAL VALUE ØF N1 IS   ?2

  M1:N1***M2:N2
ALPHA,LENGTH    P***Q***R     CØ.CØEFF.        P-AMB          REDUN?
                                               (PCT)

 5 : 2 *** 20 : 5
 5 , 20          2  3  15      3.18142E-2      10.483          99999

 5 : 2 *** 20 : 10
 5 , 20          4  6  10     -6.62266E-2      9.89453         2

 5 : 2 *** 20 : 15
 5 , 20          6  9  5      -0.159071        10.483          99999  <----
```

Table 5-4d—Program CLSIII Printout for $\ell = 20$, $m_1 = 5$; Trial $n_1 = 3$

```
550 DATA 20,5

CLSIII


SIGMA-CHANNEL-PAIR = 23.2379  ELECTRICAL DEGREES
OVERALL ARRAY LENGTH = 20 HALF-WAVELENGTHS
M1 = 5

THE TRIAL VALUE OF N1 IS   ?3

  M1:N1***M2:N2
ALPHA,LENGTH    P***Q***R      CO.COEFF.        P-AMB          REDUN?
                                                (PCT)

 5 : 3 *** 20 : 5
 5 , 20          3  2  15      -0.190885        10.483         99999


 5 : 3 *** 20 : 10
 5 , 20          6  4  10      -0.264906        9.89453        2


 5 : 3 *** 20 : 15
 5 , 20          9  6  5       -0.318142        10.483         99999  <-----
```

Class III

Over any span of array length, there are many more overall lengths in Class III than in Class I and Class II. To avoid unnecessary iteration through CLSIII, it is desirable to know which m_1 are good starting choices for particular lengths ℓ. Consideration of the optimum m_1 for Class I and the candidate m_1 for Class II arrays should lead one to the belief that

- If ℓ lies between i^2 and $i(i+1)$, choose $m_1 = i$
- If ℓ lies between $i(i-1)$ and i^2, choose $m_1 = i$.

The following are examples of this procedure.

- For $\ell = 17$; $i^2 = 16$, $i(i+1) = 20$, choose $m_1 = 4$
- For $\ell = 21$; $i(i-1) = 20$, $i^2 = 25$, choose $m_1 = 5$.

Figure 5-1 gives a geometric interpretation to this procedure. The trial m_1 for Class III are given with question marks following the trial integer, anticipating a later discussion of lengths where this intuitive trial m_1 fails (these cases are "pathological" in the sense that they are associated with m_1, n_1 pairs that are not as near the $n_1 = m_1/2$ criterion as their neighbors (see Table 3-4)). In any event, as will be seen, this geometric-selection criterion for m_1 in Class III arrays is natural, and stems directly from the fact that the cascaded end-phase configuration is based on a common-factor concept that *most simply*

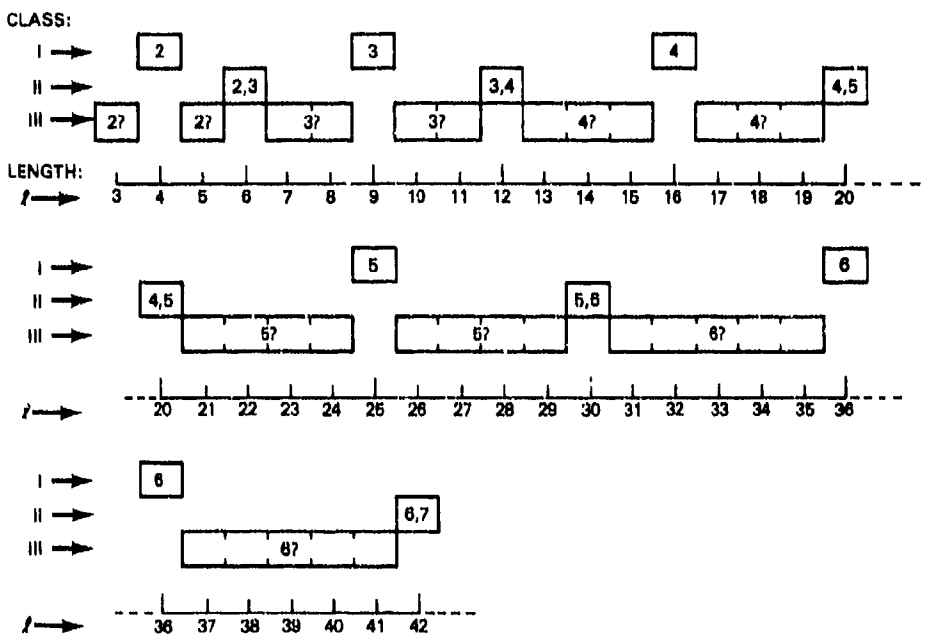

Fig. 5-1—m_1 for Class I and II; candidate m_1 for Class III: $3 \leq \ell \leq 42$

expresses the subarray parameters in terms of the overall length. This is in contrast to array representations that have been used by others.

Tables 5-5a and b shows the result of the application of CLSIII to the example $\ell = 21$. The optimum array is 5:3 ⊕ 21:10, 5; −0.258501.

Exact p_a, *Including Correlation*

Two additional computer programs are given in Appendix B, named AMBIG1 and AMBIG2. AMBIG1 is configured to solve the relations beginning in Sec. 5.4 at Eq. (5-39) for *arbitrary* m_1, n_1, m_2, n_2, α, and arbitrary channel-pair phase errors $\sigma_{1,2}$, $\sigma_{1,3}$, and $\sigma_{1,4}$. AMBIG2 is configured to provide p_a for arrays under the assumption that all channel-pair phase error variances are identical. Thus, AMBIG1 has the nature of an experimenter's tool, giving the designer, for example, the ability to examine the effect of putting higher-quality components in one channel-pair. AMBIG2 is more useful for tabulating p_a of various arrays over a range of channel-pair phase error distribution one-sigma values.

Table 5-6 provides p_a vs channel-pair phase error for several arrays of $\ell = 16$, 20, and 25. AMBIG2 was used to calculate the p_a. Figure 5-2 is a plot of p_a vs channel-pair phase error for $\ell = 16$, and Fig. 5-3 is the corresponding plot for $\ell = 25$. In both cases, because of the proximity of p_a vs channel-pair phase error for certain arrays, only two curves are shown. Table 5-6 makes these relationships clear.

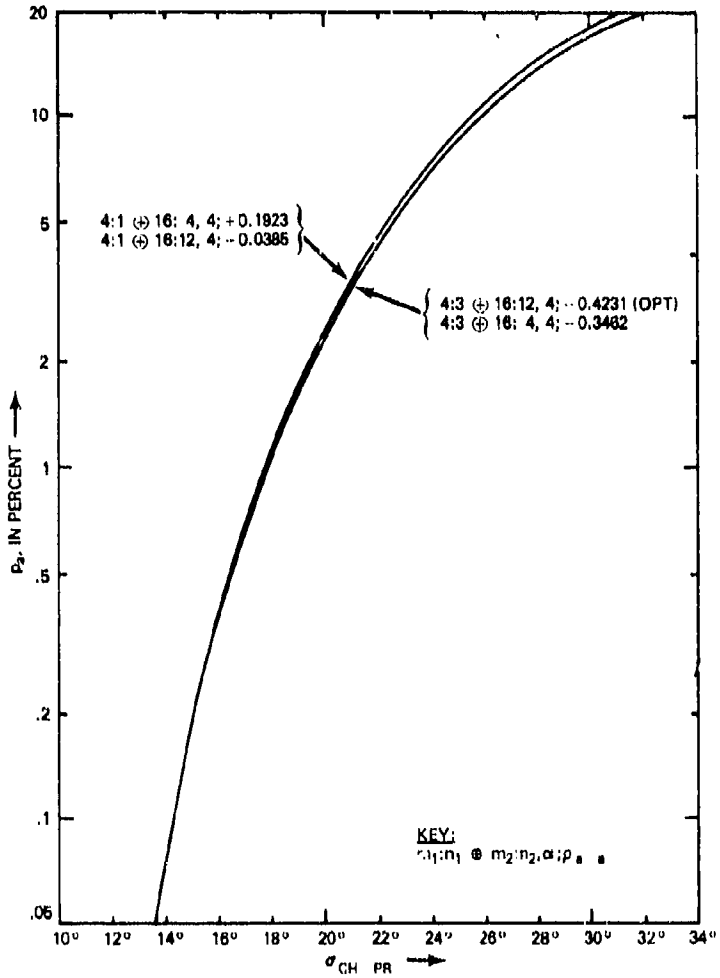

Fig. 5·2—p_a vs $\sigma_{CH\text{-}PR}$ for arrays of $\ell = 16$ ($i = 4$), Class I

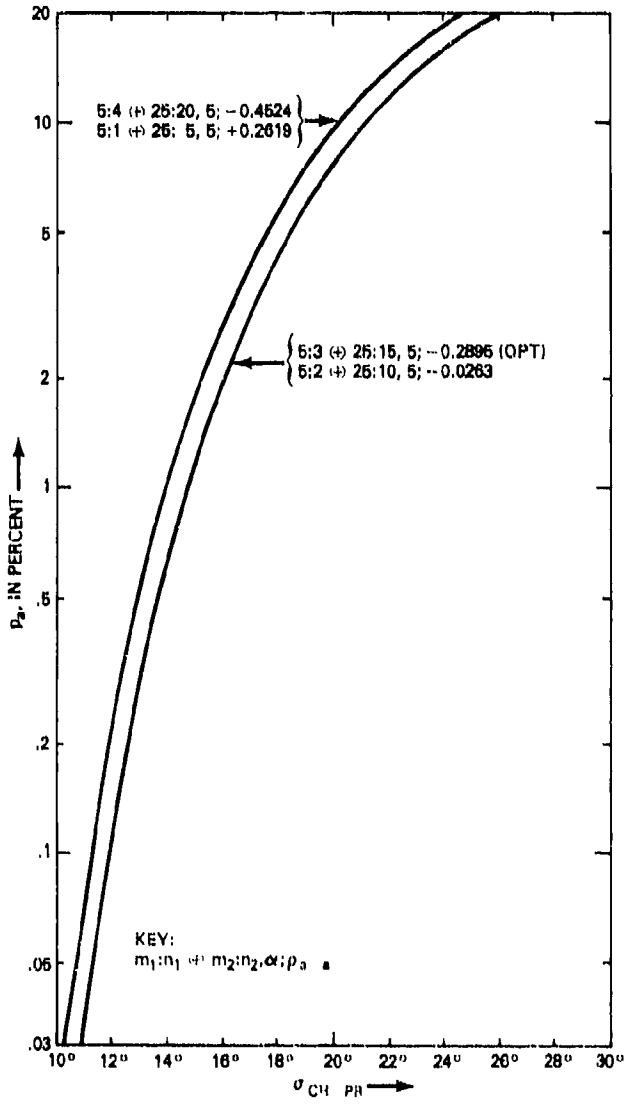

Fig. 5-3—p_a vs $\sigma_{CH\text{-}PR}$ for arrays of $\ell = 25$ ($i = 5$), Class I

Comparison of Approximate and Exact Synthesis Procedures

It was emphasized in the beginning of this subsection that an approximate synthesis procedure was sought, in part to eliminate the necessity of calculating a bivariate density function for *every* array configuration analyzed. An additional reason was to keep the theory behind the basic synthesis of an array from being obscured. Table 5-7 shows the approximate performance of the procedure.

This table is a list, over the range $3 \leq \ell \leq 42$, of the optimum m_1, as selected by three different criteria.

- Geometric-mean criteria—Fig. 5-1
- CLSIII program
- AMBIG2 program.

A check appearing in the "comments" column means that all three methods indicated the same (and correct) m_1. In the case of Class II arrays, the inability of the two simpler criteria to indicate the proper m_1 cannot be faulted, as they *do* indicate the proper m_1—i or $i + 1$—within the constraint of *not* considering array-to-array correlation.

Table 5-5a—Program CLSIII Printout for $\ell = 21$, $m_1 = 5$; Trial $n_1 = 3$

```
$50 DATA 21,5

CLSIII


SIGMA-CHANNEL-PAIR = 22.6779  ELECTRICAL DEGREES
OVERALL ARRAY LENGTH = 21 HALF-WAVELENGTHS
M1 = 5

THE TRIAL VALUE OF N1 IS   ?3

  M1:N1***M2:N2
ALPHA,LENGTH    P***Q***R     CO.COEFF.       P-AMB          REDUN?
                                              (PCT)


 5 : 3 *** 21 : 5
 5 , 21          3  2  16     -0.187155       10.2819        99999


 5 : 3 *** 21 : 10
 5 , 21          6  4  11     -0.258501       9.57561        99999  <-----


 5 : 3 *** 21 : 15
 5 , 21          9  6  6      -0.312255       10.0414        3


 5 : 3 *** 21 : 20
 5 , 21          12 8  1      -0.341022       11.8056        99999
```

Table 5-5b—Program CLSIII Printout for $\ell = 21$, $m_1 = 5$; Trial $n_1 = 2$

```
550 DATA 21,5

CLSIII


SIGMA-CHANNEL-PAIR = 22.6779  ELECTRICAL DEGREES
OVERALL ARRAY LENGTH = 21 HALF-WAVELENGTHS
M1 = 5

THE TRIAL VALUE OF N1 IS   ?2


  M1:N1***M2:N2
ALPHA,LENGTH   P***Q***R     CO.COEFF.        P-AMB          REDUN?
                                              (PCT)


 5 : 2 *** 21 : 5
 5 , 21         2  3  16      3.62235E-2      10.2819        99999


 5 : 2 *** 21 : 10
 5 , 21         4  6  11      -5.67442E-2     9.57561        99999  <----


 5 : 2 *** 21 : 15
 5 , 21         6  9  6       -0.146944       10.0414        3


 5 : 2 *** 21 : 20
 5 , 21         8  12  1      -0.21803        11.8056        99999
```

The situation is different for array lengths between 31 and 42. The reason can be deduced from Table 3-4. For $m_1 = 6$, the only allowable n_1 are either 1 or 5. Now, the ideal-unrealizable quadratic form for $m_1 = 6$ is $(6 \cdot 6 - 6 \cdot 3 + 3 \cdot 3)^{1/2} = 5.1962$. By contrast, the two *realizable* quadratic forms are $(6 \cdot 6 - 6 \cdot 1 + 1 \cdot 1)^{1/2} = (6 \cdot 6 - 6 \cdot 5 + 5 \cdot 5)^{1/2} = 5.5678$. For $m_1 = 5$, the ideal-unrealizable quadratic form is $(5 \cdot 5 - 5 \cdot 2.5 + 2.5 \cdot 2.5)^{1/2} = 4.3301$. The realizable quadratic forms for $m_1 = 5$ are $(5 \cdot 5 - 5 \cdot 3 + 3 \cdot 3)^{1/2} = (5 \cdot 5 - 5 \cdot 2 + 2 \cdot 2)^{1/2} = 4.3589$. For $m_1 = 7$, the ideal-unrealizable quadratic form is $(7 \cdot 7 - 7 \cdot 3.5 + 3.5 \cdot 3.5)^{1/2} = 6.0622$. The realizable quadratic forms are $(7 \cdot 7 - 7 \cdot 4 + 4 \cdot 4)^{1/2} = (7 \cdot 7 - 7 \cdot 3 + 3 \cdot 3)^{1/2} = 6.0828$.

The calculations above show that the subarray 1 ambiguity variable--(see Eq. (5-1))—for $m_1 = 6$ (realizable) is proportionally farther from its ideal-unrealizable variable than are the realizable variables for $m_1 = 5$ or $m_1 = 7$ from their ideal-unrealizable counterparts. The practical impact of this deficiency for arrays using $m_1 = 6$ is that as the array length migrates farther in either direction from $\ell = 36$, eventually an array utilizing $m_1 = 5$ or $m_1 = 7$ will perform better than one using $m_1 = 6$, even though the "geometric-mean criteria of Fig. 5-1 are met.

The foregoing discussion illustrated one way in which the approximate analysis leads to incorrect conclusions on the optimum-realizable array for a given length. Another way

Table 5-6—Probability of Ambiguity (p_a) vs $\sigma_{CH\text{-}PR}$ for Several Class I and Class II Four-Element, Cascaded End-Phase Arrays

$\sigma_{CH\text{-}PR}$ ↓	Array Parameter*													
	Class I, $\ell = 16$				Class I, $\ell = 20$						Class II, $\ell = 25$			
	4:3 ⊕ 16:12, 4; −0.4231	4:3 ⊕ 16:4, 4; −0.3462	4:1 ⊕ 16:4, 4; +0.1923	4:1 ⊕ 16:12, 4; −0.0385	4:3 ⊕ 20:12, 4; −0.4136	5:3 ⊕ 20:15, 5; −0.3181	5:3 ⊕ 20:5, 5; −0.1909	5:2 ⊕ 20:15, 5; −0.1591	5:2 ⊕ 20:5, 5; −0.0318	4:1 ⊕ 20:12, 4; +0.0318	5:3 ⊕ 25:15, 5; −0.2895	5:2 ⊕ 25:10, 5; −0.0263	5:4 ⊕ 25:20, 5; −0.4524	5:1 ⊕ 25:5, 5; +0.2619
10°	1.0E-4	1.0E-4	1.0E-4	1.0E-4	3.7E-3	3.7E-3	3.7E-3	3.7E-3	3.7E-3		7.3E-3	7.3E-3	1.71E-2	1.71E-2
12°	6.3E-3	6.3E-3	6.4E-3	6.4E-3	6.1E-2	6.1E-2	6.1E-2	6.1E-2	6.1E-2		0.115	0.116	0.209	0.212
14°	7.19E-2	7.22E-2	7.24E-2	7.25E-2	0.352	0.353	0.354	0.354	0.354		0.631	0.635	0.974	0.994
16°	0.356	0.358	0.360	0.361	1.15	1.16	1.16	1.16	1.16		1.94	1.96	2.69	2.76
18°	1.08	1.09	1.10	1.11	2.66	2.69	2.71	2.71	2.72		4.23	4.31	5.45	5.64
20°	2.41	2.44	2.48	2.49	4.94	5.01	5.07	5.08	5.10		7.48	7.64	9.12	9.48
22°	4.41	4.48	4.56	4.60	7.93	8.05	8.17	8.19	8.23		11.46	11.73	13.43	14.00
24°	7.03	7.14	7.29	7.36	11.45	11.66	11.85	11.89	11.96		15.93	16.33	18.10	18.91
26°	10.13	10.31	10.56	10.66	15.35	15.65	15.93	15.98	16.09		20.64	21.18	22.93	23.95
28°	13.60	13.86	14.21	14.36	19.46	19.86	20.23	20.29	20.43		25.42	26.08	27.73	28.95
30°	17.30	17.63	18.09	18.29	23.64	24.14	24.60	24.68	24.85		30.12	30.88	32.59	33.78
	↑ OPTIMUM REALIZABLE				↑ OPTIMUM REALIZABLE						↑ OPTIMUM REALIZABLE			

*Key: $m_1{:}n_1$ ⊕ $m_2{:}n_2$, α; $\rho_{\alpha\text{-}\alpha}$

Note: p_a is expressed in percent.

Table 5-7—Optimum m_1 for $3 \leqslant \ell \leqslant 42$ as Selected by Three Different Criteria

Class	ℓ	m_1 via A	m_1 via B	m_1 via AMBIG	Comments	Class	ℓ	m_1 via A	m_1 via B	m_1 via AMBIG	Comments
III	3	2	2	2	√	III	23	5	5	5	√
I	4	2	2	2	√	III	24	5	5	5	√
III	5	2	2	2	√	I	25	5	5	5	√
II	6	2 or 3	2 or 3	3	√	III	26	5	5	5	√
III	7	3	3	3	√	III	27	5	5	5	√
III	8	3	3	3	√	III	28	5	5	5	√
I	9	3	3	3	√	III	29	5	5	5	√
III	10	3	3	3	√	II	30	5 or 6	5 or 6	5	√
III	11	3	3	3	√	III	31	6	5	5	A fails
II	12	3 or 4	3 or 4	4	√	III	32	6	5	5	A fails
III	13	4	4	4	√	III	33	6	5	6	B fails
III	14	4	4	4	√	III	34	6	5	6	B fails
III	15	4	4	4	√	III	35	6	6	6	√
I	16	4	4	4	√	I	36	6	7	6	B fails
III	17	4	4	4	√	III	37	6	7	6	B fails
III	18	4	4	4	√	III	38	6	7	6	B fails
III	19	4	4	4	√	III	39	6	7	6	B fails
II	20	4 or 5	4 or 5	4	√	III	40	6	7	6	B fails
III	21	5	5	5	√	III	41	6	7	7	A fails
III	22	5	5	5	√	II	42	6 or 7	6 or 7	7	√

Criterion A: m_1 selected by "geometric mean."
Criterion B: m_1 selected by Program CLSIII.
AMBIG2: m_1 verified by exact analysis program, at a $\sigma_{\text{CH-PR}}$ more likely to be used in practical applications.

in which the approximate procedure leads to the wrong conclusions is as follows. The approximate procedure is based on the attempt to force the overall p_a toward a value of 8.9%—by forcing the channel-pair phase error to assume a value based on overall array length—without regard to correlation of ambiguities between the subarrays. As an example of the effect of correlated ambiguities on array design, consider $\ell = 37$. On the basis of the overall array length-square root criterion, one would probably evaluate candidate arrays based on $m_1 = 6$ and $m_1 = 7$ by program CLSIII. This approximate procedure indicates the following two arrays.

6:5 ⊕ 37:18,6	$p_a = 10.4165\%$	Program CLSIII, $\sigma_{\text{CH-PR}} = 17.0848°$
7:4 ⊖ 37:21,7	$p_a = 10.3100\%$	

(assuming independence of subarray ambiguities)

When program AMBIG1 is applied to the same array parameters, and to the same channel-pair phase error distributions, the results are

6:5 ⊕ 37:18,6; -0.46517	$p_a = 9.7912\%$	Program AMBIG1, $\sigma_{\text{CH-PR}} = 17.0848°$
7:4 ⊕ 37:21,7; -0.255752	$p_a = 10.1879\%$	

(including effects of subarray correlation)

For selected values of channel-pair phase error that are more likely to be used in a system design, Program AMBIG2 yields

6:5 ⊕ 37:18,6, -0.46517	$p_a = 0.1945\%, 1.1632\%$	Program AMBIG2, $\sigma_{\text{CH-PR}} = 10°, 12°$, respectively
7:4 ⊕ 37:21,7; -0.255752	$p_a = 0.3171\%, 1.4693\%$	

(including effects of subarray correlation)

The above tabulations show that on the basis of the approximate procedure employing program CLSIII one might be tempted to choose the array based on $m_1 = 7$ as the best performer. However, more precise evaluation of the arrays with the aid of AMBIG1 and AMBIG2 (once the simpler procedure exemplified by CLSIII is used to identify candidate arrays), shows the optimum array to be based on $m_1 = 6$.

Tabulated p_a *vs* $\sigma_{CH\text{-}PR}$

Table 5-8 gives p_a vs $\sigma_{\text{CH-PR}}$ for the optimum-realizable four-element cascaded end-phase array over an ℓ range from 4 to 42 half-wavelengths. The arrays have optimum p, q, and r spacings such that p_a of 0.1 to 15% for the $\sigma_{\text{CH-PR}}$ specified results.

It can be seen from the table that the optimum-realizable array for array lengths 24, 30, and 36 actually have a p_a *greater* than the arrays one half-wavelength longer, or 25, 31, and 37 half-wavelengths, respectively. This fact has apparently not been reported previously in the literature on multielement interferometers. The reason for this behavior is that lengths 24, 30, and 36 are highly composite numbers, i.e.,

Table 5-8—p_a vs Array Length—Optimum-realizable Four-element Arrays—$4 \leqslant \ell \leqslant 42$ (p_a expressed in percent)

ℓ	Class	p	q	r	$\Re_1$	$\Re_2$	α	p_a for given $\sigma_{\text{CH-PR}}$			
								10°	12°	15°	20°
4	I	1	1	2	2:1	4:2	2	–	–	–	–
5	III	1	1	3	2:1	5:2	2	–	–	–	3.7E-3
6	II	2	1	3	3:2	6:3	3	–	–	6E-4	6.70E-2
7	III	2	1	4	3:2	7:3	3	–	–	6E-4	6.79E-2
8	III	2	1	5	3:2	8:3	3	–	–	6E-4	7.83E-2
9	I	4	2	3	3:2	9:6	3	–	–	1.1E-3	0.1331
10	III	2	1	7	3:2	10:3	3	–	–	5.7E-3	0.3041
11	III	4	2	5	3:2	11:6	3	–	2E-4	1.66E-2	0.5289
12	II	3	1	8	4:3	12:4	4	1E-4	3.2E-3	8.80E-2	1.3152
13	III	6	2	5	4:3	13:8	4	1E-4	3.2E-3	8.97E-2	1.3895
14	III	3	1	10	4:3	14:4	4	1E-4	3.3E-3	9.93E-2	1.6215
15	III	6	2	7	4:3	15:8	4	1E-4	3.6E-3	0.1090	1.7684
16	I	9	3	4	4:3	16:12	4	1E-4	6.3E-3	0.1727	2.4140
17	III	6	2	9	4:3	17:8	4	2E-4	7.8E-3	0.1974	2.6136
18	III	3	1	14	4:3	18:4	4	1.1E-3	2.79E-2	0.4211	3.9239
19	III	6	2	11	4:3	19:8	4	1.4E-3	3.13E-2	0.4501	4.0385
20	II	9	3	8	4:3	20:12	4	3.7E-3	6.10E-2	0.6707	4.9441
21	III	6	4	11	5:3	21:10	5	3.7E-3	6.16E-2	0.6851	5.1190
22	III	9	6	7	5:3	22:15	5	4.0E-3	6.95E-2	0.7888	5.7743
23	III	6	4	13	5:3	23:10	5	4.3E-3	7.52E-2	0.8511	6.1414

24	III	3	2	19	5:3	24:5	5	7.7E-3	0.1204	1.2049	7.6950
25	I	9	6	10	5:3	25:15	5	7.3E-3	0.1154	1.1657	7.4757
26	III	9	6	11	5:3	26:15	5	1.05E-2	0.1481	1.3666	8.1906
27	III	6	4	17	5:3	27:10	5	1.77E-2	0.2087	1.6885	9.2463
28	III	9	6	13	5:3	28:15	5	2.45E-2	0.2569	1.9064	9.8221
29	III	9	6	14	5:3	29:15	5	3.76E-2	0.3397	2.2507	10.7278
30	II	3	2	25	5:3	30:5	5	0.1262	0.7627	3.6747	13.9890
31	III	9	6	16	5:3	31:15	5	2.8E-3	8.39E-2	0.5782	3.0944
32	III	9	6	17	5:3	32:15	5	5.0E-3	0.1208	0.7398	3.5933
33	III	10	2	21	6:5	33:12	6	5.6E-3	0.1405	0.8746	4.1906
34	III	15	3	16	6:5	34:18	6	5.8E-3	0.1458	0.9079	4.3207
35	III	15	3	17	6:5	35:18	6	6.1E-3	0.1574	0.9764	4.5865
36	I	25	5	6	6:5	36:30	6	1.06E-2	0.2406	1.3591	5.8009
37	III	15	3	19	6:5	37:18	6	7.8E-3	0.1945	1.1632	5.2218
38	III	15	3	20	6:5	38:18	6	9.4E-3	0.2223	1.2850	5.5916
39	III	20	4	15	6:5	39:24	6	1.27E-2	0.2697	1.4710	6.1024
40	III	15	3	22	6:5	40:18	6	1.52E-2	0.3023	1.5927	6.4332
41	III	12	9	20	7:4	41:21	7	2.26E-2	0.3465	1.6641	6.4894
42	II	20	15	7	7:4	42:35	7	2.69E-2	0.4280	2.0340	7.6303

Note: For arrays of 31 halfwavelengths or greater, the p_c shown in the last four columns of the table are for $\sigma_{CH\text{-}PR}$ = 8°, 10°, 12° and 15° respectiveiy.

$$24 = 2 \cdot 2 \cdot 2 \cdot 3,$$
$$30 = 2 \cdot 3 \cdot 5,$$
$$36 = 2 \cdot 2 \cdot 3 \cdot 3.$$

There are fewer degrees of freedom in synthesizing these arrays, than, for example, in $\ell = 26 = 2 \cdot 13$. In each of the lengths 24, 30, or 36, $m_2 : n_2$ is either much greater, or much less than 2:1. This is in marked contrast to the example $\ell = 26$, where the $m_2 : n_2$ ratio is 26:15, which is extremely close to the ideal-unrealizable ratio of 2:1.

As an aid to the system designer in making tradeoffs, the information in Table 5-8 is graphed in Figs. 5-4a and 5-4b.

A figure of merit for optimum-realizable arrays may be defined as the ratio of p_a ideal-unrealizable, given $\sigma_{\text{CH-PR}}$ as per Eq. (5-23), to the p_a optimum-realizable, given the same $\sigma_{\text{CH-PR}}$, evaluated in Program AMBIG1. That is,

$$\text{Figure of Merit} = \Gamma = \frac{p_{a\text{-ID}} \mid \sigma_{\text{CH-PR}},\ \text{Eq. (5-23)}}{p_{a\text{-RE}} \mid \sigma_{\text{CH-PR}},\ \text{Eq. (5-23)}}$$

$$\Gamma = \frac{0.088281}{p_{a\text{-RE}} \mid \sigma_{\text{CH-PR}},\ \text{Eq. (5-23)}}. \tag{5-45}$$

Figure 5-5 shows the figure of merit, Γ vs array length for $4 \leq \ell \leq 42$. Several relationships may be deduced from the graph.

- With the exception of the ideal-unrealizable array for $\ell = 4$, Class I ($\ell = i^2$) arrays whose m_1 are even do not have as great a Γ as arrays whose m_1 are odd

- Class II ($\ell = i(i + 1)$) do not have as great a Γ as the adjacent Class I arrays—exceptions are $\ell = 16, 36$

- Arrays whose lengths are prime have Γ greater than the mean Γ of 0.898—the only exceptions are $\ell = 7, 13$

Table 5-9 gives p_a vs $\sigma_{\text{CH-PR}}$ for the optimum-realizable four-element cascaded end-phase arrays, Classes I and II over an ℓ range from 4 to 100. The tabulated p_a are graphed in Fig. 5-6. Figure 5-7 shows the figure of merit for these arrays. It should be noted that as the array length exceeds 23 half-wavelengths, the p_a exceeds 0.1%, for $\sigma_{\text{CH-PR}} = 12°$. If $\sigma_{\text{CH-PR}}$ is reduced to 10°, arrays up to length 31 are realized before a p_a of 0.1% is exceeded. Arrays longer than this require some form of calibration (see Sec. 3.1) if the larger p_a associated with uncalibrated arrays longer than this are unsuitable for a particular application.

5.6 Concluding Remarks on Four-element Array Synthesis

The synthesis concepts presented in this section for four-element arrays enable the ESM system designer to rapidly synthesize arrays of any length. These techniques are

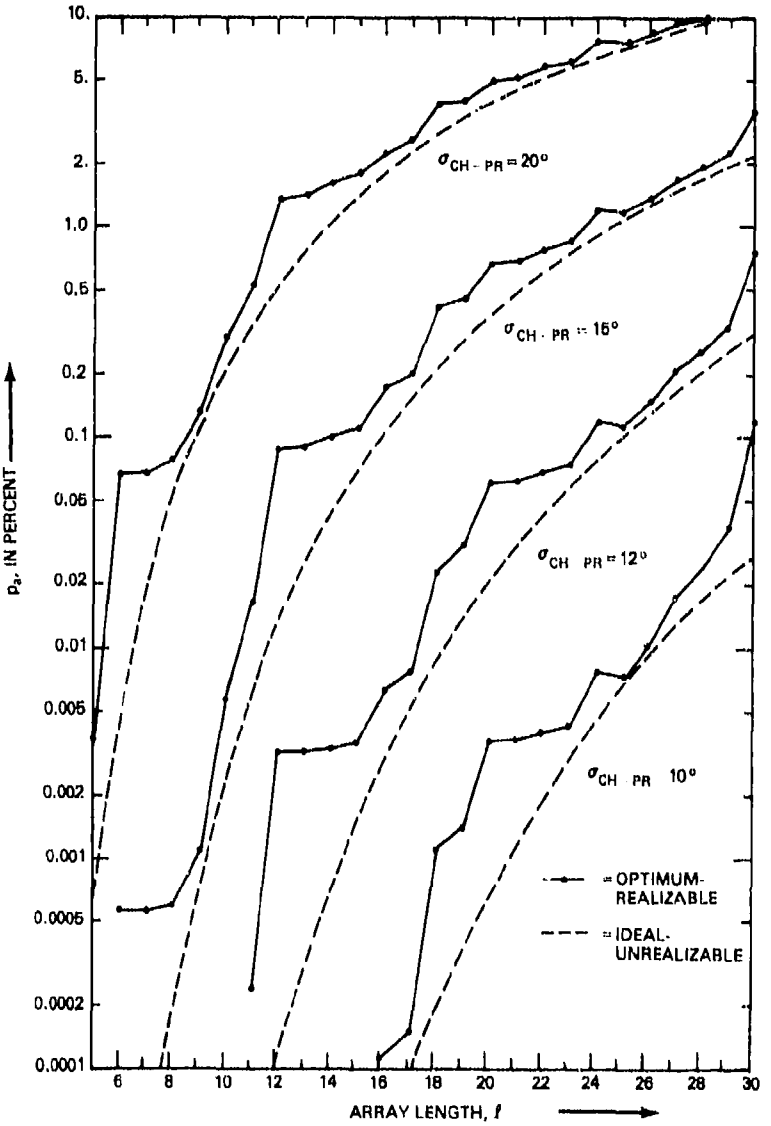

Fig. 5-4a — p_a vs array length, with σ_{CH-PR} as a parameter, $5 < \ell < 30$

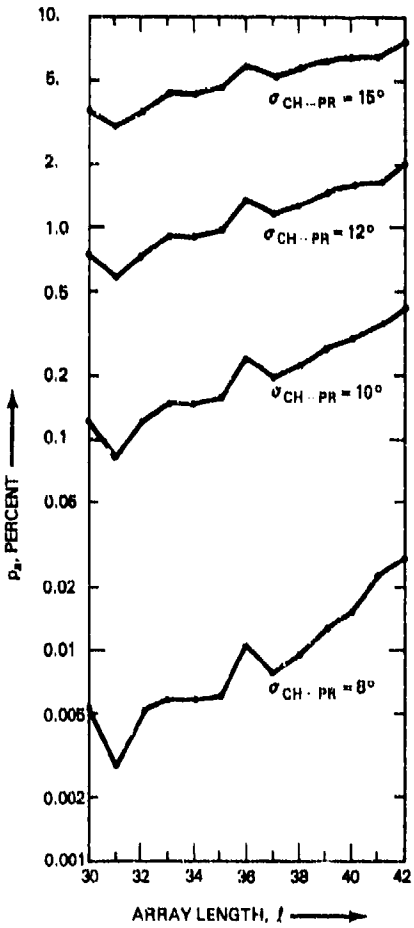

Fig. 5-4b—p_a vs array length, with σ_{CH-PR} as a parameter, $30 \leq \ell \leq 42$

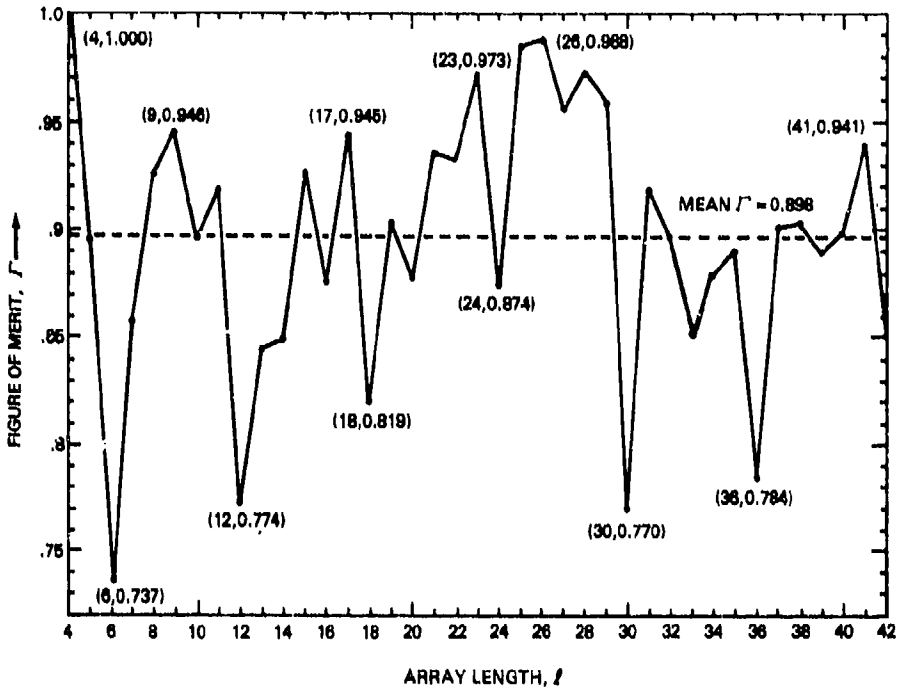

Fig. 5-5—Figure of merit, Γ vs array length for four-element arrays

based on the concept of the ideal-unrealizable array. The two-step procedures given, in conjunction with the computer-aided techniques exemplified in the programs CLSIII, AMBIG1 and AMBIG2, provide the designer with (a) an approximate synthesis leading to several candidate arrays, and (b) exact analyses to fix the parameters of the optimum-realizable array once the approximate synthesis has been performed.

Although there is a small amount of trial and error in the procedures, this should be viewed in the context that a brute-force analysis for arrays of length $\ell = 16$ leads to well over 75 arrays, all of whose p_a have to be evaluated before the optimum-realizable array spacings can be specified.

By means of the concepts presented in this report, it has been possible to answer in the affirmative the speculation of Hanson [21] on the existence of optimum four-element arrays.

A final observation (not stressed in the development) is that one need *not* be restricted to implementing the optimum-realizable array for a given length if one or more of the spacings are too small with respect to the overall frequency range of operation desired. The computer programs in Appendix B allow the designer latitude to choose between array spacings that will minimize the overall p_a vs those which are close to the optimum-realizable, but which will maximize the *minimum* interelement spacing in the array.

Table 5-9—p_a vs Array Length—Optimum-realizable Four-element Arrays—$4 \leqslant \ell \leqslant 100$, Classes I and II

ℓ	Class	p	q	r	$\mathcal{R}_1$	$\mathcal{R}_2$	α	p_a* for Given $\sigma_{CH\text{-}PR}$			
								10°	12°	15°	20°
4	I	1	1	2	2:1	4:2	2	–	–	–	–
6	II	2	1	3	3:2	6:3	3	–	–	6E-4	6.70E-2
9	I	4	2	3	3:2	9:6	3	–	–	1.1E-3	0.1331
12	II	3	1	8	4:3	12:4	4	1E-4	3.2E-3	8.80E-2	1.3152
16	I	9	3	4	4:3	16:12	4	1E-4	6.3E-3	0.1727	2.4140
20	II	9	3	8	4:3	20:12	4	3.7E-3	6.10E-2	0.6707	4.9441
25	I	9	6	10	5:3	25:15	5	7.3E-3	0.1154	1.1657	7.4757
30	II	3	2	25	5:3	30:5	5	0.1262	0.7627	3.6747	13.9890
								p_a for Given $\sigma_{CH\text{-}PR}$			
								8°	10°	12°	15°
30	II	3	2	25	5:3	30:5	5	5.3E-3	0.1262	0.7627	3.6747
36	I	25	5	6	6:5	36:30	6	1.06E-2	0.2406	1.3591	5.8009
42	II	20	15	7	7:4	42:35	7	2.69E-2	0.4280	2.0340	7.6303
								p_a for Given $\sigma_{CH\text{-}PR}$			
								6°	8°	10°	12°
42	II	20	15	7	7:4	42:35	7	1E-4	2.69E-2	0.4280	2.0340
49	I	16	12	21	7:4	49:28	7	2E-4	4.32E-2	0.6125	2.6834
56	II	20	15	21	7:4	56:35	7	1.9E-3	0.1521	1.3090	4.4740
56	II	15	9	32	8:5	56:24	8	1.9E-3	0.1521	1.3090	4.4740
64	I	25	15	24	8:5	64:40	8	3.6E-3	0.2598	1.9839	6.1700
72	II	25	15	32	8:5	72:40	8	1.41E-2	0.5237	3.0628	8.3234
81	I	25	20	36	9:5	81:45	9	2.45E-2	0.7875	4.1438	10.4911
90	II	35	28	27	9:5	90:63	9	8.59E-2	1.5157	6.2105	13.8315
100	I	49	21	30	10:7	100:70	10	0.1463	2.2014	8.0579	16.6744

*p_a expressed in percent.

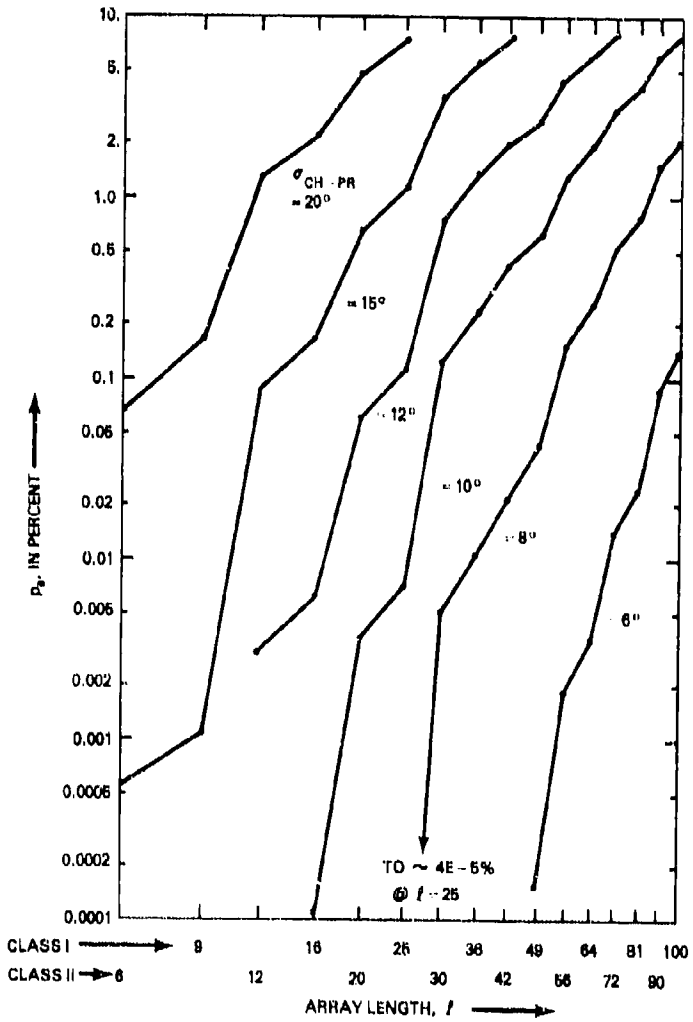

Fig. 5-6—p_a vs array length, with σ_{CH-PR} as a parameter, Class I and II, $4 \leq \ell \leq 100$

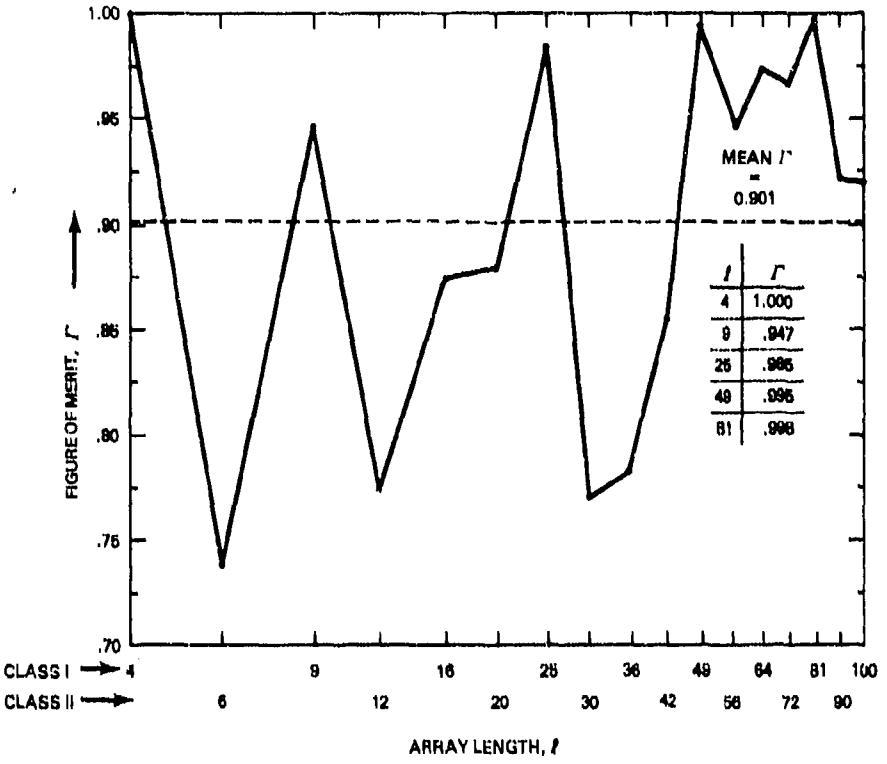

Fig. 5-7—Figure of merit, Γ vs array length for four-element arrays, Class I and II, $4 \leq \ell \leq 100$

6.0 SUMMARY AND CONCLUSIONS

This report presented a theory of three- and four-element phase-only interferometers for application to high resolution, low probability of ambiguity direction finding.

Although three-element interferometers have been widely used, the theoretical fundamentals of these arrays apparently have not been widely published in a form accessible to the system designer. With respect to four-element arrays, it was possible to establish with use of some geometric aids, in conjunction with the concepts of the ideal-unrealizable array and the subarray-to-subarray correlation coefficient, (a) the cascaded end-phase array as the optimum configuration for four-element three-integer set arrays, and (b) the optimum (i.e., the lowest probability of ambiguity subject to zero-mean channel-pair errors with equal standard deviation in all channel-pairs) four-element array spacings for arbitrary overall array length.

Work is in progress to extend the results reported here to arrays of more than four elements, and to define the improvement in accuracy of estimated angle when phase information from all the apertures, rather than from only the farthest-spaced pair of apertures, is used.

It is hoped that the theory and computer-aided design procedures given here will stimulate both further research into, as well as wider usage of, phase-only interferometer arrays in those applications requiring good angular resolution over wide fields of view.

ACKNOWLEDGMENTS

The writer gratefully acknowledges stimulating technical discussions with A. Spezio, the assistance of S. Leroy in programming Monte Carlo simulations used to verify the theory, and a critical review of the manuscript by Drs. D. C. Wu and G. E. Friedman. In addition, thanks are due to Ms. R. Long and Mrs. M. Ledford for their dedicated efforts in typing the manuscript.

REFERENCES

1. D.N. Travers and S.M. Hixon, *Abstracts of the Available Literature on Radio Direction Finding 1899–1965*, Southwest Research Institute, San Antonio, Texas, July 1, 1966 (AD 800110).
2. D.K. Barton, "International Cumulative Index on Radar Systems," *IEEE Trans.* AES-11, p. 428 ff. (29 citations on interferometers) (May 1975).
3. , "Cumulative Index on Radar Systems—Update," *IEEE Trans.* AES-9, 336–346 (Mar. 1973).
4. , "Cumulative Index on Radar Systems," *IEEE Trans.* AES-8, 91–128 (Jan. 1972).
5. A.V. Titov, "Characteristics of Two Methods of Obtaining Single-Valued Phase Readings in the Case of Multifrequency Radiation," *Radio Eng. Electr. Phys.* 19, No. 4, 132–135 (Apr. 1974).
6. V.P. Ipatov and A.V. Titov, "Uniqueness and Accuracy of Phase Measurements in the Case of Two-Frequency Radiation," *Radio Eng. Electr. Phys.* 18, No. 1, 140–144 (Jan. 1973).
7. A.V. Titov, "Discrete Methods of Measurement of Time Position of Pulsed Signals Immersed in Noise," *Radio Eng. Electr. Phys.* 14, No. 5, 684–690 (May 1969).
8. P.J. Butterly, "Some Accuracy Considerations in Passive Location Finding," Johns Hopkins University, Air Force Technical Report AFAL-TR-66-98, Air Force Avionics Laboratory, Wright-Patterson Air Force Base, Ohio, May 1966 (AD 482 431).
9. L.H. Wegner, "On the Accuracy Analysis of Airborne Techniques for Passively Locating Electromagnetic Emitters," Report R-722-PR, U.S. Air Force Project RAND, June 1971 (AD 729 767).
10. N.M. Blachman, "Position Determination from Radio Bearings," *IEEE Trans.* AES-5, 558–560 (May 1969).
11. C.J. Ancker, Jr., "Airborne Direction Finding—the Theory of Navigation Errors," *IRE Trans.* ANE-5, 199–210 (Dec. 1958).

12. W.B. Kendall, "Unambiguous Accuracy of an Interferometer Angle-Measuring System," *IEEE Trans.* SET-11, 62-70 (June 1965).

13. D.L. Margerum, "Self-Phased Arrays," in Ch. 5 *Microwave Scanning Antennas—Vol. III, Array Systems*, R.C. Hansen, editor, Academic Press, New York, 1966.

14. D.N. Travers and W.M. Sherrill, *et al.*, "Interferometer Direction Finder System for 2 to 10 MHz," Research and Development Technical Report No. ECOM-0198-F, Final Report on Contract DAAB07-C-0198, Southwest Research Institute, Department of Applied Electromagnetics, San Antonio, Texas, March 1969.

15. K.E. Bailey and J.K. Moller, "Integrated Missile Flight Test Safety System at Vandenberg/Point Arguello," *IRE Trans.* MIL-5, 294-299 (Oct. 1961).

16. E.C. Watters, F.L. Rees, and R.A. Enstrom, "High-Precision Angle Determination by Means of Radar in a Search Mode," *IRE Trans.* MIL-5, 317-325 (Oct. 1961).

17. M. Watanabe, T. Tamama, and N. Yamauchi, "A Japanese 3-D Radar for Air Traffic Control," *Electronics* 44, No. 13, 68-72 (June 1971).

18. A. Papoulis, *Probability, Random Variables, and Stochastic Processes*, McGraw-Hill, New York, 1965.

19. M. Abramowitz and I. Stegun, eds. *Handbook of Mathematical Functions with Formulas, Graphs, and Mathematical Tables*, U.S. Nat. Bur. Stds. AMS No. 55, June 1964.
    a. Equation 7.1.23, p. 298.
    b. Equation 26.3.29, p. 940.

20. I. Niven and H.S. Zuckerman, *An Introduction to the Theory of Numbers*, 3d ed., John Wiley and Sons, New York, 1972.

21. J.E. Hanson, "On Resolving Angle Ambiguities of *n*-Channel Interferometer Systems for Arbitrary Antenna Arrangements in a Plane," Technical Report No. TG 1224, Applied Physics Laboratory, Johns Hopkins University (performed under Navy Contract No. N00017-72-C-4401), Oct. 1973.

22. A.T. Moffett, "Minimum-Redundancy Linear Arrays," *IEEE Trans.* AP-16, 172-175 (Mar. 1968).

23. R.F. Morrison, Jr. and N.M. Sarachan, "Digital Direction Finder Utilizing Binary Array," U.S. Patent No. 3,213,453,19 (Oct. 1965).

24. "Tables of the Bivariate Normal Distribution Function and Related Functions," U.S. Nat. Bur. Stds. AMS No. 50, June 15, 1959.

25. N.L. Johnson and S. Kotz, *Distributions in Statistics: Continuous Multivariate Distributions*, Wiley, New York, 1972.

Appendix A

EXPANSION OF THE NORMAL PROBABILITY INTEGRAL (BETWEEN SYMMETRIC LIMITS) AROUND THE NORMALIZED ARGUMENT 2.000

This Appendix provides an expansion of the normal probability integral (between symmetric limits) around a normalized argument of 2.000. The expansion is the basis of the approximate four-element array synthesis computer-aided procedure (see Appendix B—Program CLSIII) used in Sec. 5.5 of the main body of this report.

Three functions from Ref. A1 related to normal error functions appropriate to the expansion desired are

NBS No. 26.2.2

$$P(x) = \frac{1}{\sqrt{2\pi}} \int_{-\infty}^{x} \exp \frac{-t^2}{2} \, dt , \tag{A1}$$

NBS No. 26.2.4

$$A(x) = \frac{1}{\sqrt{2\pi}} \int_{-x}^{x} \exp \frac{-t^2}{2} \, dt = 2P(x) - 1 , \tag{A2}$$

NBS No. 26.2.9

$$\frac{\partial}{\partial x} P\left(\frac{x - m}{\sigma}\right) = \frac{1}{\sigma} \cdot \frac{1}{\sqrt{2\pi}} \exp \frac{-(x - m)^2}{2\sigma^2}$$

$$= \frac{1}{\sigma} Z\left(\frac{x - m}{\sigma}\right), \tag{A3}$$

where

$$Z(x) = \frac{1}{\sqrt{2\pi}} \exp \frac{-x^2}{2} .$$

A Taylor's series expansion for Eq. (A2) in the vicinity of argument x is

$$A(x \pm \Delta) \approx A(x) \pm \Delta A'(x) + \frac{\Delta^2}{2!} A''(x) \pm \frac{\Delta^3}{3!} A'''(x) . \tag{A4}$$

Now we have

$$A'(x) = \frac{\partial}{\partial x} P(x) - \frac{\partial}{\partial x} P(-x)$$

$$= 2Z(x)\,, \tag{A5}$$

$$A''(x) = 2Z'(x) = -2xZ(x)\,, \tag{A6}$$

and

$$A'''(x) = 2Z(x)[x^2 - 1]\,. \tag{A7}$$

The use of Eqs. (A5, 6, and 7) in Eq. (A4) yields

$$A(x \pm \Delta) \approx A(x) \pm 2\Delta Z(x) - \frac{2\Delta^2}{2!}\, xZ(x) \pm \frac{2\Delta^3}{3!}\,(x^2 - 1)Z(x)\,. \tag{A8}$$

The transformation $x + \Delta \rightarrow \frac{x + \Delta}{\sigma}$ results in

$$A\left(\frac{x + \Delta}{\sigma}\right) \approx A\left(\frac{x}{\sigma}\right) + Z\left(\frac{x}{\sigma}\right)\left[2\left(\frac{\Delta}{\sigma}\right) - \left(\frac{\Delta}{\sigma}\right)^2\left(\frac{x}{\sigma}\right) + \frac{1}{3}\left(\frac{\Delta}{\sigma}\right)^3\left(\frac{x^2}{\sigma^2}\right) - 1\right]\,. \tag{A9}$$

For $x/\sigma = 2.000$, Eq. (A9) simplifies to

$$A\left(2 + \frac{\Delta}{\sigma}\right) \approx A(2) + \frac{e^{-2}}{\sqrt{2\pi}}\left[2\left(\frac{\Delta}{\sigma}\right) - 2\left(\frac{\Delta}{\sigma}\right)^2 + \left(\frac{\Delta}{\sigma}\right)^3\right]. \tag{A10}$$

From Ref. A1, exact values of $A(2)$ and $Z(2) = \frac{1}{\sqrt{2\pi}}\, e^{-2}$ are

$$A(2) = 0.95449\ 97361$$
$$Z(2) = 0.05399\ 09665\,.$$

Over a range of −0.4 to +0.4 relative to a mean value of $x = 2.000$, the approximate value of $A(x + \Delta)$ compared to the exact value from Ref. A2 is given in the table below.

$(x + \Delta)/\sigma$ = Arg.	A (Arg.) Eq. (A10)	A (Arg.) Ref. A2	Error
1.6	0.890574	0.890401	1.73E-04
1.7	0.910929	0.910869	5.99E-05
1.8	0.928152	0.928139	1.27E-05
1.9	0.942568	0.942567	7.97E-07
2.0	0.9545	0.9545	0.
2.1	0.964272	0.964271	8.64E-07
2.2	0.972209	0.972193	1.56E-05
2.3	0.978634	0.978552	8.19E-05
2.4	0.983871	0.983605	2.66E-04

REFERENCES

A1. M. Abramowitz and I. Stegun, eds., *Handbook of Mathematical Functions with Formulas, Graphs, and Mathematical Tables*, U.S. Nat. Bur. Stds., AMS No. 55, June 1964.

A2. *Tables of Normal Probability Functions*, U.S. Nat. Bur. Stds., AMS No. 23, June 5, 1953.

Appendix B

COMPUTER PROGRAM LISTINGS AND COMMENTS ON THEIR USE

This Appendix provides listings of three computer programs for analyzing and synthesizing four-element cascaded end-phase arrays, along with examples of their use. The programs are written in BASIC language, and have run satisfactorily on a time-shared system utilizing a Digital Equipment Corporation System 10 at the Naval Research Laboratory.

The three programs are called CLSIII, AMBIG1, and AMBIG2. Descriptions of the programs are given below.

CLSIII

Figure B1 is a listing of program CLSIII. The user specifies the desired overall array length, ℓ and a trial subarray ratio 1 numerator, m_1 as data input via line 550. The program automatically selects a channel-pair phase error, $\sigma_{\text{CH-PR}}$ based on overall array length ℓ (according to Eq. (5-23) of Sec. 5.3 of the body of this report) that would result in a probability of ambiguity of approximately 8.89% for the ideal-unrealizable array of the given length. The program will then query the user for his trial subarray ratio 1 denominator, n_1.

The program then prints out the parameters of all possible array configurations for the particular set of ℓ, m_1 and n_1 chosen, listing

- $m_1:n_1 \oplus m_2:n_2$ ratios
- Factor α, and length ℓ
- Array spacings p, q, and r
- Array-to-array correlation coefficient, $\rho_{a,a}$
- Approximate p_a, in percent, assuming independence of subarray-to-subarray ambiguities
- Indication of redundancy in array spacings: "99999" indicates "no redundancy"; a small integer indicates that the spacings p, q, and r have this factor in common.

An example of a CLSIII printout is given in Fig. B2 for $\ell = 21$, $m_1 = 5$, and $n_1 = 3$. The printout shows that the array whose spacings are $p = 6$, $q = 4$, and $r = 11$ is the best-performing array of length 21, given $m_1 = 5$ and $n_1 = 3$. Actually, as pointed in the main body of the report, this is the optimum array for length 21. The user has the freedom to

```
CLSIII


10 DIM X(10),Y(10),G(10)
20 DIM D(10),E(10),F(10),P(10),Ø(10),Z(10)
30 READ L,M1
40 LET K9 = SQRT(3*L)
50 LET S9 = 180/K9
60 PRINT"SIGMA-CHANNEL-PAIR ="JS9J" ELECTRICAL DEGREES"
70 LET C1 = EXP(-2)/SQRT(2*3.14159Ø6)
80 PRINT"ØVERALL ARRAY LENGTH ="JL"HALF-WAVELENGTHS"
90 PRINT"M1 ="JM1
100 LET J9 = INT(L/M1)
110 IF J9*M1-L=0 THEN 130
120 GØ TØ 140
130 LET J9 = J9-1
140 PRINT
150 PRINT"THE TRIAL VALUE ØF N1 IS  "J
160 INPUT N1
170 PRINT
180 PRINT
190 PRINT"  M1:N1***M2:N2"
200 PRINT"ALPHA"J","J"LENGTH"," P***Ø***R","C0.C0EFF."," P-AMB","REDUN?"
210 PRINT "    ","    ","    "," (PCT)"
220 PRINT
230 PRINT
240 FØR J = 1 TØ J9
250 LET A = M1*M1-M1*N1+N1*N1
260 LET B = L*L-L*J*M1+J*M1*J*M1
270 LET C = (M1-N1)*(L-J*M1)-N1*L
280 LET P(J) = .5*C/SQRT(A*B)
290 LET D1 = K9/SQRT(A) - 2
300 LET D2 = M1*K9/SQRT(B) - 2
310 LET G1 = .9544997 + C1*(2*D1 - 2*D1*D1 + D1*D1*D1)
320 LET G2 = .9544997 + C1*(2*D2 - 2*D2*D2 + D2*D2*D2)
330 LET G3 = G1*G2
340 LET Ø(J) = 100*(1-G3)
350 LET D(J) = N1*J
360 LET E(J) = (M1-N1)*J
370 LET F(J) = L - J*M1
380 FØR K = J9 + 2 TØ 2 STEP -1
390 LET T = D(J)/K - INT(D(J)/K)
400 LET U = E(J)/K - INT(E(J)/K)
410 LET V = F(J)/K - INT(F(J)/K)
420 LET W = T + U + V
430 IF W = 0 THEN 470
440 NEXT K
450 LET G(J) = 99999
460 GØ TØ 480
470 LET G(J) = K
480 NEXT J
490 FØR J = 1 TØ J9
500 PRINT M1J":"JN1J"***"JLJ":"JJ*M1
510 PRINT M1J","JL,D(J)JE(J)JF(J),P(J),Ø(J),G(J)
520 PRINT
530 PRINT
540 NEXT J
550 DATA 25,5
560 END
```

Fig. B1—Listing of program CLSIII

```
550 DATA 21,5

CLSIII


SIGMA-CHANNEL-PAIR = 22.6779  ELECTRICAL DEGREES
ØVERALL ARRAY LENGTH = 21 HALF-WAVELENGTHS
M1 = 5

THE TRIAL VALUE ØF N1 IS   ?3


  M1:N1***M2:N2
ALPHA,LENGTH    P***Q***R      CØ.CØEFF.        P-AMB          REDUN?
                                                (PCT)

 5 : 3 *** 21 : 5
 5 , 21          3  2  16      -0.187155        10.2819         99999

 5 : 3 *** 21 : 10
 5 , 21          6  4  11      -0.258501        9.57561         99999

 5 : 3 *** 21 : 15
 5 , 21          9  6  6       -0.312255        10.0414         3

 5 : 3 *** 21 : 20
 5 , 21          12  8  1      -0.341022        11.8056         99999
```

Fig. B2—Example of program CLSIII printout

explore the performance of other arrays of length 21 by modifying his m_1 and n_1 inputs, should he wish to search, for example, for arrays whose minimum spacings exceed those obtained for the optimum-realizable arrays (from p_a considerations) discussed in the main text of this report.

If a radically unsuitable trial m_1 is chosen, say $m_1 = 2$, for $\ell = 21$, the program will indicate an overall p_a that is grossly in error, compared to the exact-independent p_a, because the range of validity of the expansion for the probability integral for subarray 2 will have been exceeded. Normally, trial m_1 will be chosen by reference to Fig. 5-1 in Sec. 5.5 of the body of this report. Figure B3 shows the exact probability of ambiguity (independence assumed) for a four-element array in terms of the normalized arguments for the individual subarrays, centered on a normalized argument of 2.000 for each subarray. That is, if each subarray has a normalized probability function argument of 2.000, then, the p_a for this array is 8.89%. Suppose an array is characterized by a normalized argument of 1.9 for subarray 1 and 2.3 for subarray 2. The *exact* p_a for the overall array would be 7.765%; the *approximate* p_a returned by program CLSIII would be 7.757%, or 0.008 percentage points low. It can be seen that the extremes of error in program CLSIII occur when both arguments are nearly the same value. That is, if both arguments are 1.6 (normalized), the exact p_a is 20.719%, and the approximate p_a is 0.031 percentage points low. It can be appreciated, however, that in most array syntheses, when the normalized argument of one subarray is *less* than 2.000, the normalized argument of the

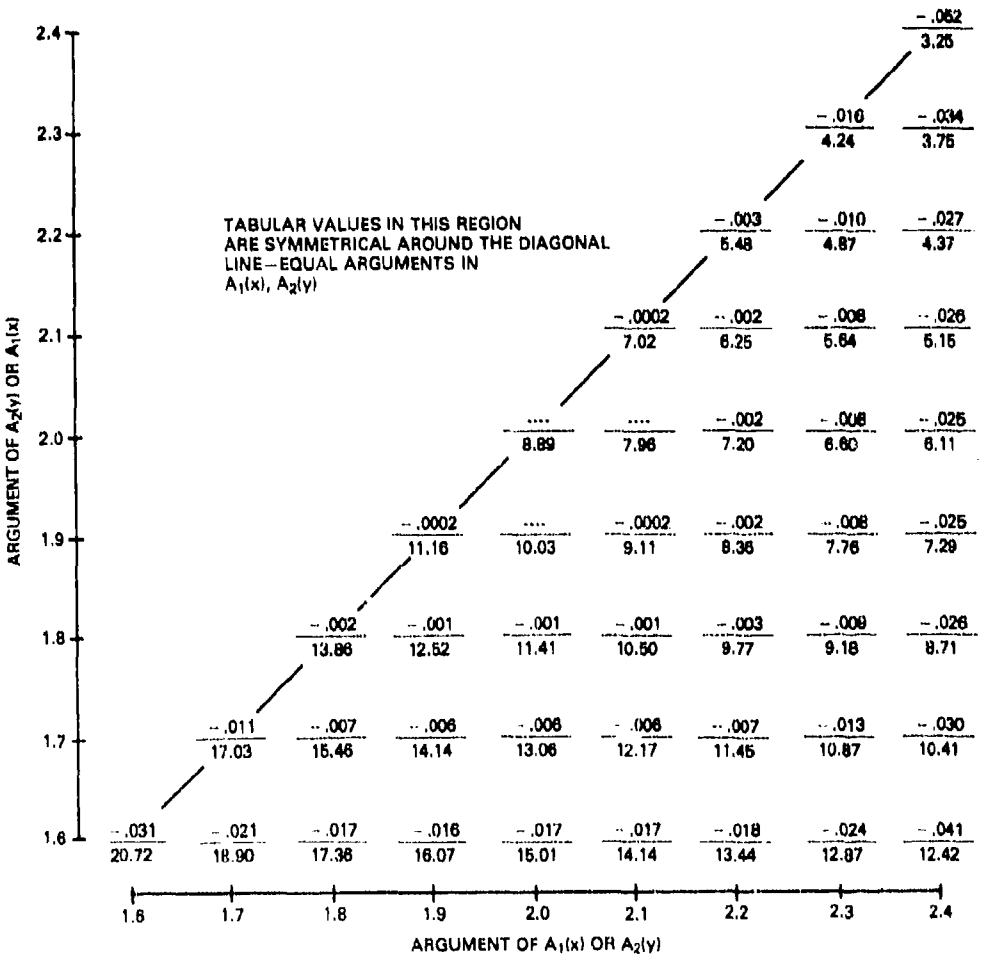

NOTES: 1) $p_a = 1 - A_1(x)A_2(y)$; $1.6 \le x \le 2.4$, $1.6 \le y \le 2.4$.
2) −.002/8.36 INDICATES EXACT $p_a = 8.36\%$, APPROXIMATE p_a IS 0.002 PERCENTAGE POINTS LESS.

Fig. B3—Comparison of approximate and exact p_a for normalized arguments $A_1(x)$, $A_2(y)$

other subarray is generally *larger* than 2.000; Fig. B3 shows that the errors in the approximation tend to cancel when this condition exists.

In summary, program CLSIII is suited to the purposes for which it is intended: to eliminate the need to calculate the *exact* p_a for each array candidate, and to provide the user with a readily applied overview of the performance of various arrays on a relative basis.

AMBIG1

Figure B4 is a listing of program AMBIG1. This program provides an exact calculation of p_a for a four-element cascaded end-phase array upon the user's specifying the following data inputs:

- Subarray 1—(line 1110)

  m_1, n_1, and $\rho_{1,2;1,3}$*

- Subarray 2--(line 1120)

  $m_2 = \ell$, $n_2 = j\alpha$, $\rho_{1,3;1,4}$

- Miscellaneous parameters—(line 1130)

  $\sigma_{1,2}$, $\sigma_{1,3}$, $\sigma_{1,4}$, $\rho_{1,2;1,4}$, α

An example of an AMBIG1 printout for $\mathcal{R}_1 = 5{:}3$, $\mathcal{R}_2 = 21{:}10$, $\alpha = 5$, $\sigma_{1,2} = \sigma_{1,3} = \sigma_{1,4} = 12.5°$, and $\rho_{1,2;1,3} = \rho_{1,3;1,4} = \rho_{1,2;1,4} = +0.5000$ is given in Fig. B5.

Program AMBIG1 can also be used to calculate the p_a of arrays in which the $\sigma_{1,j}$, $j = 2, 3, 4$ are not equal. For example, suppose that

$$\sigma_{1,2} = 10°,$$
$$\sigma_{1,3} = 14°,$$
$$\sigma_{1,4} = 12°.$$

Suppose further that the channel-pair phase error correlation coefficients are known (by measurement of the joint channel-pair phase errors) to be

$$\rho_{1,2;1,3} = 0.457143,$$
$$\rho_{1,3;1,4} = 0.380952,$$
$$\rho_{1,2;1,4} = 0.533333.$$

*$\rho_{1,2;1,3}$ is the correlation coefficient between channel-pair errors in the 1, 2 channel-pair to the 1, 3 channel-pair. The value of this coefficient (and the two below in lines 1120 and 1130) is usually set at +0.5000 for design purposes.

AMBIG1

```
10 READ M1,N1,P1
20 READ M2,N2,P2
30 READ S1,S2,S3,P3,Q
40 DIM H(31,2),L(2),U(2),Z(2)
50 PRINT"FØUR-ELEMENT PHASE INTERFERØMETER:"
60 PRINT"CØMPØUND PRØB.-ØF-AMBIGUITY FØR ARRAY SYNTHESIZED"
70 PRINT"BY CASCADING TWØ THREE-ELEMENT INTERFERØMETERS-----"
80 PRINT
90 PRINT "SIGMA,CH-PR--1,2 =";S1;"ELECTRICAL DEGREES"
100 PRINT "SIGMA,CH-PR--1,3 =";S2;"ELECTRICAL DEGREES"
110 PRINT "SIGMA,CH-PR--1,4 =";S3;"ELECTRICAL DEGREES"
120 PRINT
130 PRINT
140 PRINT"     ARRAY NØ.1 PARAMETERS:"
150 PRINT"     'LARGE' =";M1,"  'SMALL' =";N1
160 PRINT
170 PRINT"     ARRAY NØ.2 PARAMETERS:"
180 PRINT"     'LARGE' =";M2,"  'SMALL' =";N2
190 PRINT
200 PRINT"     ARRAY NØ.2-ARRAY NØ.1 RESØLUTIØN FACTØR:";Q
210 PRINT
220 LET A1 = SQR(((M1*S1)↑2)-2.*P1*(M1*S1)*(N1*S2)+((N1*S2)↑2))
230 LET A9 = SQR(((M2*S2)↑2)-2.*P2*(M2*S2)*(N2*S3)+((N2*S3)↑2))
240 LET P8 = M1*M2*P1*S1*S2 + N1*N2*P2*S2*S3
250 LET P9 = -M1*N2*P3*S1*S3 - N1*M2*S2*S2 + P8
260 LET P4 = P9/(A1*A9)
270 LET C1 = 1/(2*3.1415926)
280 LET C2 = 1./SQR(1.-P4*P4)
290 LET A2 = A9/Q
300 PRINT"SIG-Z(ARRAY NØ.1) =";A1,"DEGREES"
310 PRINT
320 PRINT"SIG-W(ARRAY NØ.2) =";A9,"DEGREES"
330 PRINT"SIG-W(ARRAY NØ.2) =";A2,"DEGREES(RESØLVED BY NØ.1)"
340 PRINT"----------"
350 PRINT"E(Z*W) =";P9,"DEGREES"
360 PRINT"----- ----"
370 PRINT"ARRAY-TØ-ARRAY CØRR. CØEFF'T. =";P4
380 PRINT"----------"
390 PRINT
400 PRINT"----------"
410 LET U1 = 180/A1
420 LET U2 = 180/A2
430 PRINT"PRØBABILITY FUNCTIØN PARAMETERS:"
440 PRINT
450 PRINT"ARGUMENT F(1) =";U1
460 PRINT"ARGUMENT F(2) =";U2
470 LET U(1) = U1
480 LET U(2) = U2
490 FØR J = 1 TØ 2
500 IF U(J)>5.4513 THEN 630
510 LET Z3 = 0.
520 LET T = U(J)/(2↑.5)
530 LET S = T
540 LET Y2 = U(J)*U(J)/2
550 LET D = 1
560 LET D = D + 2
```

Fig. B4—Listing of program AMBIG1

```
570 LET T = T*(2*Y2/D)
580 LET S = S + T
590 IF(T/S-1E-10)>0 THEN 560
600 LET Z3 = (2/SQRT(3.1415926))*S*EXP(-Y2)
610 LET Z(J) = (1.-Z3)/2
620 GØ TØ 640
630 LET Z(J) = 2.5E-08
640 NEXT J
650 LET A1 = 1 - 2*Z(1)
660 LET B1 = 1 - 2*Z(2)
670 FØR J = 1 TØ 2
680 IF U(J) >5.4513 THEN 950
690 LET H(0,J) = 1
700 LET H(1,J) =-U(J)
710 LET A =-U(J)
720 LET B = 1
730 FØR I = 2 TØ 20
740 LET C = A
750 LET A =-A*U(J) -(I-1)*B
760 LET B = C
770 LET H(I,J) = A
780 NEXT I
790 NEXT J
800 FØR J = 1 TØ 2
810 LET E = 1
820 LET F = 0
830 FØR K = 0 TØ 20
840 LET X = P4*(3-2*J)
850 LET D = H(K,1)*H(K,2)*(X↑(K+1))
860 LET E = E*(K+1)
870 LET F = F + D/E
880 NEXT K
890 LET U3 = U(1)*U(1) + U(2)*U(2)
900 LET F1 = F*C1*EXP(-U3/2)
910 LET L(J) = Z(1)*Z(2) + F1
920 NEXT J
930 PRINT"L(1) ="JL(1)," L(2) ="JL(2)
940 GØ TØ 960
950 LET L(1) = L(2) = 0
960 PRINT"PRØB.-CØRR(1) ="JA1," PRØB.-CØRR(2) ="JB1
970 PRINT"PRØB.-AMB(1) ="J2*Z(1)," PRØB.-AMB(2) ="J2*Z(2)
980 PRINT"----------"
990 PRINT
1000 LET E1 = 2. - (A1+B1+2.*L(1)+2.*L(2))
1010 PRINT
1020 PRINT"----------"
1030 LET E2 = 100*E1
1040 LET E3 = INT(E2*10↑4 + .5)/10↑4
1050 PRINT "PRØB. ØF AMBIGUITY ="JE3J"PERCENT(INCL. CØRRELATIØN)"
1060 PRINT
1070 LET D2 = 100*(1-A1*B1)
1080 LET D3 = INT(D2*10↑4 + .5)/10↑4
1090 PRINT "PRØB. ØF AMBIGUITY ="JD3J"PERCENT(ASSUMING INDEPENDENCE)"
1100 PRINT"----------"
1110 DATA 5,3,.5
1120 DATA 21,10,.5
1130 DATA 12.5,12.5,12.5,.5,5
1140 END
```

Fig. B4—Listing of program AMBIG1 (continued)

```
1110 DATA 5,3,.5
1120 DATA 21,10,.5
1130 DATA 12.5,12.5,12.5,.5,5


AMBIG1



F0UR-ELEMENT PHASE INTERFER0METER:
C0MP0UND PR0B.-0F-AMBIGUITY F0R ARRAY SYNTHESIZED
BY CASCADING TV0 THREE-ELEMENT INTERFER0METERS-----

SIGMA,CH-PR--1,2 = 12.5 ELECTRICAL DEGREES
SIGMA,CH-PR--1,3 = 12.5 ELECTRICAL DEGREES
SIGMA,CH-PR--1,4 = 12.5 ELECTRICAL DEGREES


     ARRAY N0.1 PARAMETERS:
     'LARGE' = 5                'SMALL' = 3

     ARRAY N0.2 PARAMETERS:
     'LARGE' = 21               'SMALL' = 10

     ARRAY N0.2-ARRAY N0.1 RES0LUTI0N FACT0R: 5

SIG-Z(ARRAY N0.1) = 54.4862 DEGREES

SIG-W(ARRAY N0.2) = 227.418 DEGREES
SIG-W(ARRAY N0.2) = 45.4835 DEGREES(RES0LVED BY N0.1)
----------
E(Z*W) =-3203.13            DEGREES
----------
ARRAY-T0-ARRAY C0RR. C0EFF'T. =-0.258501
----------

----------
PR0BABILITY FUNCTI0N PARAMETERS:

ARGUMENT F(1) = 3.30359
ARGUMENT F(2) = 3.95748
L(1) = 1.07035E-10              L(2) = 4.10727E-7
PR0B.-C0RR(1) = 0.999045        PR0B.-C0RR(2) = 0.999924
PR0B.-AMB(1)  = 9.54531E-4      PR0B.-AMB(2)  = 7.57352E-5
----------


----------
PR0B. 0F AMBIGUITY = 0.1029 PERCENT(INCL. C0RRELATI0N)

PR0B. 0F AMBIGUITY = 0.103 PERCENT(ASSUMING INDEPENDENCE)
----------
```

Fig. B5—Example of program AMBIG1 printout—equal channel-pair phase errors

These two sets of values define zero-mean *channel* errors, according to Eq. (3-7) of Sec. 3.2 of the main text (for $\rho_{1,2;1,3}$, and with suitable subscript changes—the other correlation coefficients)

$$\sigma_1 = 8.0000^\circ,$$

$$\sigma_2 = (\sigma_{1,2}^2 - \sigma_1^2)^{1/2} = (100 - 64)^{1/2} = 6.0000^\circ,$$

$$\sigma_3 = (\sigma_{1,3}^2 - \sigma_1^2)^{1/2} = (196 - 64)^{1/2} = 11.4892^\circ,$$

$$\sigma_4 = (\sigma_{1,4}^2 - \sigma_1^2)^{1/2} = (144 - 64)^{1/2} = 8.9443^\circ.$$

Figure B6 shows the AMBIG1 printout for the data inputs

$$m_1 = 5,\ n_1 = 3,\ \rho_{1,2;1,3} = 0.457143 \quad \text{(line 1110)}$$

$$m_2 = 21,\ n_2 = 10,\ \rho_{1,3;1,4} = 0.380952 \quad \text{(line 1120)}$$

$$\sigma_{1,2} = 10^\circ,\ \sigma_{1,3} = 14^\circ,\ \sigma_{1,4} = 12^\circ, \quad \text{(line 1130)}$$

$$\rho_{1,2;1,4} = 0.533333,\ \alpha = 5.$$

AMBIG2

Figure B7 is a listing of program AMBIG2. This program is similar to program AMBIG1, providing exact calculations of p_a for a four-element cascaded end-phase array. The details of the probability functions are omitted in the printout, and all channel-pair phase error distributions are presumed equal to $\sigma_{\text{CH-PR}}$ in the input. Hence, in AMBIG2, all the channel-pair phase error correlation coefficients are forced to equal +0.5000.

Figure B8 shows a printout for the same example that was used in the printout given as Fig. B5. The data input on line 860 of AMBIG2 has the form:

$$m_1 = 5,\ n_1 = 3,\ m_2 = 21,\ n_2 = 10,\ \alpha = 5.$$

The exact p_a (including the effect of subarray-to-subarray correlation) is calculated over the range on $\sigma_{\text{CH-PR}}$ from 10 to 25 electrical degrees in 1-degree steps in this example. The range and step size on $\sigma_{\text{CH-PR}}$ can be varied readily by altering lines 290 and 300 in the program as required.

```
1110 DATA 5,3,.457143
1120 DATA 21,10,.380952
1130 DATA 10.,14.,12.,.533333,5


AMBIG1



F0UR-ELEMENT PHASE INTERFER0METER:
C0MP0UND PR0B.-0F-AMBIGUITY F0R ARRAY SYNTHESIZED
BY CASCADING TW0 THREE-ELEMENT INTERFER0METERS-----

SIGMA,CH-PR--1,2 = 10 ELECTRICAL DEGREES
SIGMA,CH-PR--1,3 = 14 ELECTRICAL DEGREES
SIGMA,CH-PR--1,4 = 12 ELECTRICAL DEGREES


     ARRAY N0.1 PARAMETERS:
     'LARGE' = 5                'SMALL' = 3

     ARRAY N0.2 PARAMETERS:
     'LARGE' = 21               'SMALL' = 10

     ARRAY N0.2-ARRAY N0.1 RES0LUTI0N FACT0R: 5

SIG-Z(ARRAY N0.1) = 48.4149 DEGREES

SIG-W(ARRAY N0.2) = 271.949 DEGREES
SIG-W(ARRAY N0.2) = 54.3897 DEGREES(RES0LVED BY N0.1)
----------
E(Z*W) =-6908.              DEGREES
----------
ARRAY-T0-ARRAY C0RR. C0EFF'T. =-0.524671
----------

----------
PR0BABILITY FUNCTI0N PARAMETERS:

ARGUMENT F(1) = 3.71787
ARGUMENT F(2) = 3.30945
L(1) =-1.59428E-13              L(2) = 7.61799E-6
PR0B.-C0RR(1) = 0.999799        PR0B.-C0RR(2) = 0.999065
PR0B.-AMB(1)  = 2.00920E-4      PR0B.-AMB(2)  = 9.34742E-4
----------


----------
PR0B. 0F AMBIGUITY = 0.112 PERCENT(INCL. C0RRELATI0N)

PR0B. 0F AMBIGUITY = 0.1135 PERCENT(ASSUMING INDEPENDENCE)
----------
```

Fig. B6 – Example of program AMBIG1 printout—unequal channel-pair phase errors

AMBIG2

```
10 READ M1,N1,M2,N2,Q
20 DIM S(50)
30 DIM H(31,2),L(2),U(2),Z(2)
40 PRINT"FØUR-ELEMENT PHASE INTERFERØMETER:"
50 PRINT"CØMPØUND PRØB.-ØF-AMBIGUITY FØR ARRAY SYNTHESIZED"
60 PRINT"BY CASCADING TWØ THREE-ELEMENT INTERFERØMETERS-----"
70 PRINT
80 PRINT"      ARRAY NØ.1 PARAMETERS:"
90 PRINT"      'LARGE' =";M1,"  'SMALL' =";N1
100 PRINT
110 PRINT"      ARRAY NØ.2 PARAMETERS:"
120 PRINT"      'LARGE' =";M2,"  'SMALL' =";N2
130 PRINT
140 PRINT"      ARRAY NØ.2-ARRAY NØ.1 RESØLUTIØN FACTØR:";Q
150 PRINT
160 LET A1 = SQRT(M1*M1-M1*N1+N1*N1)
170 LET A9 = SQRT(M2*M2-M2*N2+N2*N2)
180 LET P9 = (M1-N1)*(M2-N2)-N1*M2
190 LET P4 = .5*P9/(A1*A9)
200 LET C1 = 1/(2*3.1415926)
210 LET C2 = 1./SQR(1.-P4*P4)
220 LET A2 = A9/Q
230 PRINT
240 PRINT"ARRAY-TØ-ARRAY CØRR. CØEFF'T. =";P4
250 PRINT
260 PRINT"CP.PR.SIG.","#1 P-CØRR.","#2 P-CØRR.","CØMP'D.AMB."
270 PRINT"   (DEGR)","      ","      ","  (PCT)"
280 PRINT
290 FØR M = 6 TØ 26
300 LET S(M) = 5 +(M-1)
310 LET U1 = 180./(S(M)*A1)
320 LET U2 = 180./(S(M)*A2)
330 LET U(1) = U1
340 LET U(2) = U2
350 FØR J = 1 TØ 2
360 IF U(J)>5.4513 THEN 490
370 LET Z3 = 0.
380 LET T = U(J)/(2↑.5)
390 LET S = T
```

Fig. B7—Listing of program AMBIG2

```
400 LET Y2 = U(J)*U(J)/2
410 LET D = 1
420 LET D = D + 2
430 LET T = T*(2*Y2/D)
440 LET S = S + T
450 IF(T/S-1E-10)>0 THEN 420
460 LET Z3 = (2/SQRT(3.1415926))*S*EXP(-Y2)
470 LET Z(J) = (1.-Z3)/2
480 GØ TØ 500
490 LET Z(J) = 2.5E-08
500 NEXT J
510 LET A7 = 1 - 2*Z(1)
520 LET B7 = 1 - 2*Z(2)
530 FØR J = 1 TØ 2
540 IF U(J)>5.4513 THEN 800
550 LET H(0,J) = 1
560 LET H(1,J) =-U(J)
570 LET A =-U(J)
580 LET B = 1
590 FØR I = 2 TØ 20
600 LET C = A
610 LET A =-A*U(J) -(I-1)*B
620 LET B = C
630 LET H(I,J) = A
640 NEXT I
650 NEXT J
660 FØR J = 1 TØ 2
670 LET E = 1.
680 LET F = 0.
690 FØR K = 0 TØ 20
700 LET X = P4*(3-2*J)
710 LET D = H(K,1)*H(K,2)*(X↑(K+1))
720 LET E = E*(K+1)
730 LET F = F + D/E
740 NEXT K
750 LET U3 = U(1)*U(1) + U(2)*U(2)
760 LET F1 = F*C1*EXP(-U3/2)
770 LET L(J) = Z(1)*Z(2) + F1
780 NEXT J
790 GØ TØ 810
800 LET L(1) = L(2) = 0
810 LET E1 = 2. - (A7+B7+2.*L(1)+2.*L(2))
820 LET E2 = 100*E1
830 LET E3 = INT(E2*10↑4 + .5)/10↑4
840 PRINT S(M),A7,B7,E3
850 NEXT M
860 DATA 5,3,21,10,5
870 END
```

Fig. B7—Listing of program AMBIG2 (continued)

```
290 FØR M = 6 TØ 21
860 DATA 5,3,21,10,5


AMBIG2



FØUR-ELEMENT PHASE INTERFERØMETER:
CØMPØUND PRØB.-ØF-AMBIGUITY FØR ARRAY SYNTHESIZED
BY CASCADING TWØ THREE-ELEMENT INTERFERØMETERS-----

     ARRAY NØ.1 PARAMETERS:
     'LARGE' = 5                'SMALL' = 3

     ARRAY NØ.2 PARAMETERS:
     'LARGE' = 21               'SMALL' = 10

     ARRAY NØ.2-ARRAY NØ.1 RESØLUTIØN FACTØR: 5


ARRAY-TØ-ARRAY CØRR. CØEFF'T. =-0.258502

CP.PR.SIG.     #1 P-CØRR.     #2 P-CØRR.     CØMP'D.AMB.
   (DEGR)                                      (PCT)

 10              0.999964       0.999999       0.0037
 11              0.999826       0.999993       0.0181
 12              0.999421       0.999963       0.0616
 13              0.99851        0.999358       0.163
 14              0.996818       0.99959        0.3583
 15              0.994095       0.999026       0.6851
 16              0.990146       0.99801        1.1766
 17              0.984864       0.996385       1.8573
 18              0.978219       0.994009       2.7409
 19              0.970251       0.990775       3.8303
 20              0.961053       0.986617       5.119
 21              0.95075        0.981509       6.5929
 22              0.939487       0.97546        8.2329
 23              0.927414       0.968508       10.0165
 24              0.91468        0.960715       11.9201
 25              0.901423       0.952155       13.9199
```

Fig. B8—Example of program AMBIG2 printout

Naval Research Laboratory
Technical Library
Research Reports Section

DATE: February 12, 2004

FROM: **Mary Templeman**, Code 5596.3

TO: **Code 5700 Dr Klemm**

C: Tina Smallwood, Code 1221.1 ts 6/16/04

SUBJ: Review of NRL Report

Dear Sir/Madam:

Please review NRL Report 8005 for:

- ☑ Possible Distribution Statement Change To "A"
- ☐ Possible Change in Classification

Thank you,

Mary Templeman
(202)767-3425
maryt@library.nrl.navy.mil

---

767 6357

The subject report can be:

- ☑ Changed to Distribution A (Unlimited)
- ☐ Changed to Classification _____
- ☐ Other:

Ted A. Roberts 6/15/04
Signature Date

TEd A Roberts
5722